MASS. INST. OF TECHNOLOGY
SEP 13 1965
LIBRARIES

ANALYSIS OF THE HEAT CAPACITY RESULTS OF ANTIFERROMAGNETIC COMPOUNDS AND COMPOUNDS WHICH EXHIBIT ROTATION

by

David Smith

B.S. (magna cum laude) Providence College

(1961)

Submitted in Partial Fulfillment of the Requirements

for the Degree of Doctor of Philosophy

at the

MASSACHUSETTS INSTITUTE OF TECHNOLOGY

September 1965

Signature of Author Signature redacted
Department of Chemistry, August 31, 1965

Certified by Signature redacted
Thesis Supervisor

Accepted by Signature redacted
Chairman, Departmental Committee on Graduate Students

This Doctoral Thesis has been

Examined by a Committee of the Department of Chemistry

as Follows

Professor Clark C. Stephenson
Thesis Supervisor

Signature redacted

Professor Irwin Oppenheim
Chairman

Signature redacted

Professor Carl W. Garland

Signature redacted

ANALYSIS OF HEAT CAPACITY RESULTS OF ANTIFERROMAGNETIC COMPOUNDS AND COMPOUNDS WHICH EXHIBIT ROTATION

by

DAVID SMITH

Submitted in Partial Fulfillment of the Requirements for the Degree of Doctor of Philosophy, at the Massachusetts Institute of Technology, August, 1965.

ABSTRACT

The heat capacity results of a number of antiferromagnetic compounds and of compounds which exhibit rotation have been analyzed in this thesis. In order to study the heat capacities of magnetic compounds and compounds which exhibit rotation, the lattice heat capacities of these compounds must be known. It was found that a sum of Debye and Einstein functions can accurately represent the lattice heat capacity of a compound.

The heat capacity of antiferromagnetic $MnTiO_3$ was measured from 30°K to 300°K using the existing calorimeter[1] and cryostat.[2] The entropy at 298.16°K is 25.08 e.u. ± 0.1 e.u.

The magnetic heat capacity results of compounds with the corundum structure and the transition metal fluorides and chlorides have been analyzed. Three compounds with the corundum structure have no magnetic contribution below room temperature, Al_2O_3, Ti_2O_3, and Fe_2O_3. Each of these compounds could be represented by a sum of the following: a Debye function with four degrees of freedom, a Debye function with two degrees of freedom, an Einstein function with three degrees of freedom, and an Einstein function with six degrees of freedom. It was found that the Debye characteristic temperatures were linear functions of molecular weight multiplied by molar volume and the Einstein characteristic temperatures were linear functions of the square root of the reduced mass multiplied by the molar volume. Given these relationships it was possible to determine the characteristic temperatures for the magnetic compounds with the same crystal structure (Cr_2O_3 and $MnTiO_3$). From the characteristic temperatures, the lattice heat capacity was computed. The same general procedure was followed to determine the lattice heat capacity of the magnetic fluorides and chlorides. Given the lattice heat capacities for these compounds, the magnetic heat capacities may then be computed.

The entropy associated with the magnetic transition in Cr_2O_3 was about one-half the expected value. This was explained by assuming that there is pairwise interaction between Cr-Cr ions, but no higher order interaction above the Néel temperature.

The entropy associated with the magnetic transition at 62.3°K in $MnTiO_3$ was determined to be 3.51 e.u. which is in excellent agreement with the expected 3.56 e.u. (R ln6 for Mn^{+2}). Only 55% of the magnetic entropy and 37% of the magnetic enthalpy is acquired at the Néel temperature. The anamolous magnetic susceptibility results[3] could not be explained from the heat capacity results.

Three of the magnetic compounds analyzed exhibited both cooperative and non-cooperative (Schottky) effects, $CoCl_2$, CoF_2, and FeF_2. For the cobalt salts, there are six Kramers doublets with a separation of less than 2000 cm^{-1}. It was possible to determine the energy of the doublets from the heat capacity results. For Co^{+2} in $CoCl_2$ the energy levels of the doublets are: 0, 205 cm^{-1}, 425 cm^{-1}, 890 cm^{-1}, 946 cm^{-1}, and 1020 cm^{-1}, where the lowest doublet is given a value of zero. For Co^{+2} in CoF_2 the energy of the doublets are: 0, 153 cm^{-1}, 750 cm^{-1}, and 1300 cm^{-1}. The highest two Kramers doublets make no contribution to the heat capacity below room temperature.

The energy levels for a three-dimensional hindered rotor were evaluated for a tetrahedron in a cubic environment using the potential function given by Gutowsky et. al.[4] Using perturbation theory it was possible to evaluate the energy levels by assuming that below the barrier to rotation harmonic oscillator wave functions are the zero-order wave functions of the problem and above the barrier to rotation free-rotor wave functions are the zero-order wave functions. The theory was applied to the hindered rotation of the ammonium ion in the ammonium halides and the borohydride ion in the alkali borohydrides. The torsional frequencies of NH_4^+ evaluated from the heat capacity results both above and below the order-disorder transitions in the ammonium halides are in good agreement with torsional frequencies determined by other techniques. The rotational heat capacity of BH_4^- in $NaBH_4$ and KBH_4 was computed from the observed heat capacity. The theoretical evaluation of the rotational heat capacity of BH_4^- was in reasonable agreement with the observed heat capacity of BH_4^- in the case of KBH_4, but in poor agreement in the case of $NaBH_4$.

---

1) H.E. Adams, "The Heat Capacity of Manganese Fluoride, etc.", thesis, MIT, (1942)
2) R. W. Blue and J.F. Hicks, J. Am. Chem. Soc., 52, 1962, (1937)
3) S. Kern and B. Feldman, Solid State Research Report, Lincoln Laboratory, MIT, (1962), #2, p. 35
4) H. S. Gutowsky, G. E. Pake, and R. Bersohn, J. Chem. Phys., 22, 643, (1954)

Thesis Supervisor: Clark C. Stephenson

Title: Professor of Chemistry

TO MY PARENTS

ACKNOWLEDGMENT

The author gratefully acknowledges the assistance given to him by Professor Clark C. Stephenson during the author's tenure at MIT.

Thanks are due to Professor Robert E. Newnham for providing the sample of $MnTiO_3$ used for the heat capacity measurements and to Dr. O. R. Lundell for his help in collecting the experimental data.

The author is most grateful to Professor J. C. Slater for the financial assistance received during the summer of 1963.

Thanks are due to the Computation Center at MIT for providing the author with time on the IBM 7094 computer.

TABLE OF CONTENTS

		Page
I.	INTRODUCTION	1
	Motion of Ionic Groups in Solids	
	Antiferromagnetism in Transition Metal Compounds	
II.	HEAT CAPACITY MEASUREMENTS	10
	Experimental Measurements	
III.	DETERMINATION OF THE MAGNETIC HEAT CAPACITY OF ANTIFERROMAGNETIC COMPOUNDS	20
	Corundum Structure Compounds	
	Ilmenites	
	Transition Metal Fluorides	
	Transition Metal Chlorides	
	Cupric Oxide	
	Summary	
IV.	DISCUSSION OF MAGNETIC HEAT CAPACITY RESULTS	73
	Compounds with Magnetic Transitions in the Liquid Helium Temperature Region	
	Hydrated Cobalt Salts	
	Cobalt Chloride	
	Cobalt Fluoride	
	Cupric Chloride and Chromous Chloride	
	Chromic Oxide	

TABLE OF CONTENTS (CONTINUED)

Page

Cupric Oxide

Ferrous Fluoride and Manganese Fluoride

Manganese Titanate

V. MOTION OF IONIC GROUPS IN SOLIDS 102

One-Dimensional Hindered Rotation

Three-Dimensional Hindered Rotation

Ammonium Chloride

Deutero-Ammonium Chloride

Ammonium Bromide

Deutero-Ammonium Bromide

Ammonium Iodide (Tetragonal)

Sodium Borohydride

Potassium Borohydride

Ammonium Fluoborate

Lithium Borohydride

Ammonium Fluoride

Ammonium Nitrate

Discussion on Three-Dimensional Hindered Rotation

Ammonium Iodide (Face-Centered Cubic)

Hydroxides

Ice

TABLE OF CONTENTS (CONTINUED)

Page

Hydrogen Peroxide

Ferrocene

Quartic Oscillator

Summary

APPENDIX I. MAGNETIC HEAT CAPACITIES OF ANTIFERROMAGNETIC COMPOUNDS 176

APPENDIX II. ENERGY LEVELS OF THREE-DIMENSIONAL HINDERED ROTOR 190

APPENDIX III. COMPUTER PROGRAMS 214

REFERENCES..... 244

BIOGRAPHY 254

LIST OF TABLES

		Page
1.	Order of Heat Capacity Measurements	11
2.	Experimental Heat Capacity of $MnTiO_3$	13
3.	Thermodynamics Functions of $MnTiO_3$	14
4.	Maxima in Frequency Distribution of Alkali Halides	28
5.	Values of $C_p - C_v$ for NaCl and KCl	31
6.	Lattice Parameters of Corundum Structure Compounds	34
7.	Lattice Parameters of Transition Metal Fluorides	35
8.	Lattice Parameters of Transition Metal Chlorides	35
9.	Debye and Einstein Characteristic Temperatures for Corundum Structure Compounds	37
10.	Debye and Einstein Characteristic Temperatures for Transition Metal Fluorides	59
11.	Debye and Einstein Characteristic Temperatures for Transition Metal Chlorides	66
12.	Accuracy of Representing Heat Capacity Results by Debye and Einstein Functions	69
13.	Accuracy of Various Debye and Einstein Representations for ZnF_2	70
14.	Exchange Parameters for Magnetic Compounds With Néel Temperatures below 10°K	79
15.	Exchange Parameters for Magnetic Compounds with Spin ½	79

LIST OF TABLES (CONTINUED)

Page

16. Exchange Parameters for Magnetic Compounds with Néel Temperatures Above 10°K 100

17. Energy Levels of One-Dimensional Hindered Rotor 107

18. Heat Capacity of One-Dimensional Hindered Rotor 109

19. Debye and Einstein Characteristic Temperatures for Some Nitrates 146

20. Torsional Frequencies for the Ammonium Halides 148

21. Heights of Barriers to Rotation for Ammonium Halides 149

22. Debye and Einstein Characteristic Temperatures for the Ammonium Halides in their Low Temperature Phases 150

23. Debye and Einstein Characteristic Temperatures for Solid Solutions of NH_4I and KI 155

24. The Heat Capacity of the Ammonium Ion in a Solid Solution 45.8% NH_4I and 54.2% KI between 15°K and 60°K .. 156

25. The Heat Capacity of the Ammonium Ion in a Solid Solution 45.8% NH_4I and 54.2% KI between 15°K and 300°K 158

26. Torsional Frequencies for the Hydroxides 162

27. Torsional Frequencies of Water Molecule in H_2O and D_2O Lattices 164

28. Accuracy of Torsional Frequency of OH^- in NaOH 173

29. Accuracy of Torsional Frequency of OH^- in LiOH 174

30. Accuracy of Torsional Frequency of Ammonium Ion in NH_4Cl 175

LIST OF TABLES (CONTINUED)

		Page
31.	Magnetic Heat Capacity and Entropy of Chromic Oxide	177
32.	Magnetic Heat Capacity and Entropy of Manganese Titanate	178
33.	Magnetic Heat Capacity and Entropy of Manganese Fluoride	180
34.	Magnetic Heat Capacity of Ferrous Fluoride	181
35.	Magnetic Heat Capacity and Entropy of Cobalt Fluoride ...	183
36.	Magnetic Heat Capacity and Entropy of Chromous Chloride .	185
37.	Magnetic Heat Capacity and Entropy of Cupric Chloride ...	187
38.	Magnetic Heat Capacity of Cobalt Chloride	188

LIST OF FIGURES

		Page
1.	Experimental Heat Capacity of $MnTiO_3$	18
2.	Frequency Distribution of Sodium Chloride	25
3.	Debye Temperatures (θ_1) for Corundum Structure Compounds	38
4.	Debye Temperatures (θ_2) for Corundum Structure Compounds	41
5.	Einstein Temperatures (θ_4) for Corundum Structure Compounds	45
6.	Magnetic Heat Capacity of Chromic Oxide	48
7.	Separation of Observed Heat Capacity of $MnTiO_3$ into Lattice and Magnetic Contributions	52
8.	Magnetic Heat Capacity of Manganese Titanate	54
9.	Magnetic Entropoy of Manganese Titanate	57
10.	Magnetic Heat Capacity of Cobalt Chloride	82
11.	The Contribution of the Six Kramers Doublets to the Magnetic Heat Capacity of $CoCl_2$ above 100°K	86
12.	Magnetic Heat Capacity of Cobalt Fluoride	89
13.	The Contribution of the Kramers Doublets to the Magnetic Heat Capacity of CoF_2 above 100°K	91
14.	Crystal Structure of Corundum Compounds	95
15.	Rotational Heat Capacity of BH_4^- in $NaBH_4$	128

LIST OF FIGURES (CONTINUED)

Page

16. Rotational Heat Capacity of BH_4^- in KBH_4 132

17. Comparison of Observed and Theoretical Heat Capacity of BH_4^- in $NaBH_4$ and KBH_4 137

18. Rotational Heat Capacity of NH_4^+ in NH_4BF_4 141

I. INTRODUCTION

Specific heat measurements have been a useful tool in the study of the microscopic properties of solids. They have been used to study cooperative effects, such as order-disorder phenomena and magnetic transitions in solids, and non-cooperative effects, namely Schottky effects in dilute magnetic salts, and the motion of ionic groups in solids.

In order to study any of these phenomena it is necessary to know the lattice heat capacity, so that it may be possible to determine the contribution of the phenomena under study to the observed heat capacity. Three methods have been used to evaluate the lattice heat capacity in solid compounds. One method is to compare the heat capacity of a compound under study, e.g. an antiferromagnetic compound, with that of an isomorphous diamagnetic salt. The lattice heat capacity of the compound under study is simply taken to be equal to the heat capacity of the isomorphous salt. An analysis of this type was used to determine the lattice heat capacity of UO_2 and NpO_2 using ThO_2 as the diamagnetic salt.[1]

Stout and Catalino,[2] using the principle of corresponding states, computed the lattice heat capacity of antiferromagnetic salts which have Néel temperatures under $80^{\circ}K$. They derived the lattice

heat capacity from the heat capacity versus temperature curve of an isomorphous diamagnetic salt by changing the temperature scale by an appropriate factor. This factor, which differs only slightly from one, is found by matching the entropy at relatively high temperatures.

The third method for determining the lattice heat capacity is to assume that the lattice heat capacity can be represented by a sum of Debye and Einstein functions. This method has been used to evaluate the torsional frequencies of a number of ammonium salts.[3,4,5]

The first theoretical analysis of heat capacity data was developed by Einstein.[6] He considered 3N independent harmonic oscillators in one dimension, each having the identical frequency ν. The partition function, Z, for the assembly is

$$Z = \sum_{n=0}^{\infty} e^{-(n+\frac{1}{2})h\nu/kT}$$

He was able to express the heat capacity of the system as

$$C = 3Nk\left(\frac{\theta_E}{T}\right)^2 \frac{e^{\theta_E/T}}{\left(e^{\theta_E/T}-1\right)^2}$$

where $\theta_E = h\nu/k$, is the Einstein characteristic temperature.

The Einstein model does not represent the heat capacity of solids at very low temperatures. The model treated each atom as an independent oscillator which executes harmonic motion about a fixed.

point in space. However, atoms in a real crystal do not all have the same frequency.

In a solid that has 3N normal modes of vibration there are $f(\nu)d\nu$ modes in the frequency range $d\nu$ at ν. The total heat capacity is

$$C = k \int_{\text{all permissible frequencies}} \left(\frac{h\nu}{kT}\right)^2 \frac{e^{h\nu/kT}}{\left(e^{h\nu/kT} - 1\right)^2} f(\nu)d\nu$$

Debye was able to determine the value of $f(\nu)$ by assuming that the acoustical spectrum of a solid can be treated as if the solid were an elastic continuum.[7] The Debye theory limits the frequencies possible to all those below the frequency ν_{max}, which is found from the requirement that the total number of oscillators be 3N, so that

$$\int_0^{\nu_{max}} f(\nu)d\nu = 3N$$

The distribution function derived by Debye is

$$f(\nu) = \frac{9N\nu^2 d\nu}{\nu_{max}^2}$$

The heat capacity becomes

$$C = 9Nk \frac{1}{x_m^3} \int_0^{x_m} \frac{x^4 e^x}{(e^x - 1)^2} \, dx$$

$$x = \frac{h\nu}{kT} \qquad x_m = \frac{h\nu_{max}}{kT} = \frac{\theta_D}{T}$$

$$\nu_{max} = \frac{9}{4\pi} \frac{N}{V} \left[\frac{1}{\frac{1}{v_l^3} + \frac{2}{v_t^3}} \right]$$

v_l = velocity of longitudinal vibrations in the crystal

v_t = velocity of transverse vibrations in the crystal

The Debye theory disregards frequencies greater than ν_{max}, although in solids there are frequencies having values greater than ν_{max}. Neither the Debye nor the Einstein theory accurately represents the heat capacity of solids. The heat capacities of a number of compounds, however, have been represented by a sum of Debye and Einstein functions.

Given a method for determining the lattice heat capacity, many different types of problems may be attacked. Two of these problems, the motion of ionic groups in solids and antiferromagnetism in the transition metal compounds, will be studied in this thesis.

Motion of Ionic Groups in Solids

Three types of motion may be displayed by an ionic group in a solid: free rotation, hindered rotation, and torsional oscillation. Torsional oscillation is simply harmonic vibration. Hindered rotation is intermediate between torsional oscillation and free rotation.

The ammonium halides have been extensively studied, since in these salts all three types of motion are exhibited. The ammonium halides, with the exception of the fluoride, have a lambda-point in their specific heat. Pauling[18] first explained the lambda-point as the onset of free rotation in these salts. However, Frenkel[19] proposed that the lambda-point was due to a disordering of the ammonium ions. Stephenson, Blue, and Stout[17] substantiated Frenkel's picture by determining the entropy associated with the transition in the heat capacity results. They found about 1.4 e.u., or R ln2, associated with the transition. This is the value expected, if there were two possible orientations of the ammonium ion.

From their heat capacity results, Stephenson et. al.[17] concluded that the ammonium ion acted as a torsional oscillator at low temperatures in the ammonium halides. At room temperature there was no evidence of free rotation, except in the case of ammonium iodide. At about 250^{o}K ammonium iodide undergoes a first-order transition with a decrease in the heat capacity of about 4 cal/mole/deg.[20] This

decrease in the heat capacity may be explained by assuming that the ammonium ion acts as a torsional oscillator in the low temperature phase and as a free rotor in the high temperature phase.

Other ammonium salts presumably exhibit pseudo-free rotation at room temperature. These include ammonium fluosilicate (hexagonal form),[4] ammonium fluoborate,[21] and ammonium chlorostannate.[22] In all these salts the heat capacity of the ammonium ion has a rounded maximum between 150°K and 200°K. As room temperature is approached the rotational heat capacity of the ammonium ion in these salts decreases toward 3/2R, the classical value of the heat capacity of a three-dimensional free rotor.

The heat capacity results of many of the ammonium salts have been reexamined in this thesis in order to obtain a better understanding of the motion of the ammonium ion in its salts.

Antiferromagnetism in Transition Metal Compounds

The Weiss Molecular Field Theory is generally used in interpreting the magnetic properties of antiferromagnets and ferromagnets. This model assumes that a single spin interacts with a uniform field. The Heisenberg Hamiltonian for a magnetic substance

in no external field is

$$\mathcal{H} = -\sum_{nn'} J_{nn'}\, \vec{S}_n \cdot \vec{S}_{n'} \tag{5}$$

where $J_{nn'}$ is an exchange integral. For antiferromagnetic compounds $J_{nn'} < 0$; for ferromagnetic compounds $J_{nn'} > 0$. Using the molecular field approximation the effective Hamiltonian for spin n is

$$\mathcal{H}_n = -\vec{S}_n \left[2\sum_{n'} J_{nn'} \langle S_{n'} \rangle \right] = -\vec{S}_n \vec{H}_n$$

$$H_n = 2\sum_{n'} J_{nn'} \langle S_{n'} \rangle = 2zJ \langle S_{n'} \rangle$$

where z is the number of nearest neighbors. The average value of the spin S_n is well known to be

$$\langle S_n \rangle = S B_S \left(\frac{S H_n}{kT} \right)$$

where S is the total spin quantum number and B_S is the Brillouin function for spin S. The solution of the molecular field problem has been treated in detail elsewhere.[23] The important results of

this theory are

$$T_N = \frac{2}{3}\frac{zJ[S(S+1)]}{k}$$

$$E = \frac{zS^2|J|}{k}$$

where T_N is the Néel temperature and E is the total magnetic energy. This model predicts that there will be no magnetic heat capacity above the Néel temperature.

Specific heat results of magnetic substances have been used to determine the exchange parameter using the molecular field model.[24] Recently an extended molecular field theory has been proposed to explain the magnetic heat capacity above the Néel temperature in $CuCl_2 \cdot 2H_2O$.[25-27]

The Weiss molecular field theory considers only nearest neighbors. Usually, this is a good approximation. However, it has been proposed that in hexagonal $MnTiO_3$ two types of interactions are important; the interactions between Mn ions within the hexagonal layers and the interactions between Mn ions on different hexagonal layers. Usually the interactions between the hexagonal layers are much greater than the interactions within the layers. It is believed that as a result of the two different types of important interactions,

$MnTiO_3$ exhibits anomalous magnetic properties. Neutron diffraction[89] results and antiferromagnetic resonance data[168] show that the Néel temperature of $MnTiO_3$ is 61.5^oK. The powder magnetic susceptibility, however, exhibits no peak at 61.5^oK, but rather exhibits a rounded maximum at about 95^oK.[88] In order to obtain a better understanding of the magnetic interactions present in $MnTiO_3$, its heat capacity has been measured.

II. HEAT CAPACITY MEASUREMENT

The heat capacity measurements were made in a calorimeter[28] and a cryostat[29] previously described. Temperatures were measured by means of a platinum-rhodium resistance thermometer with the laboratory designation R222. R222 was originally calibrated against a helium gas thermometer, as described by Blue and Hicks,[29] from 11°K to 300°K. Measurements were made on a Leeds and Northrup Wenner potentiometer and a Leeds and Northrup type HS galvanometer. Two auxiliary galvanometers were used to maintain adiabatic conditions between the calorimeter and the surrounding shield. All calculations were based upon a calorie defined by 1 calorie = 4.1833 international joules, and upon an ice-point of 273.16°K. The heat capacity of a 99.8171 grams (vacuum mass) or 0.66179 moles of manganese titanate was measured. The molecular weight of the compound was taken as 150.83.

A detailed description of the method of measuring and calculating the heat capacities is found in the appendix to the thesis by T. G. Maple.[30] Computer programs have been written to perform these calculations. These programs are given in Appendix III.

$MnTiO_3$ was prepared by heating a 50-50 mixture of $MnCO_3$ and TiO_2 at 1000°C. No impurities were noticed from x-ray diffraction measurements.

Table 1 gives the series of measurements in the order they were performed.

TABLE 1

Order of Heat Capacity Measurements

Series	Number of C_p Measurements	Temperature Range ^{o}K	Coolant
A	15	61.2 - 104.7	pumped liquid N_2
B	14	110.2 - 182.3	liquid N_2
C	18	187.7 - 296.6	liquid N_2
D	3	285.3 - 299.2	liquid N_2
E	13	59.0 - 78.9	pumped liquid N_2
F	11	30.7 - 69.4	liquid H_2

Four values from series B and C have been omitted because of a failure in the potentiometer. The first two values in Series E have been omitted because of unfavorable conditions. The first five values listed under Series E in Table 2 are not as accurate as other runs because the temperature interval was only $0.5^{o}K$. The Néel temperature is $62.3^{o}K \pm 0.1^{o}K$.

Smooth-curve values of the heat capacity are listed in Table 3. Also listed in this Table are the thermodynamic functions S, $(H - E_o)/T$, and $-(F - E_o)/T$.

The entropy below 31°K was estimated by assuming that the magnetic entropy at 31°K is equal to about one-half the magnetic heat capacity. The lattice entropy was computed from the Debye and Einstein functions for $MnTiO_3$ given in the next chapter. The total entropy at 31°K is estimated to be 0.67 e.u. ± 0.10 e.u.

The precision of the heat capacity runs are: 1% in the temperature range 30°K to 40°K, 0.3% in the range 40°K to 100°K, and 0.1% above 100°K. Below 100°K the precision is not as good as is usually attainable using the apparatus in this laboratory. One source of difficulty is that $MnTiO_3$ is bulky, so only 0.6 moles could be packed into the calorimeter. The heat capacity of the empty calorimeter contributed 40% to 60% to the heat capacity of the calorimeter and sample. The accuracy of the heat capacity measurements is 2% between 30°K and 40°K, 0.5% between 40°K and 100°K, and 0.2% above 100°K.

TABLE 2

Experimental Heat Capacity of $MnTiO_3$

Values in calories $degree^{-1}$ $mole^{-1}$

T	C_p	T	C_p	T	C_p
Series A		Series B		Series C	
62.21	6.88	115.07	11.23	187.69	17.70
63.90	6.71	120.10	11.72	193.57	18.16
66.80	6.64	125.31	12.24	199.55	18.59
69.88	6.82	130.75	12.75	205.63	18.91
72.79	7.05	136.24	13.27	211.57	19.38
75.55	7.29	141.80	13.78	217.62	19.75
78.20	7.47	147.40	14.34	223.74	20.14
80.74	7.76	153.03	14.84	230.06	20.52
83.30	7.99	158.72	15.39	236.54	20.91
85.99	8.21	164.56	15.90	243.15	21.23
89.12	8.58	176.34	16.90	249.92	21.58
92.71	8.88	182.26	17.30	256.56	21.91
96.45	9.30			263.13	22.31
100.44	9.70			269.83	22.66
104.70	10.15			276.41	22.92
				282.87	23.31
				289.50	23.65
Series D		Series E		Series F	
285.30	23.42	60.04	6.56	30.63	1.66
291.99	23.69	60.56	6.73	33.10	1.98
299.18	23.97	61.05	6.94	35.93	2.18
		61.55	7.04	39.27	2.69
		62.03	7.13	43.31	3.27
		62.52	6.90	47.75	3.97
		63.60	6.78	52.44	4.83
		65.75	6.63	57.20	5.87
		69.19	6.84	61.29	6.92
		73.77	7.19	65.12	6.66
		78.93	7.62	69.38	6.84

TABLE 3

Thermodynamic Functions of $MnTiO_3$

The thermodynamic functions are in calories degrees^{-1} mole^{-1}.

T	C_p	S	$(H - E_o)/T$	$-(F - E_o)/T$
31	1.71	0.67	0.48	0.19
32	1.81	0.73	0.52	0.21
34	2.03	0.84	0.60	0.24
36	2.27	0.97	0.69	0.28
38	2.52	1.09	0.78	0.32
40	2.79	1.23	0.87	0.36
42	3.08	1.37	0.97	0.40
44	3.38	1.52	1.07	0.45
46	3.67	1.68	1.18	0.50
48	4.00	1.84	1.29	0.55
50	4.36	2.01	1.41	0.61
52	4.74	2.19	1.53	0.67
54	5.16	2.38	1.65	0.73
56	5.60	2.57	1.79	0.79
58	6.07	2.78	1.93	0.85
59	6.38	2.89	2.00	0.89
60	6.57	2.99	2.07	0.92
61	6.83	3.11	2.15	0.96
62	7.10	3.22	2.23	0.99
62.3	7.18	3.25	2.25	1.00
63	6.83	3.33	2.30	1.03

TABLE 3 (Continued)

T	C_p	S	$(H - E_o)/T$	$-(F - E_o)/T$
64	6.73	3.44	2.37	1.06
65	6.66	3.54	2.44	1.10
66	6.63	3.64	2.50	1.14
68	6.70	3.84	2.62	1.22
70	6.87	4.04	2.74	1.29
72	7.01	4.23	2.86	1.37
74	7.17	4.43	2.97	1.45
76	7.33	4.62	3.09	1.53
78	7.50	4.81	3.20	1.62
80	7.69	5.00	3.31	1.70
85	8.15	5.48	3.58	1.91
90	8.64	5.96	3.85	2.12
95	9.14	6.44	4.11	2.33
100	9.66	6.93	4.38	2.55
105	10.19	7.41	4.64	2.77
110	10.70	7.90	4.90	2.99
115	11.21	8.38	5.17	3.22
120	11.72	8.87	5.43	3.44
125	12.20	9.36	5.69	3.67
130	12.68	9.85	5.95	3.90
135	13.15	10.33	6.21	4.13
140	13.63	10.82	6.46	4.36
145	14.10	11.31	6.72	4.59
150	14.57	11.79	6.97	4.82
155	15.04	12.28	7.23	5.05

TABLE 3 (Continued)

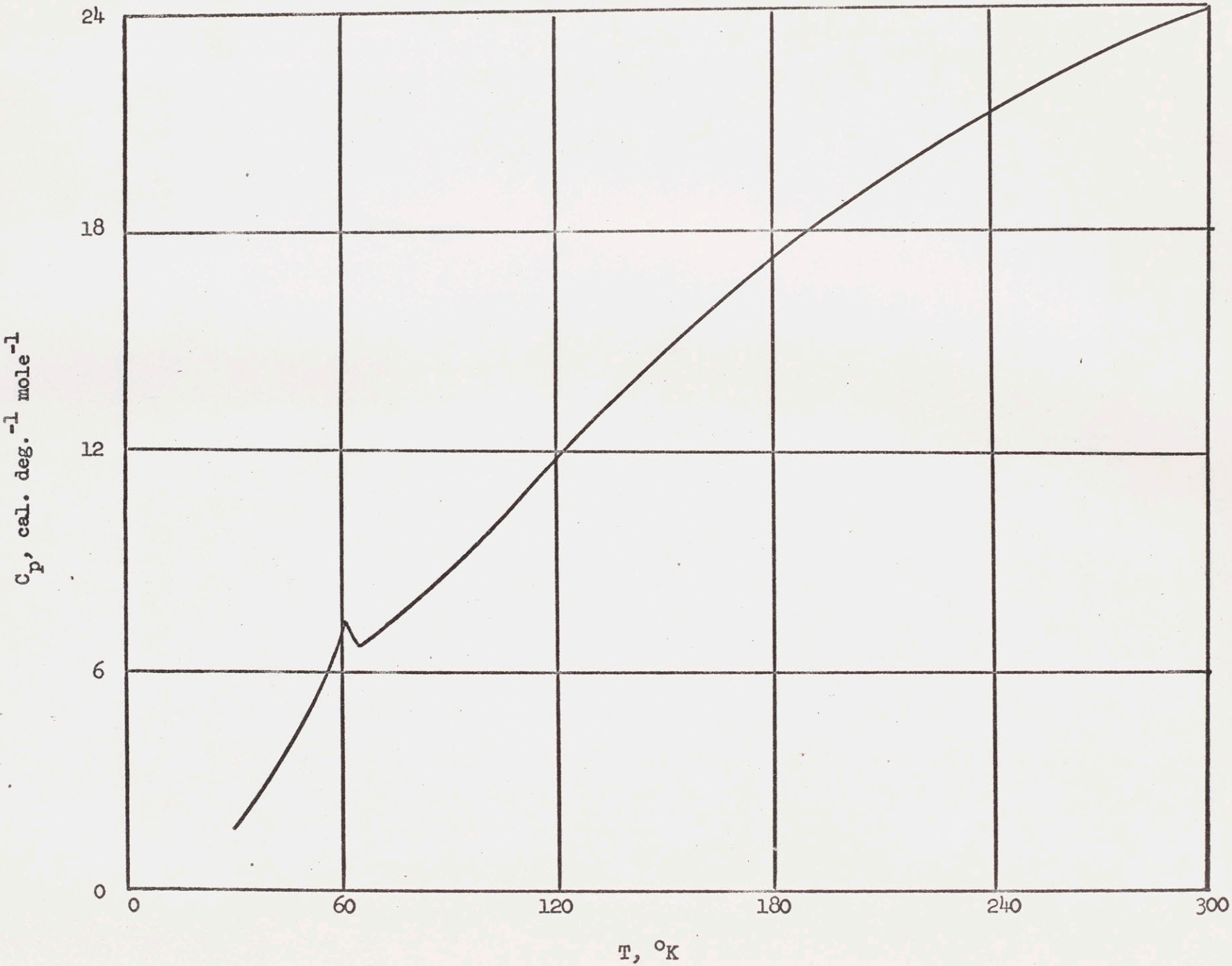
T	C_p	S	$(H - E_o)/T$	$-(F - E_o)/T$
160	15.50	12.76	7.48	5.29
165	15.95	13.25	7.73	5.52
170	16.38	13.73	7.98	5.75
175	16.78	14.21	8.22	5.00
180	17.15	14.69	8.46	6.22
185	17.52	15.16	8.70	6.46
190	17.89	15.64	8.94	6.70
195	18.24	16.11	9.18	6.93
200	18.59	16.57	9.41	7.17
205	18.93	17.04	9.63	7.40
210	19.25	17.50	9.86	7.64
215	19.58	17.95	10.08	7.87
220	19.90	18.41	10.30	8.10
225	20.22	18.86	10.52	8.34
230	20.52	19.30	10.73	8.57
235	20.81	19.75	10.94	8.81
240	21.08	20.19	11.15	9.04
245	21.33	20.63	11.36	9.27
250	21.58	21.06	11.56	9.50
255	21.84	21.49	11.76	9.73
260	22.13	21.92	11.95	9.96
265	22.40	22.34	12.15	10.19
270	22.67	22.76	12.34	10.42
275	22.93	23.18	12.53	10.65

TABLE 3 (Continued)

T	C_p	S	$(H - E_o)/T$	$-(F - E_o)/T$
280	23.18	23.60	12.72	10.88
285	23.41	24.01	12.91	11.10
290	23.63	24.42	13.09	11.33
295	23.82	24.82	13.27	11.55
300	24.00	25.23	13.45	11.78
298.16	23.93	25.08	13.38	11.70

Figure 1

Experimental Heat Capacity of Manganese Titanate


24
18
12
6
0
0
60
120
180
240
300
C_p, cal. deg.$^{-1}$ mole^{-1}
T, °K

III. DETERMINATION OF THE MAGNETIC HEAT CAPACITY OF ANTIFERROMAGNETIC COMPOUNDS

In order to analyze the heat capacity results of a magnetic compound it is necessary to separate the magnetic heat capacity from the lattice heat capacity. For magnetic compounds which have their Néel temperature in the liquid helium region, this separation is quite simple. Above the transition temperature the magnetic heat capacity is proportional to T^{-2} (for $T \gg T_N$).[31] The lattice heat capacity in this region is proportional to T^3. Therefore, the total heat capacity is given by

$$C = aT^3 + b/T^2$$

or

$$CT^2 = aT^5 + b$$

where "a" and "b" are constants. A plot of CT^2 versus T^5 should give a straight line, whose slope is equal to "a". The lattice heat capacity can then be calculated and subtracted from the total heat capacity to give the magnetic heat capacity. Even if the lattice heat capacity does not obey the T^3 dependence perfectly, no great error is introduced into the magnetic heat capacity, since the lattice heat capacity is very small compared to the magnetic heat capacity in this temperature region. A number of magnetic compounds have been analyzed by this method.[34-46]

For magnetic compounds whose Néel temperature is above 150°K, the problem of separating the magnetic and lattice heat capacity is no longer simple. Two schemes have been proposed to solve this problem. Weiss et. al.[24,33] proposed a Two-Debye method. They assumed that the lattice heat capacity of a binary magnetic salt may be represented by a sum of two Debye functions; one Debye function representing the positive ion and the other representing the negative ion. For A_xB_y

$$C_v = 3xD(\theta_1/T) + 3yD(\theta_2/T)$$

They also assumed that the entropy associated with the transition is given by the spin-only formula $R\ln(2S + 1)$, where R is the gas constant and S is the spin of the magnetic ion. Using these two assumptions, they were able to compute the lattice heat capacity. The magnetic heat capacity can then be calculated by subtracting the lattice heat capacity from the observed heat capacity.

Stout and Catalano[2] proposed another method, based on the principle of corresponding states, for determining the lattice heat capacity. They compared the heat capacity of a magnetic with that of an isomorphous diamagnetic compound. They assumed that

$$C^M(T) = C^D(rT)$$

and

$$S^{M}(T) = S^{D}(r'T) + R\ln(2S + 1)$$

where the superscripts M and D stand for magnetic and diamagnetic salts respectively. Stout and Catalano compared the entropies of the magnetic and diamagnetic salts rather than their heat capacities, since the low frequency vibrations, which make the major contribution to the heat capacities at low temperatures, make a larger contribution to the entropy than to the heat capacity at high temperatures. They computed values for a parameter r' by subtracting from the entropy of the magnetic salt $R\ln(2S + 1)$ at any given temperature T and then finding the temperature (T') where the diamagnetic salt has the same value of the entropy.

$$r' = T/T'$$

The value of r' is nearly independent of temperature at temperatures high above the transition point, where the magnetic heat capacity makes no contribution to the total heat capacity of the magnetic salt. The parameter r is determined by comparing the heat capacities of the magnetic and diamagnetic compounds. If the principle of corresponding states were obeyed r' would be equal to r. In practice this is not true. At very low and very high temperatures r and r' are sensitive functions of temperature. At low temperatures, this is due to the magnetic

transition; at high temperatures, it is due to the contribution of high frequency vibrations to the heat capacity.

With the calculated values of r' at various temperatures, the lattice heat capacity of magnetic compounds can be calculated by using the equation

$$C^{M}_{lattice}\ (T) = C^{D}(rT)(1 + d\ln r'/d\ln T)$$

Once the lattice heat capacity is known for the magnetic salt, the magnetic heat capacity can be computed.

Both methods discussed have serious shortcomings. The Two-Debye method is seriously restricted, since the lattice heat capacity can be represented by a sum of two Debye functions only for compounds which have a rutile structure. The corresponding states method can be used only for compounds which have their transition temperature below $80^{o}K$, since the principle of corresponding states begins to break down at high temperatures. This method cannot calculate accurate values of the magnetic heat capacity above $100^{o}K$. Both methods assume that the entropy associated with the transition is $R\ln(2S + 1)$.

In order to alleviate these shortcomings another method has been developed to treat the problem of calculating the lattice heat capacity of magnetic compounds. It will be assumed that the lattice heat capacity of a compound may be represented by a sum of Debye and Einstein functions. The reliability of this method will be studied by considering the heat

capacity of sodium chloride. There are six degrees of freedom associated with each sodium chloride molecule; three degrees of freedom associated with the lattice vibrations ("translatory" modes of vibration) of the sodium and chloride ions as a whole and three degrees of freedom associated with the lattice vibrations of the sodium ion with respect to the chloride ion. The three normal modes of vibration associated with the crystal as a whole are represented by a Debye function having three degrees of freedom. The three normal modes associated with the inter-ionic vibrations of the sodium and chloride ions are represented by an Einstein function having three degrees of freedom.

The frequency spectrum[8-11] of sodium chloride has been calculated by considering the electrostatic interactions in the solid. The frequency spectrum calculated by Kellermann[9,10] and refined by Karo[8] is shown in Fig. 2 together with the frequency spectrum calculated by utilizing a Debye function with three degrees of freedom. The heat capacity of sodium chloride is represented by the following Debye and Einstein functions:

$$C_V = 3D(225/T) + 3E(250/T)$$

The Debye function resembles the low (acoustical) frequencies; the Einstein function the high (optical) frequencies. The apparent lack of agreement between the frequency spectrum calculated from electrostatic forces in the solid and that evaluated from the Debye

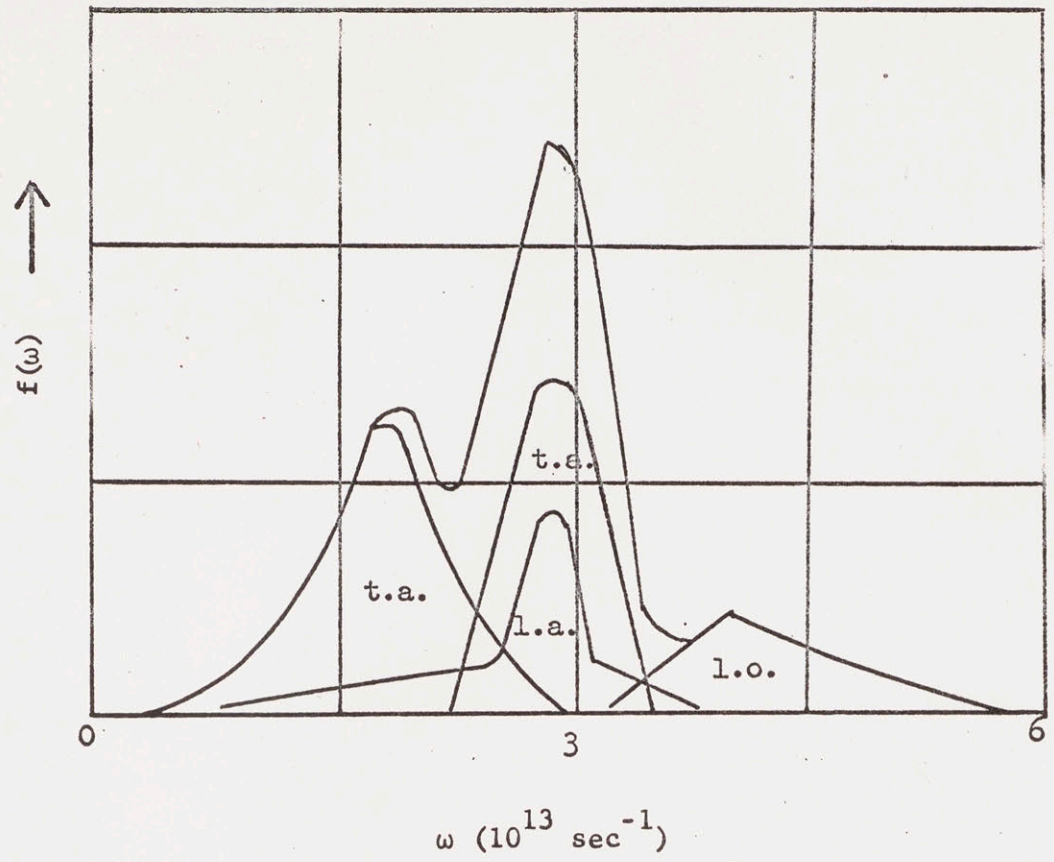
Figure 2

Frequency Distribution for Sodium Chloride

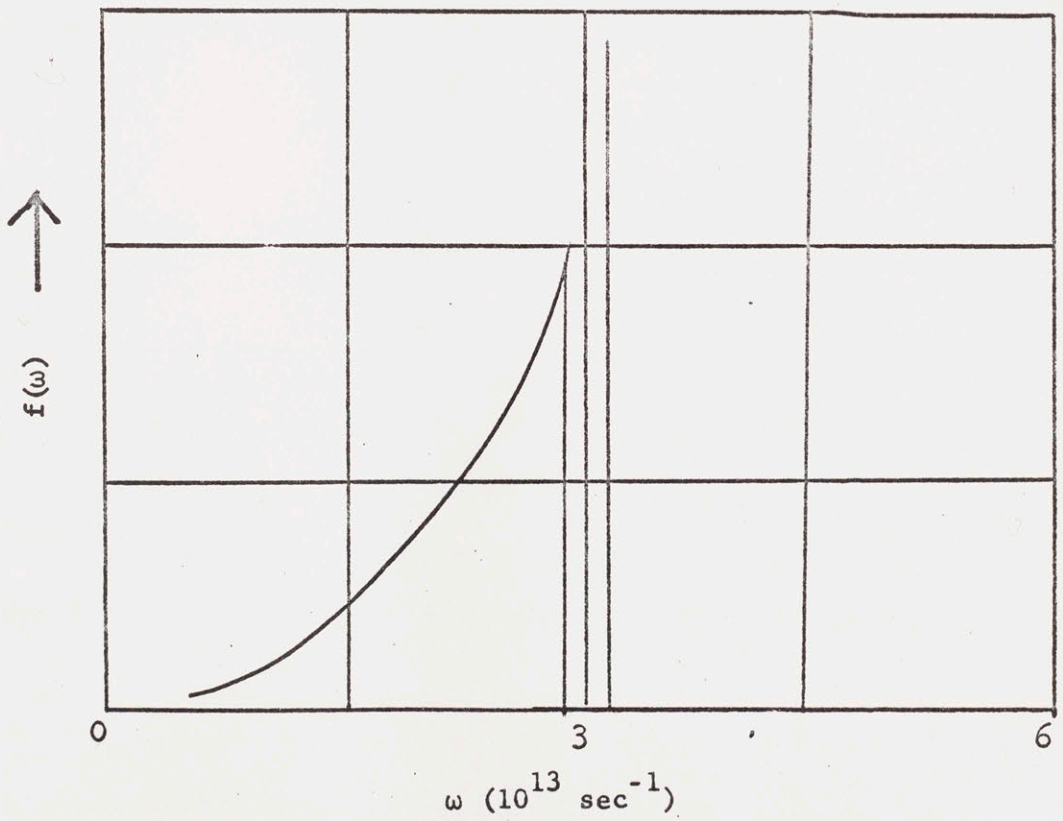
1a. Kellermann Model

1b. Debye and Einstein Models

(a)



(b)



and Einstein representation of the heat capacity data. The heat capacity results are rather insensitive to the frequency spectrum. It is interesting to note that the characteristic Debye temperature lies between the maxima of the transverse and longitudinal acoustical frequencies, and the Einstein characteristic temperature lies between the maxima of the transverse optical and longitudinal optical frequencies. This has been found to be the case, with only two exceptions, in the other alkali halides that have been studied. The exceptions are LiF and LiCl. The results are given in Table 4. It was impossible to represent the heat capacity of LiF to a Debye function with three degrees of freedom and an Einstein function with three degrees of freedom. However, if the Einstein function were split into one with two degrees of freedom and another with one degree of freedom, the heat capacity data can be reproduced.

$$C_V = 3D(524/T) + 2E(385.6/T) + E(810/T)$$

Although the Debye function does not resemble the acoustical frequencies, the split of the Einstein function does follow from Karo's frequency spectrum. The transverse and longitudinal optical frequencies are separated by an amount which does not allow a single Einstein function to reproduce it.

The heat capacity at constant volume is calculated from the Debye and Einstein functions. Experimentally, the heat capacity at constant

TABLE 4

Maxima in Frequency Spectra of Alkali Halides Expressed in 10^{13} sec^{-1}

	Karo's Calculation				Heat Capacity Results	
	ta	la	to	lo	θ_D	θ_E
LiF	3.1	4.8	4.7	11.7	7.5	5.0 , 10.6
LiCl	2.0	3.1	4.4	8.0	3.9	3.4 , 6.5
NaF	2.9	4.2	3.9	6.1	4.5	5.1
NaCl	1.9	2.9	2.8	4.0	2.9	3.2
NaBr	1.2	1.9	2.4	3.7	1.8	2.9
NaI	0.8	1.3	2.0	3.4	1.3	2.5
KF	2.0	3.0	3.1	5.1	3.0	4.0
KCl	1.7	2.4	2.2	3.1	2.2	2.9
KBr	1.1	1.6	1.9	2.5	1.6	2.4
KI	0.8	1.2	1.7	2.4	1.2	2.1
RbBr	1.0	1.4	1.4	1.8	1.3	1.7
RbI	0.8	1.1	1.2	1.5	1.1	1.5

ta - transverse acoustical mode

la - longitudinal acoustical mode

to - transverse optical mode

lo - longitudinal optical mode

θ_D - Debye characteristic temperature

θ_E - Einstein characteristic temperature

pressure is measured. The relation between them is

$$C_p - C_v = \alpha^2 VT/B \tag{1}$$

where α is the thermal expansion, B the compressibility, and V is the molar volume. Unfortunately thermal expansion and compressibility data are not available for most solids. In order to estimate $C_p - C_v$, Grüneisen's relation is used

$$\gamma = \frac{\alpha V}{BC_v}$$

γ, Grüneisen's constant, is assumed to be independent of temperature. For ionic solids (1) becomes

$$C_p - C_v = \frac{\gamma^2 BC_v^2 T}{V} \tag{2}$$

$\frac{B}{V}$ is also assumed to be independent of temperature. So (2) may be written as

$$C_p - C_v = (aC_v)^2 T \tag{3}$$

$$a^2 = \frac{\gamma^2 B}{V}$$

For molecular solids Grüneisen's relation is

$$\frac{\alpha V}{B} = (\gamma_1 C_{v1} + \gamma_2 C_{v2})$$

where C_{v1} is the contribution of the intramolecular vibrations to the heat capacity and C_{v2} is the contribution of the intermolecular vibrations to the heat capacity. For molecular solids

$$C_p - C_v = (aC_{v1} + bC_{v2})^2 T \qquad (4)$$

In practice it is usually impossible to distinguish between "a" and "b", so they are taken to be equal.

The value of the constant "a" in (3) is considered as an empirical parameter in the analysis of heat capacity data. For the alkali halides, "a" has been determine by analyzing the heat capacity results.[12] $C_p - C_v$ has been determined from thermodynamic data[13,14] (thermal expansion and compressibility) for a number of the alkali halides using Eq. (1). In Table 5 the results of the heat capacity analysis for $C_p - C_v$ and the experimental results for $C_p - C_v$ are given for NaCl and KCl. The values of $C_p - C_v$ for NaCl calculated from the analysis of the heat capacity data are in excellent agreement with the experimental results. The maximum deviation between the two sets of data is 0.02cal/mole/deg. For KCl the results

TABLE 5

Values of $C_p - C_v$ for NaCl and KCl

Temperature ^oK	NaCl		KCl	
	Thermo-dynamic Data	Heat Capacity Data	Thermo-dynamic Data	Heat Capacity Data
30	0.000	0.001	0.000	0.002
40	0.001	0.003	0.002	0.008
50	0.005	0.010	0.010	0.021
60	0.014	0.023	0.022	0.032
80	0.049	0.062	0.055	0.089
100	0.096	0.111	0.097	0.144
120	0.148	0.164	0.143	0.200
140	0.201	0.218	0.191	0.256
160	0.255	0.271	0.238	0.311
180	0.309	0.324	0.285	0.365
200	0.365	0.376	0.322	0.418
220	0.421	0.428	0.380	0.471
240	0.479	0.478	0.427	0.522
260	0.536	0.528	0.475	0.574
270	0.565	0.553	0.498	0.625

$C_p - C_v$ is expressed in calories $degree^{-1}$ $mole^{-1}$

are not in very good agreement. However, the difference between the $C_p - C_v$ values determined from experimental data and heat capacity data is due to anharmonic vibrations in KCl. The contribution of anharmonic vibrations have been estimated by other techniques[15,16] and are in agreement with the results determined here. The results for the lithium halides and the other sodium halides resemble the results for NaCl, while the results for the other potassium and rubidium halides resemble the KCl results.

The Debye and Einstein functions together with the parameter "a" (giving $C_p - C_v$) represent the heat capacities of the various alkali halides very well. Below $30^{\circ}K$ the heat capacity is represented to within 10%, between $30^{\circ}K$ and $150^{\circ}K$ to within 1%, and between $150^{\circ}K$ and room temperature to within 0.5%.

After considering the results of representing the lattice heat by a sum of Debye and Einstein functions for the alkali halides, the assumption was made that the lattice heat capacity of magnetic compounds can likewise be represented by a sum of Debye and Einstein functions.

The values of the Debye and Einstein characteristic temperatures for magnetic compounds are determined from the characteristic temperatures of isomorphous diamagnetic salts. As long as there is no strong spin-lattice interaction this is permissible. The charac-

teristic temperatures are given by

$$\theta_D = k\sqrt{M}\, V^{1/3} \qquad \theta_E = k'\sqrt{\mu}\, V^{1/3}$$

where θ_D and θ_E are the Debye and Einstein characteristic temperatures, k and k' are constants, M is the molecular weight of the compound under study, μ is the reduced mass of the compound, and V is the molar volume. In order to determine θ_D for a magnetic compound, the values of θ_D for isomorphous diamagnetic compounds are plotted against $\sqrt{M} \times V^{1/3}$. From the resulting curve, θ_D for the magnetic salt may be determined.

From a study of a number of groups of isomorphous compounds that will be given later in this chapter, it was found that θ_D and θ_E were proportional to V rather than $V^{1/3}$. Also, rather than being proportional to $\sqrt{M}$, θ_D was sometimes found to be proportional to M. Therefore, for the groups of isomorphous compounds studied in this chapter θ_D is plotted against M x V and $\sqrt{M} \times V$. The curve which is most nearly linear is used to give the dependence of θ_D on molecular weight and molar volume. The same procedure was followed for θ_E, except that the molecular weight was replaced by the reduced mass. Usually the difference in the characteristic temperatures determined assuming that θ_D depended on M x V rather than $\sqrt{M} \times V$ is small.

Three groups of isomorphous compounds are to be studied: compounds with the corundum structure, transition metal fluorides, and transition metal chlorides. The lattice parameters used to determine the molar volume are given in Tables 6, 7, and 8.

TABLE 6

Lattice Parameters for Corundum Structure Compounds

	Molecular Weight	Lattice Parameters $a(\mathring{A})$	$c(\mathring{A})$	Molar Volume cc/mole	Ref.
Al_2O_3	101.96	4.7859	12.991	25.68	72
Ti_2O_3	143.8	5.149	13.642	31.44	72
V_2O_3	149.90	4.952	14.002	29.85	72
Cr_2O_3	152.02	4.9607	13.599	29.09	72
Fe_2O_3	159.70	5.0345	13.749	30.29	72
$MgTiO_3$	120.22	5.054	13.898	30.86	75
$MnTiO_3$	150.84	5.137	14.283	32.77	73
$FeTiO_3$	151.75	5.082	14.026	30.29	74

TABLE 7

Lattice Parameters for Transition Metal Fluorides with a Tetragonal Structure

	Molecular Weight	Lattice Parameters a(Å)	c(Å)	Molar Volume cc/mole	Ref.
MgF_2	62.32	4.623	3.052	19.64	75
MnF_2	92.93	4.8734	3.3099	23.67	69
FeF_2	93.85	4.6966	3.3091	21.98	69
CoF_2	96.94	4.6951	3.1796	21.11	69
NiF_2	96.69	4.6506	3.0836	20.10	69
ZnF_2	103.38	4.7034	3.1335	20.88	69

TABLE 8

Lattice Parameters for Transition Metal Chlorides

	Molecular Weight	Lattice Parameters a(Å)	c(Å)	Molar Volume cc/mole	Ref.
$MgCl_2$	95.23	3.632	17.795	40.81	76
*$CrCl_2$	122.92			41.9	77
$MnCl_2$	125.84	3.711	17.59	42.12	76
$FeCl_2$	126.76	3.593	17.58	39.46	76
$CoCl_2$	129.85	3.553	17.39	38.17	76
$NiCl_2$	129.60	3.478	17.41	36.62	76
**$CuCl_2$	134.45			39.1	75
$ZnCl_2$	136.29	5.40	10.35	52.47	75

* crystal structure othorhombic

** crystal structure monoclinic, all other salts have hexagonal ($CdCl_2$) crystal structure.

Corundum Structure Compounds (Sesquioxides)

The low temperature heat capacities of five compounds (Al_2O_3,[47] Ti_2O_3,[48] Fe_2O_3,[49] Cr_2O_3,[50] V_2O_3[51]) which have the corundum structure ($R\bar{3}c$) have been measured. Two of these compounds, Cr_2O_3 and V_2O_3, have transitions below 320°K. The heat capacities of the three other compounds may be represented by the following:

$$C_p = 4D(\theta_1/T) + 2D(\theta_2/T) + 3E(\theta_3/T) + 6E(\theta_4/T) + (aC_v)^2T$$

C_v is the sum of Debye and Einstein terms.

It is necessary to split the six degrees of freedom for the Debye function into one Debye function with four degrees of freedom and another with two degrees of freedom. This 2-1 split is due to the high c/a ratio of these compounds. The heat capacities of other hexagonal compounds, e.g. NH_4F, H_2O, and $MnCl_2$, also require a split of the Debye function. One would expect only three degrees of freedom associated with the Debye functions, but it was necessary to have two Debye functions with a total of six degrees of freedom in order to represent the heat capacity. The extra three degrees of freedom are low frequency optical vibrations.

The characteristic temperatures and "a" values for the corundum structure compounds are given in Table 9. Both Debye functions (θ_1 and θ_2)

TABLE 9

Debye and Einstein Characteristic Temperatures

for Corundum Structure Compounds

Compound	θ_1	θ_2	θ_3	θ_4	a
Al_2O_3	660	1030	490	1000	0.0020
Fe_2O_3	373	475	470	775	0.00365
Ti_2O_3	410	630	490	750	0.0023
Cr_2O_3	432	685	490	(815)	(0.0023)
V_2O_3	(424)	(676)	(490)	(800)	(0.0023)

Numbers that are in parenthesis have been estimated.

$C_p = 4D(\theta_1/T) + 2D(\theta_2/T) + 3E(\theta_3/T) + 6E(\theta_4/T) + (aC_v)^2T$

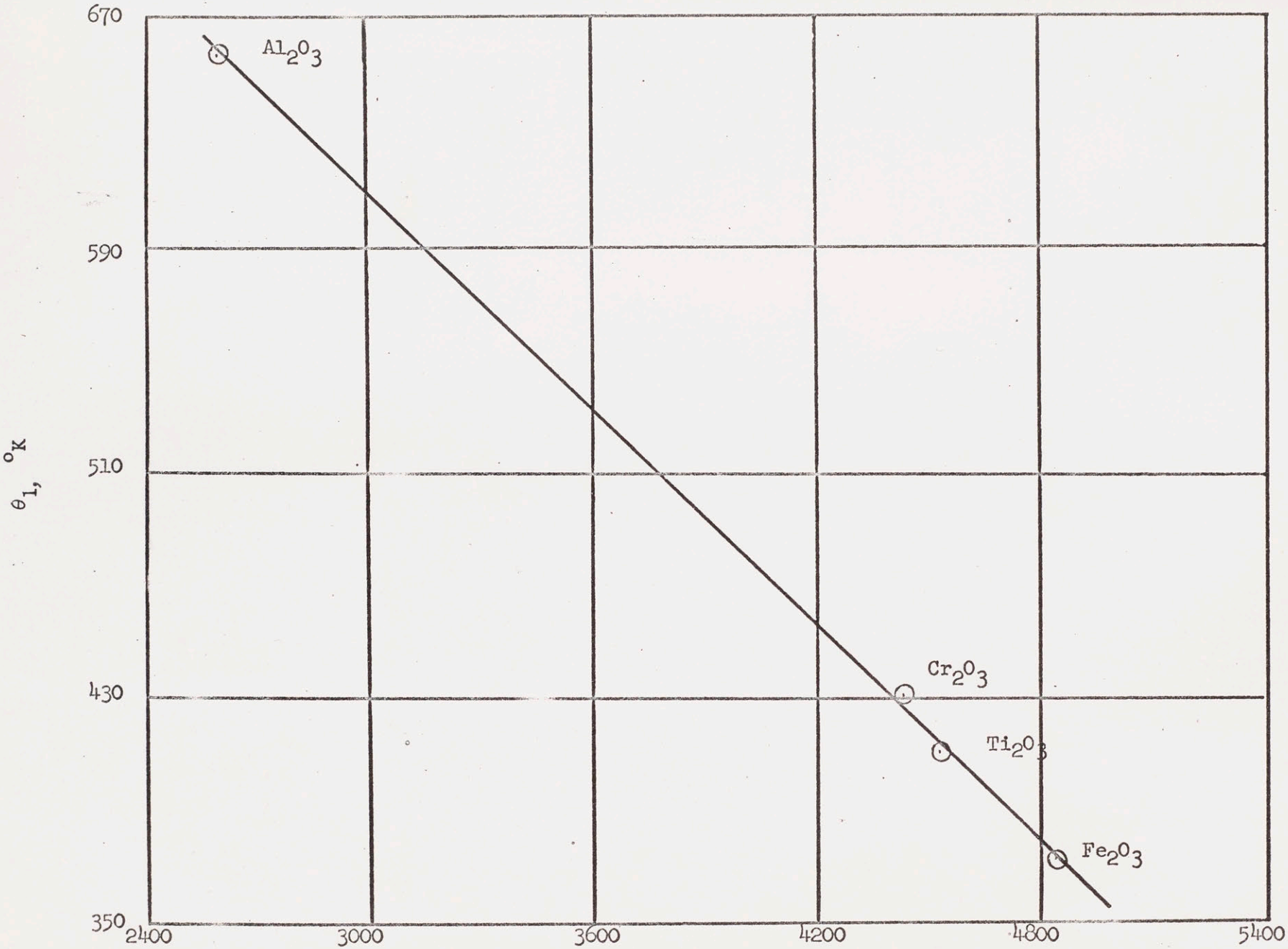
for these compounds give a straight line when plotted against M x V (Fig. 3a and Fig. 4a). θ_2 for Al_2O_3 does not lie on the straight line. Al_2O_3 has a much smaller molecular weight and molar volume than the other oxides, so the discrepancy is not surprising. The important fact is that the transition metal oxides give a straight line when plotted against M x V. The Debye characteristic temperatures (θ_1 and θ_2) are not perfectly linear functions of

Figure 3

Debye Temperatures (θ_1) for Corundum Structure Compounds

a) Debye Temperature as function of Molecular Weight x Molar Volume

b) Debye Temperature as function of $\sqrt{\text{Molecular Weight x Molar Volume}}$


670
590
510
430
350
θ_1, °K
Al_2O_3
Cr_2O_3
Ti_2O_3
Fe_2O_3
2400
3000
3600
4200
4800
5400
Molecular Weight x Molar Volume

(b)

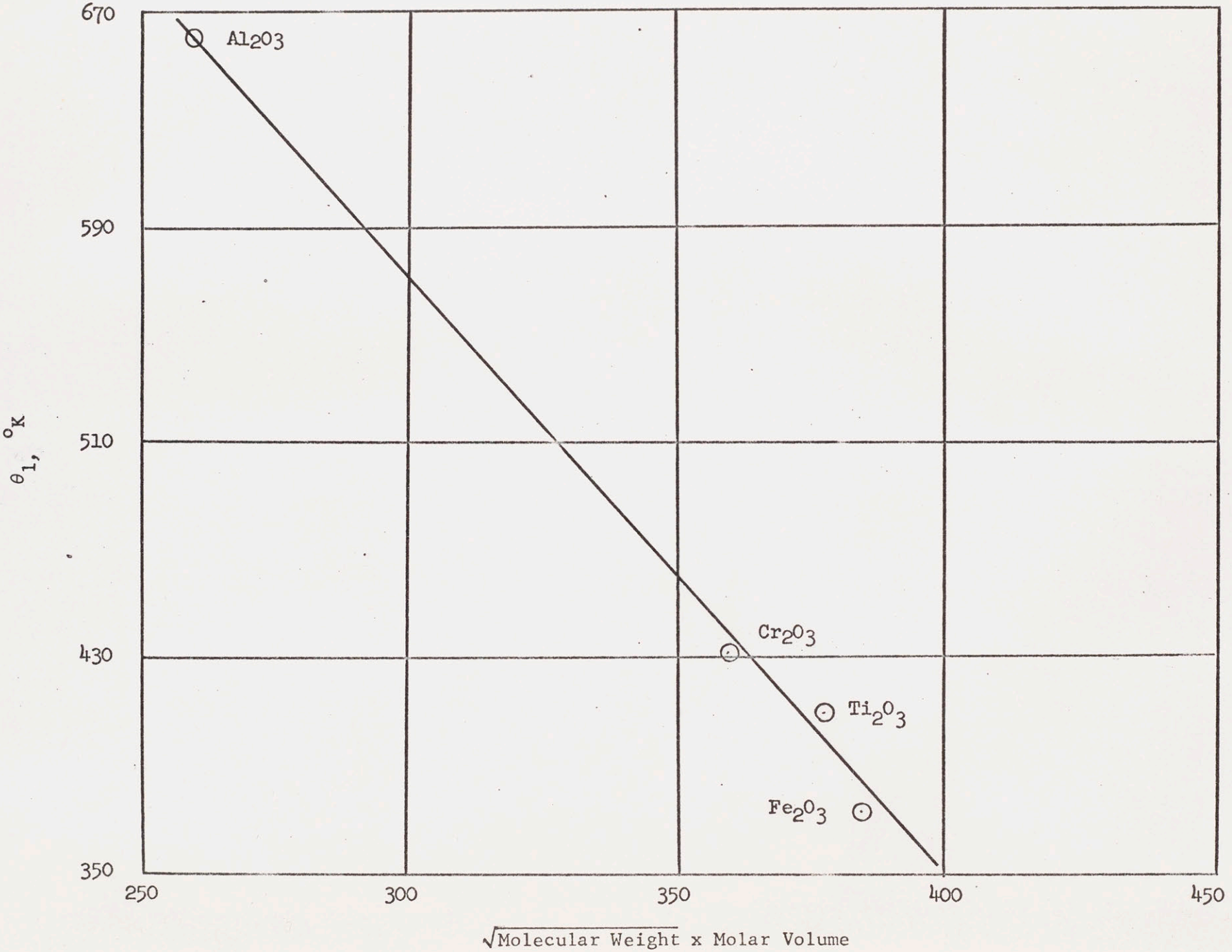

670
590
510
430
350
θ_1, °K
Al_2O_3
Cr_2O_3
Ti_2O_3
Fe_2O_3
250
300
350
400
450
$\sqrt{\text{Molecular Weight x Molar Volume}}$

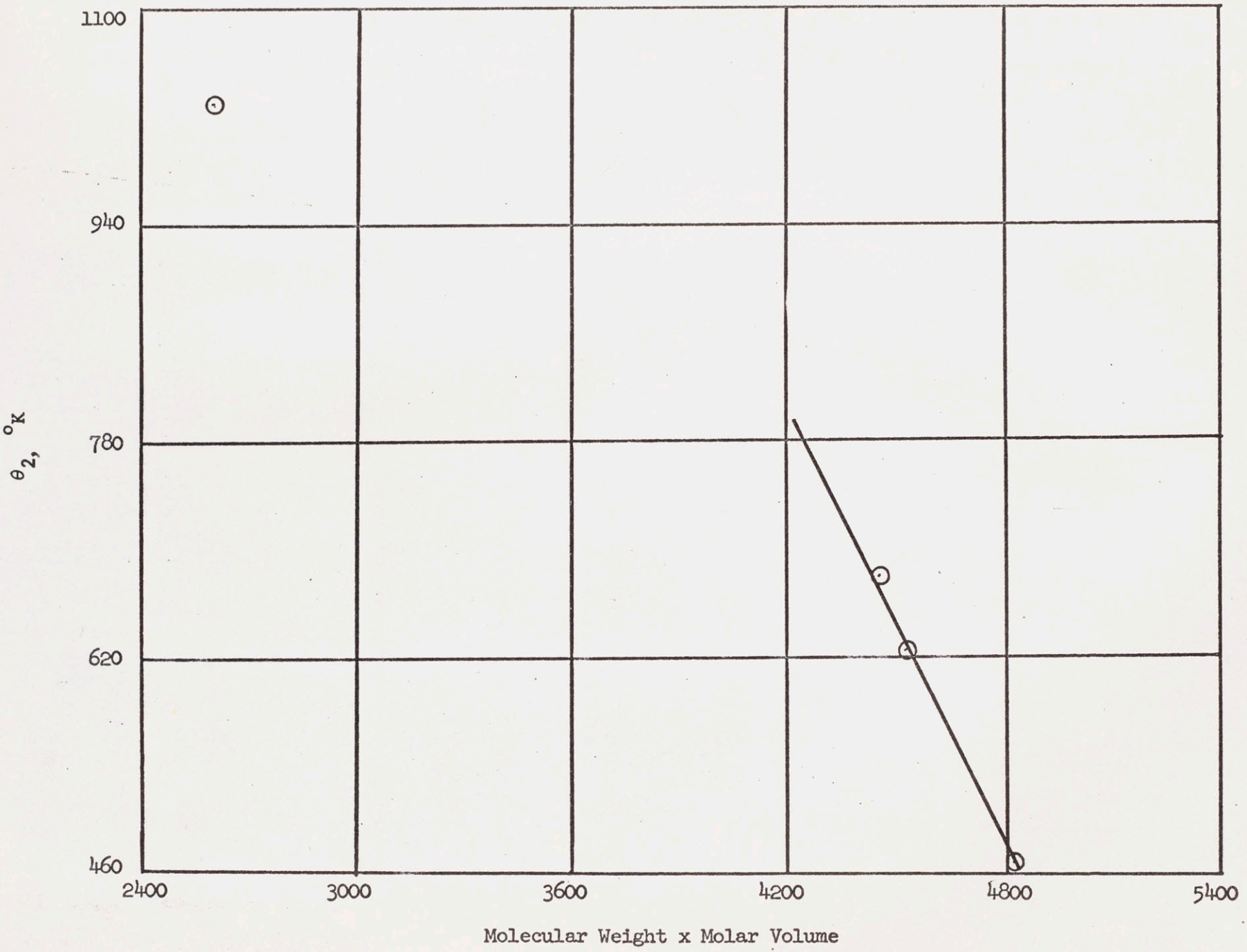
Figure 4

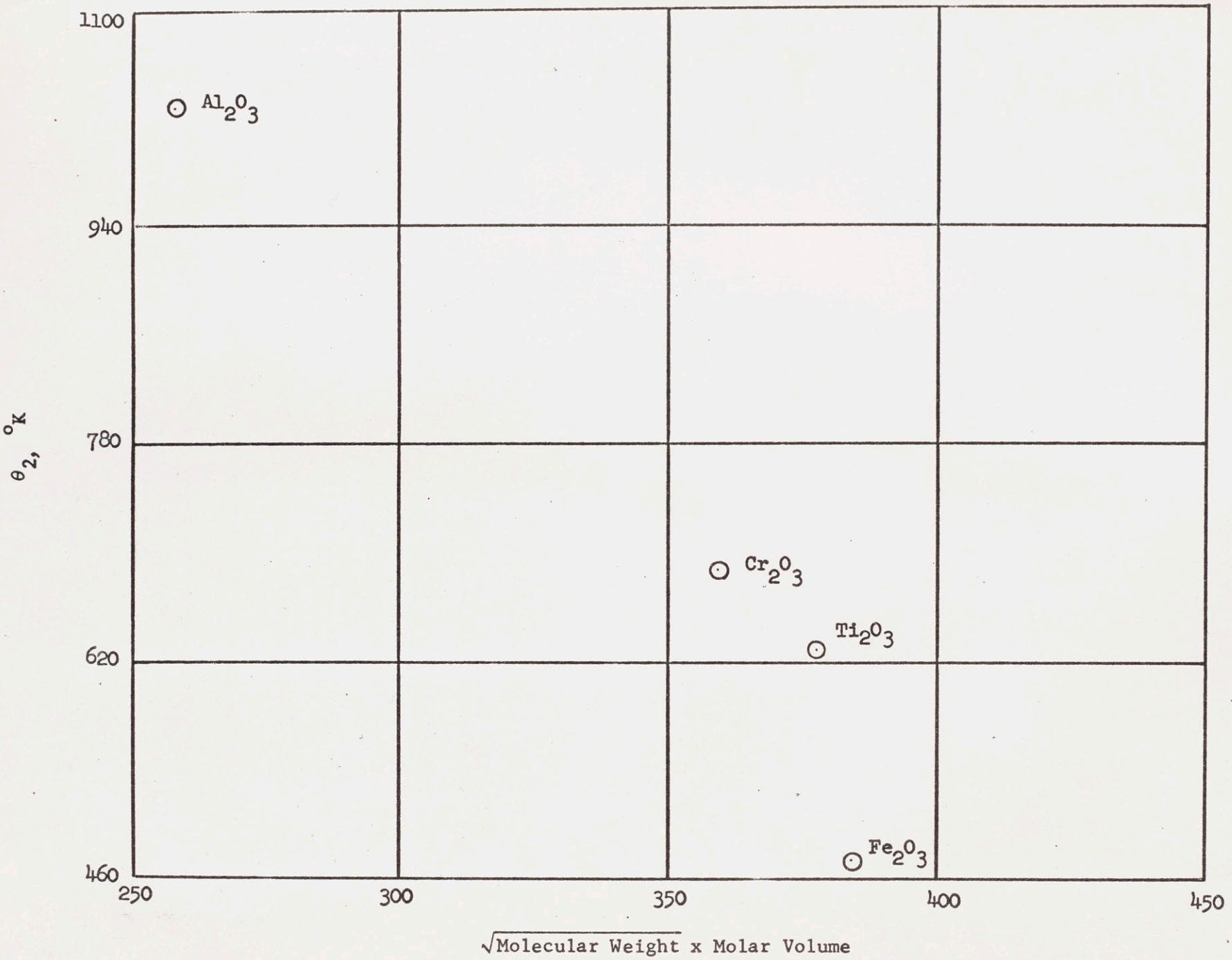
Debye Temperatures (θ_2) for Corundum Structure Compounds

a) Debye Temperature as function of Molecular Weight x Molar Volume

b) Debye Temperature as function of $\sqrt{\text{Molecular Weight}}$ x Molar Volume

(a)


1100
940
780
620
460
θ_2, °K
2400
3000
3600
4200
4800
5400
Molecular Weight x Molar Volume


1100
940
780
620
460
250
300
350
400
450
θ_2, °K
Al_2O_3
Cr_2O_3
Ti_2O_3
Fe_2O_3
√Molecular Weight x Molar Volume

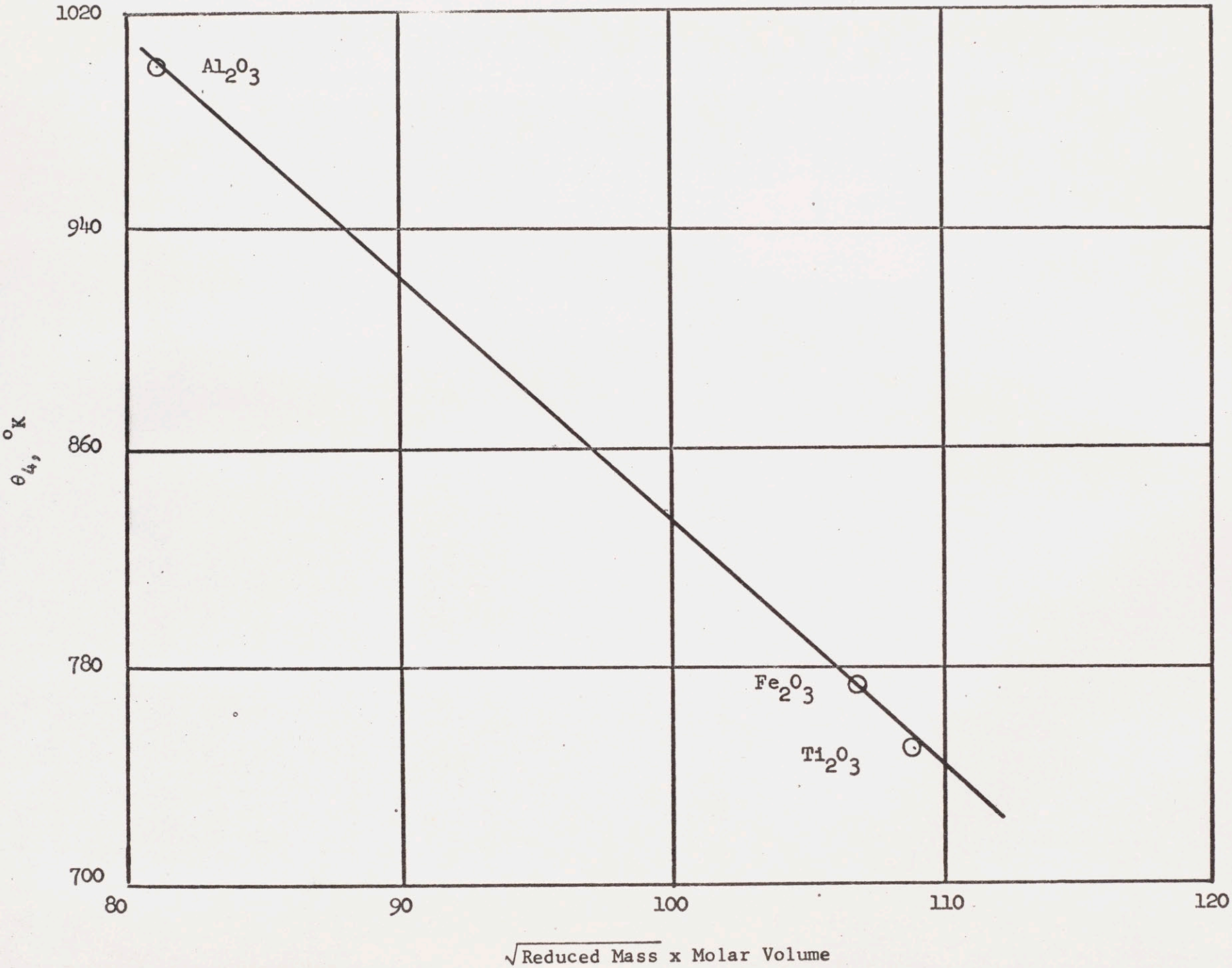
$\sqrt{M} \times V$ (Fig. 3b and 4b). However, the values of θ, determined from Fig. 3a and Fig. 3b are reasonably close to each other. One of the Einstein characteristic temperatures (θ_3) has about the same value for all the corundum structure compounds. The Einstein function (θ_4) with six degrees of freedom is a linear function of $\sqrt{\mu} \times V$ (Fig. 5), where

$$\frac{1}{\mu} = \frac{1}{M(\text{metal ion})} + \frac{1}{M(\text{oxygen})}$$

The heat capacity of Cr_2O_3 has been measured from 55°K to 335°K. It has an antiferromagnetic transition at 305.5°K. Therefore, below 100°K the magnetic heat capacity should make little, if any, contribution to the total heat capacity. It was therefore possible to calculate both Debye characteristic temperatures and the lowest Einstein temperatures (θ_3) for Cr_2O_3. The other Einstein characteristic temperature (θ_4) may be estimated using Fig. 5. The parameter "a" must also be estimated for Cr_2O_3. This parameter has been found to be principally a function of the melting point of the compound under study.[12] The value of "a" for Cr_2O_3 may be estimated from the other corundum structure compounds by taking into account the melting points of these compounds. The value of "a" for Fe_2O_3 is anomalously high. This might be due to its magnetic transition at 520°C.

Figure 5

Einstein Temperatures (θ_4) for Corundum Structure Compounds


1020
940
860
780
700
80
90
100
110
120
θ_4, °K
Al_2O_3
Fe_2O_3
Ti_2O_3
$\sqrt{\text{Reduced Mass x Molar Volume}}$

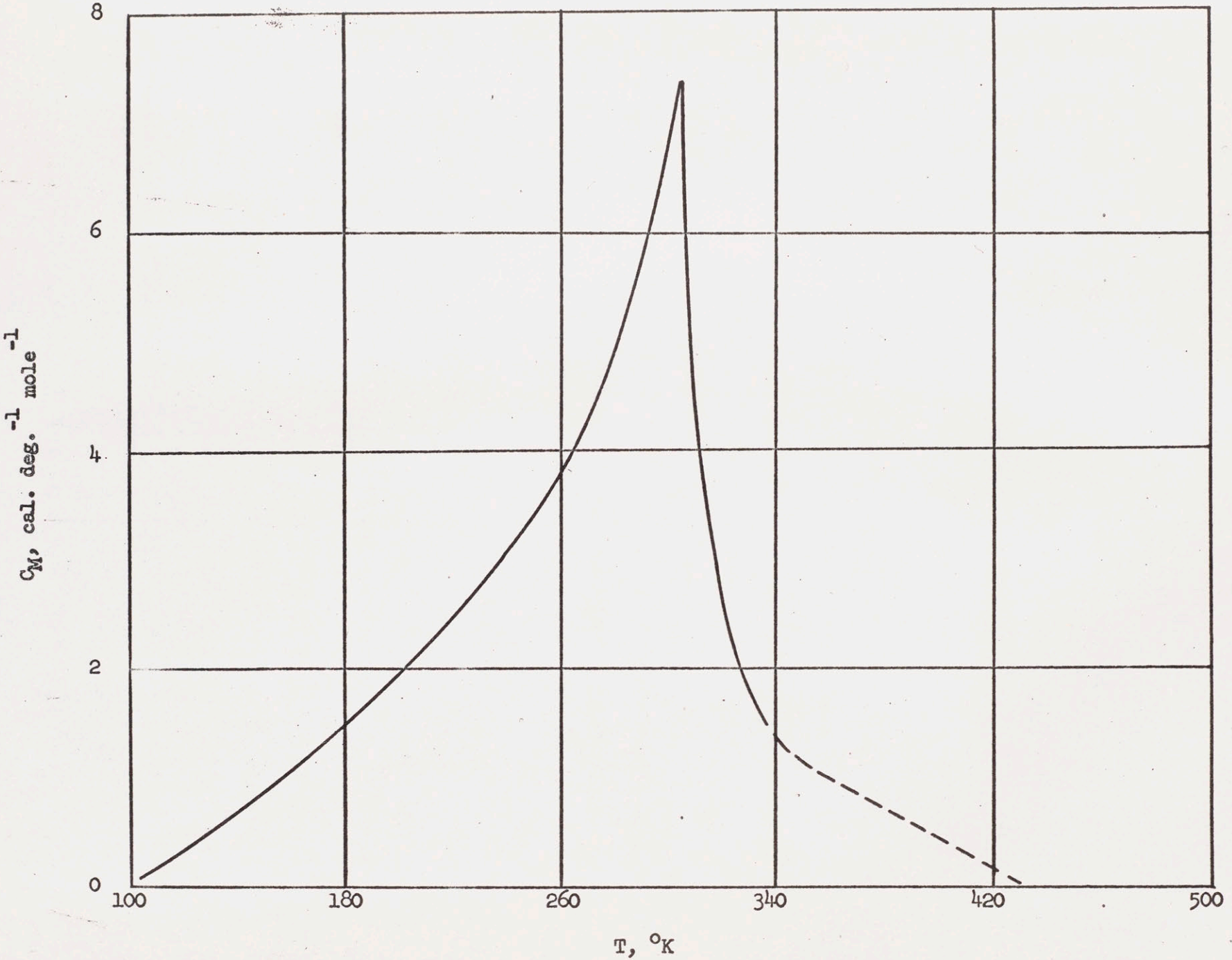
The lattice heat capacity of Cr_2O_3 can be computed from the value of "a" and the Debye and Einstein characteristic temperatures given in Table 9. The magnetic heat capacity, calculated by subtracting the lattice heat capacity from the total heat capacity, is given in Table 31 in Appendix I. The magnetic heat capacity above 335°K is estimated using the high temperature heat capacity measurements of Kelley et. al.[52] The entropy associated with the antiferromagnetic transition is 2.52 e.u. This includes the high temperature extrapolation (Fig. 6). The theoretical entropy for Cr_2O_3 is 2Rln4 (5.54 e.u.). This is outside the possible error involved in the entropy calculation. The error involved in the estimation of "a" is no more than a few tenths of an entropy unit. The same is true for θ_4. The entropy associated with the transition is close to Rln 4 (2.76 e.u.) or 2Rln 2 (2.76 e.u.). There is no reason to expect the effective spin of Cr^{+3} to be reduced from 3/2 to 1/2. Antiferromagnetic resonance[53] results indicate a spin of 3/2. This point will be further discussed in the next chapter.

V_2O_3 is isomorphous to Al_2O_3 above its transition temperature (168°K), but is pseudo-orthorhombic below the transition temperature.[54] The exact nature of the transition is open to question.[55] The entropy associated with the transition is 6.06 e.u. if the parameters given in Table 9 are used to calculate the lattice heat capacity. This is

Figure 6

Magnetic Heat Capacity of Chromic Oxide

Dotted lines signify high temperature extrapolation


8
6
4
2
0
100
180
260
340
420
500
C_M, cal. deg.$^{-1}$ mole^{-1}
T, °K

1.64 e.u. greater than 2Rln 3 (4.40 e.u.). However, this calculation assumes that the crystal structures above and below the transition have the same molar volume. The molar volume above the transition is about 15% greater than the molar volume below the transition. This is a possible explanation of the extra 1.64 e.u.

Ilmenites

The heat capacities of $MgTiO_3$[32] and $FeTiO_3$[32] (ilmenite) have been measured between 55°K and 300°K. Both of these compounds and $MnTiO_3$ have the same crystal structure as the sesquioxides (Al_2O_3, etc.), except that they have two different cations rather than only one cation. $FeTiO_3$ is antiferromagnetic with a Néel temperature of 56.3°K.[32] The heat capacity of diamagnetic $MgTiO_3$ may be represented by

$$C_p = 4D(420/T) + 2D(630/T) + 3E(490/T) + 3E(690/T) + 3E(1015/T) + (0.0017C_v)^2T$$

The Einstein function (θ_4) which had six degrees of freedom for the sesquioxides has been split into two Einstein functions each having three degrees of freedom for $MgTiO_3$. The Debye characteristic

temperatures taken from Figs. 3 and 4 do not agree with the ones given above. This is due to the difference in masses of Mg and Ti. For $MnTiO_3$ and $FeTiO_3$ Debye temperatures taken from Figs. 3 and 4 should be acceptable since the difference in the masses of the cations is small. Two of the three Einstein temperatures and the value of "a" may be determined for $MnTiO_3$ and $FeTiO_3$ from their heat capacity results above 200^oK. The third Einstein temperature is assumed to be equal to 490^oK, since this is its value for $MgTiO_3$ and most of the sesquioxides. The lattice heat capacity of $MnTiO_3$ is given by

$$C_p = 4D(360/T) + 2D(410/T) + 3E(490/T) + 3E(590/T) + 3E(880/T) + (0.0021C_v)^2T$$

The lattice heat capacity calculated from the Debye-Einstein representation and the observed heat capacity are illustrated in Fig. 7. The magnetic heat capacity is illustrated in Fig. 8 and listed in Table 32 in Appendix I.

The magnetic entropy of $MnTiO_3$ is computed to be 3.51 e.u. which is in excellent agreement with R ln6 (3.56). Therefore, manganese is divalent and titanium is tetravalent in $MnTiO_3$. For $FeTiO_3$ Mossbauer experiments[74] have proved that Fe is divalent.

There is a significant magnetic contribution to the heat

Figure 7

Separation of Observed Heat Capacity of $MnTiO_3$ into Lattice and Magnetic Contributions

The upper curve represents the observed heat capacity. The lower curve represents the lattice heat capacity.

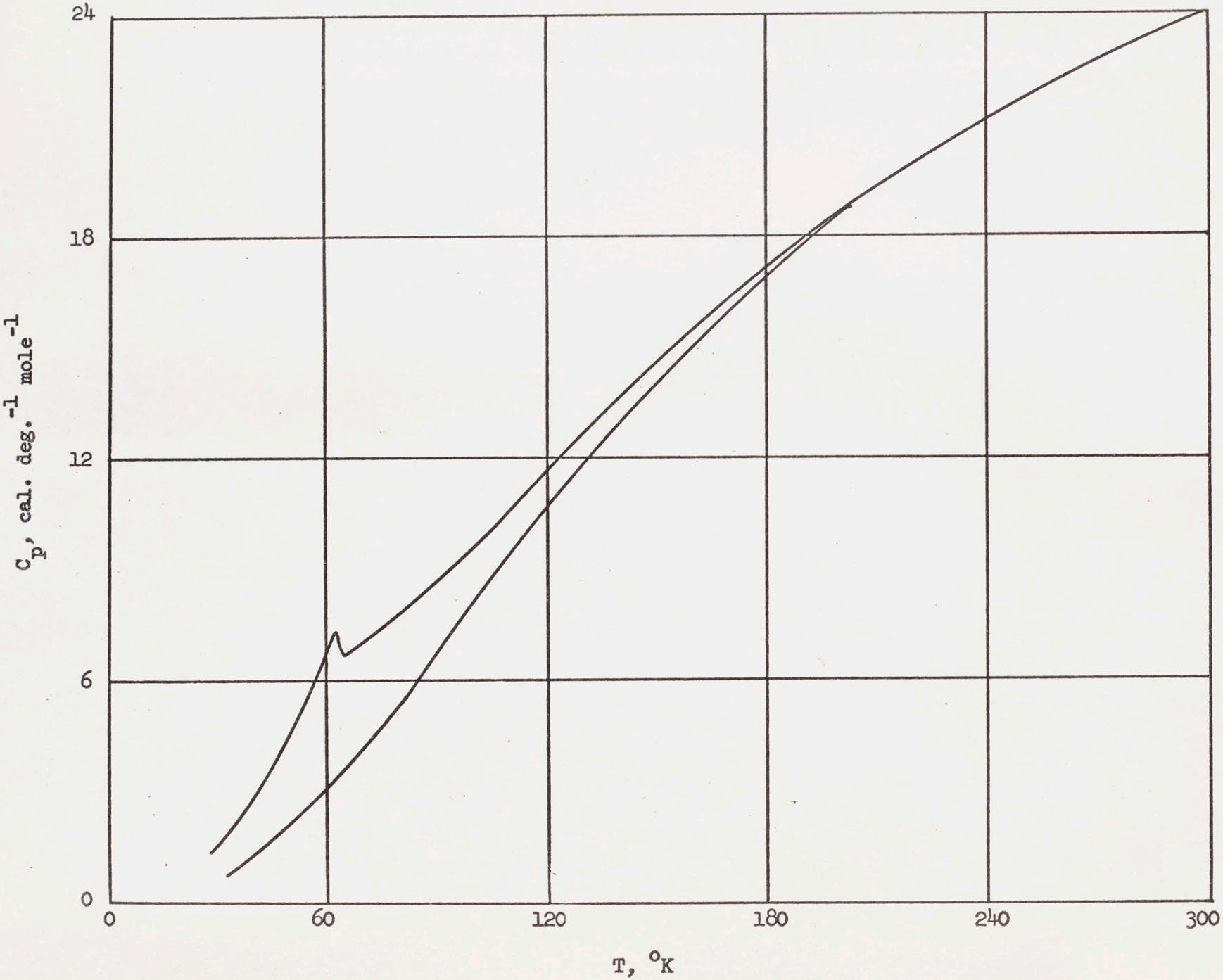
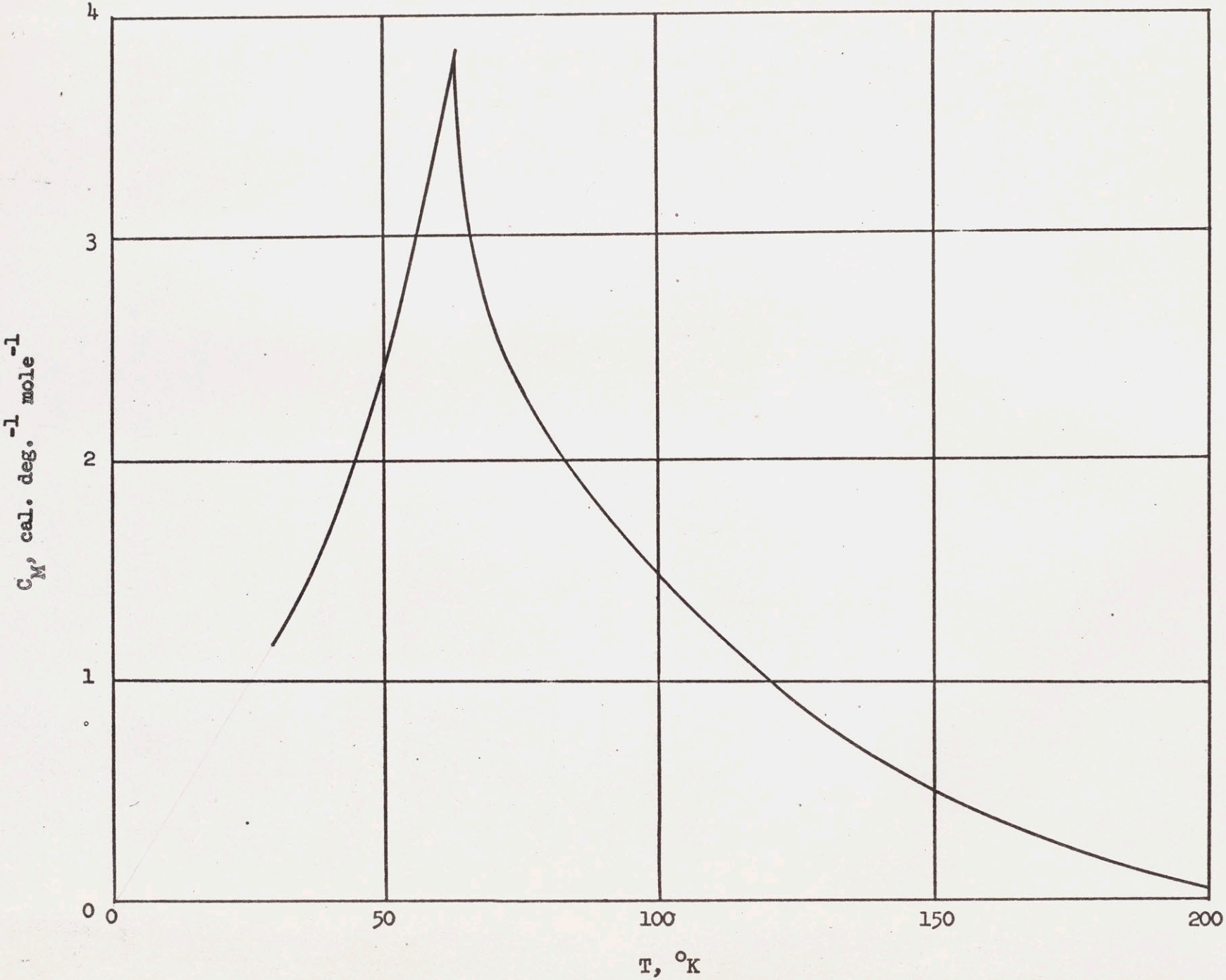

24
18
12
6
0
0
60
120
180
240
300
C_p, cal. deg.$^{-1}$ mole^{-1}
T, °K

Figure 8

Magnetic Heat Capacity of Manganese Titanate


4
3
2
1
0
0
50
100
150
200
C_M, cal. deg.$^{-1}$ mole^{-1}
T, °K

capacity above the Néel temperature. On Figure 9, the magnetic entropy is illustrated as a function of temperature for $MnTiO_3$. Only 55% of the magnetic entropy is acquired below the Néel temperature. The enthalpy associated with the cooperative effect is 223.5 calories. Only 37% of the enthalpy is acquired below the transition temperature.

The magnetic heat capacity computed for $MnTiO_3$ using the corresponding states method is in excellent agreement with that calculated using the Debye-Einstein representation. Below $70^{o}K$, the two methods agree to within 0.03 calories $degree^{-1}$ $mole^{-1}$ and above $70^{o}K$ they agree to within 0.12 calories $degree^{-1}$ $mole^{-1}$.

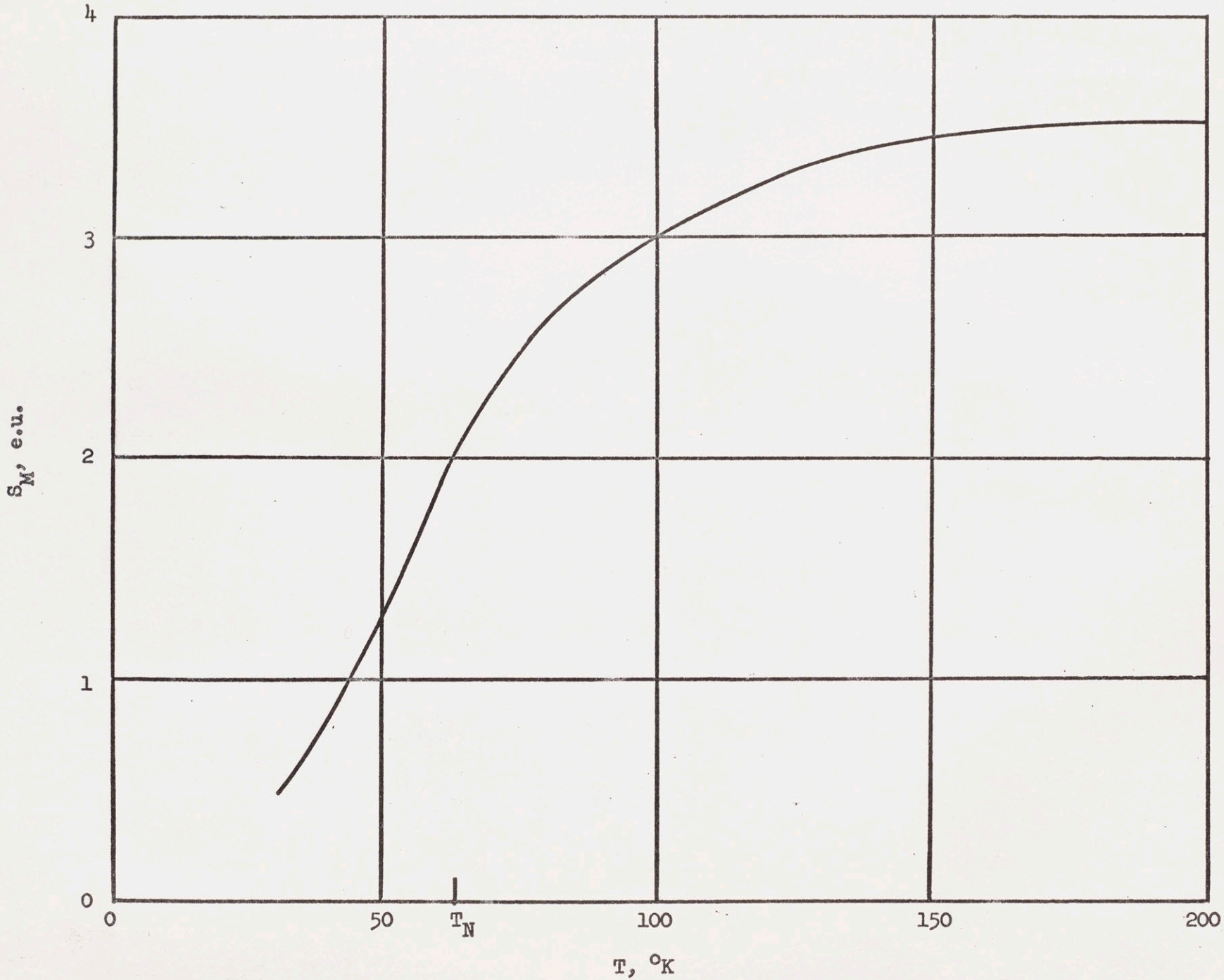
It is difficult to analyze the heat capacity results of $FeTiO_3$ because its heat capacity was measured down to only $55^{o}K$, which is just below the Néel temperature. The heat capacity results for $FeTiO_3$ did indicate substantial magnetic order above the Néel temperature ($S(\infty)-S(T_N)/R \ln(2S+1) = 0.48$). An analysis similar to that of $MnTiO_3$ is impossible, because of the lack of heat capacity data below $55^{o}K$.

Transition Metal Fluorides

The transition metal fluorides, MnF_2,[56] FeF_2,[57] CoF_2,[57] and NiF_2,[58] together with ZnF_2[2] and MgF_2[59] have a rutile structure. The heat capacities of the diamagnetic salts ZnF_2 and MgF_2 may be

Figure 9

Magnetic Entropy of Manganese Titanate


4
3
2
1
0
S_M, e.u.
0
50
T_N
100
150
200
T, °K

represented by

$$C_p = 3D(\theta_1/T) + 3E(\theta_2/T) + 3E(\theta_3/T) + (aC_v)^2T$$

The characteristic temperatures for the diamagnetic salts are given in Table 10. The Debye characteristic temperature has been determined

TABLE 10

Debye and Einstein Characteristic Temperatures for Transition Metal Fluorides

Compound	θ_1	θ_2	θ_3	a
ZnF_2	245	330	620	0.0023
MgF_2	337	450	700	0.0025
MnF_2	(245)	(297)	580	0.0028
NiF_2	(270)	(353)	700	0.0026
CoF_2	(275)	(340)	(630)	(0.0024)
FeF_2	(263)	(325)	(609)	(0.0026)

Numbers that are in parenthesis have been estimated.

$C_p = 3D(\theta_1/T) + 3E(\theta_2/T) + 3E(\theta_3/T) + (aC_v)^2T$

by Catalano[60] for both MnF_2 and CoF_2 in the liquid helium region where the magnetic heat capacity makes no contribution to the heat capacity. Usually the Debye characteristic temperature calculated from heat capacity data in the liquid helium region is higher than that calculated in the liquid hydrogen region. By assuming that the Debye temperatures (θ_1) of MnF_2 and CoF_2 are not less than 10° of that determined in the liquid helium region, θ_1 for MgF_2, CoF_2, and MnF_2 is a linear function of $\sqrt{M} \times V$. The Debye temperature (θ_1) of MnF_2 and CoF_2 estimated in this manner is $245^{\circ}K$ and $275^{\circ}K$ compared to $252^{\circ}K$ and $282^{\circ}K$ determined by Catalano in the liquid helium region. The Debye temperature (θ_1) of ZnF_2 does not lie on the line drawn to represent the Debye temperatures of MgF_2, MnF_2, and ZnF_2, but rather 20° below it. The Debye characteristic temperature of ZnF_2 calculated from individual heat capacity points is a rather sensitive function of temperature in the liquid hydrogen region. Usually, in the liquid hydrogen region the Debye characteristic temperature is not a sensitive function of temperature. The Debye characteristic temperature calculated for ZnF_2 at $15^{\circ}K$ is $263^{\circ}K$, which is the temperature expected from the θ_1 versus $\sqrt{M} \times V$ plot for the other fluorides. However, the heat capacity data as a whole is best represented by a θ_1 of $245^{\circ}K$. The assumption that θ_1 for MnF_2 and CoF_2 would be within $10^{\circ}K$ of the Debye temperature determined by Catalano in the liquid helium region would appear to be questionable

in light of the results for ZnF_2. However, if this assumption is invalid, then the entropy associated with the transition in MnF_2 and CoF_2 would be in poor agreement with the theoretical $R\ln(2S + 1)$, since the entropy associated with the transition is a very sensitive function of the Debye characteristic temperature θ_1. The magnetic entropy calculated using the parameters for MnF_2 is in excellent agreement with the theoretical $R\ln 6$, so the assumption would appear to be valid. CoF_2, likewise, gives good results.

The Einstein characteristic temperatures (θ_2) for the magnetic fluorides are estimated from the straight line representing θ_2 of MgF_2 and ZnF_2 as a function of $\sqrt{\mu} \times V$. If $\mu \times V$ were used rather than $\sqrt{\mu} \times V$, the resulting Einstein characteristic temperatures estimated for MnF_2 and FeF_2 give poor results for the entropy associated with the transition.

The Einstein characteristic temperature (θ_3) and "a" are determined for the magnetic fluorides, except CoF_2 and FeF_2, from the heat capacity results above $200^{\circ}K$. Since the Néel temperatures for these magnetic fluorides are below $80^{\circ}K$, it is safe to assume that there is little, if any, contribution of the magnetic heat capacity to the total heat capacity. The Einstein characteristic temperature (θ_3) is best expressed as a function of $\sqrt{\mu} \times V$.

The magnetic heat capacity makes a contribution to the total heat capacity of CoF_2 and FeF_2 up to room temperature. This is due

to the low lying orbital levels in Co^{+2} and Fe^{+2}. For CoF_2 and FeF_2, therefore, θ_3 is estimated from values of θ_3 of the other fluorides assuming θ_3 to be a linear function of $\sqrt{\mu} \times V$. The value of "a" is estimated using the values of "a" for the other fluorides as a guide. In computing the term $(aC_v)^2T$, C_v is usually assumed to be given by the Debye and Einstein functions alone, i.e. the magnetic heat capacity at constant volume is not included in C_v. Usually, this causes no serious difficulties, since the magnetic heat capacity makes significant contributions to the total heat capacity in temperature regions (below 120^oK) where $(aC_v)^2T$ is very small. In CoF_2 and FeF_2, however, the magnetic heat capacity at constant volume is included in C_v. In order to carry out the calculation of $(aC_v)^2T$ for CoF_2 and FeF_2, a method of successive approximations described by Orehotsky[21] was used. This procedure is not used for Cr_2O_3, which also has significant magnetic contributions to the heat capacity at room temperature, since for Cr_2O_3 there is a lambda-point near room temperature. In order to calculate an accurate value of $(C_p - C_v)$ a more sophisticated approach to the problem must be devised. This requires a knowledge of the thermal expansion and compressibility as a function of temperature. Since this data is not available, the calculation of $(C_p - C_v)$ for Cr_2O_3 does not include the magnetic heat capacity at constant volume. This obviously introduces uncertainties into the calculation of the magnetic heat capacity, but it does not

influence the magnetic entropy to any great degree.

The magnetic heat capacities of MnF_2, FeF_2, and CoF_2 are given in Tables 33, 34, and 35 respectively. An analysis of this data is left to the next chapter.

The magnetic entropy calculated for NiF_2 using the parameters in Table 10 does not agree with the theoretically predicted entropy. The nickel ion has a spin of one, so that the entropy associated with the magnetic transition should be R ln 3 (2.20 e.u.). The magnetic entropy calculated using the parameters in Table 10 is 1.4 e.u. This indicates a large error in one or more of the characteristic temperatures. This method of calculating magnetic heat capacities appears to fail for this salt.

Transition Metal Chlorides

The heat capacities of $MgCl_2$,[61] $CrCl_2$,[62] $CuCl_2$,[62] $MnCl_2$,[63-66] $ZnCl_2$,[67] $NiCl_2$,[68] and $CoCl_2$[63] have been measured. $MgCl_2$ and $ZnCl_2$ are diamagnetic; $CrCl_2$, $CuCl_2$, $NiCl_2$, and $CoCl_2$ are antiferromagnetic; and $MnCl_2$ is antiferromagnetic in the liquid helium region and paramagnetic at higher temperatures.

The heat capacity of $MnCl_2$ exhibits two peaks; one at 1.81°K and one at 1.96°K. Above 3.2°K the magnetic heat capacity of $MnCl_2$

is given by

$$C_M = 13.2/T^2 - 13.1/T^3 \qquad (6)$$

The lattice heat capacity of $MnCl_2$ above 10^oK can be calculated by subtracting from the total heat capacity the magnetic heat capacity calculated from (6). The lattice heat capacity of $MnCl_2$ may be represented by

$$C_p = 2D(\theta_1/T) + D(\theta_2/T) + 3E(\theta_3/T) + 3E(\theta_4/T) + (aC_v)^2T \qquad (7)$$

$MnCl_2$ is a hexagonal salt ($CdCl_2$ structure) belonging to the space group D^5_{3d}. As with the corundum structure compounds, it is necessary to split the Debye function into one with two degrees of freedom and one with a single degree of freedom.

$MgCl_2$ is isomorphous to $MnCl_2$ and its heat capacity may be represented by Eq. (7). $ZnCl_2$ exists in three polymorphic forms, one of which is isomorphous to $MnCl_2$. The heat capacity of $ZnCl_2$ cannot be represented by Eq. (7), but can be represented by

$$C_p = 3D(111/T) + 2E(166/T) + E(300/T) + 3E(445/T) + (0.0025C_v)^2T$$

Since this form is quite different from that of $MnCl_2$ and $MgCl_2$, the

results of $ZnCl_2$ are not used in estimating the lattice heat capacity of the magnetic chlorides.

$CoCl_2$ and $NiCl_2$ are isomorphous to $MnCl_2$. Both $CrCl_2$ and $CuCl_2$ have different structures, but they are similar to $MnCl_2$ in that they are layered compounds. The heat capacities of $CrCl_2$ and $CuCl_2$ should, therefore, be represented by Eq. (7). The Debye characteristic temperatures are estimated using $MnCl_2$ and $MgCl_2$ as guides.

The Debye characteristic temperatures (θ_1 and θ_2) are assumed to be linear functions of $\sqrt{M \times V}$. If M x V were used rather than $\sqrt{M \times V}$, the results for the magnetic entropy of $CoCl_2$ and $CuCl_2$ are poor with respect to the calculation of the magnetic entropy.

The Einstein characteristic temperature (θ_3) has the same value for both $MgCl_2$ and $MnCl_2$. Therefore, θ_3 is assumed to be equal to 220°K for $NiCl_2$ and $CoCl_2$. For $CrCl_2$ and $CuCl_2$ θ_3 is determined from the heat capacity results above 100°K. Since both of these compounds have transition temperatures below 25°K, the magnetic heat capacity should make no significant contribution to the total heat capacity above 100°K.

For $CrCl_2$, $CuCl_2$, and $NiCl_2$ "a" and θ_4 are determined from the heat capacity results above 200°K. However, $CoCl_2$ has magnetic contributions to the heat capacity up to room temperature, so that θ_3 and "a" must be estimated. The Einstein characteristic temperature, θ_3, is estimated by assuming that it is a linear function of $\sqrt{\mu \times V}$.

The calculation of $C_p - C_v$ term is the same as that described for CoF_2.

TABLE 11

Debye and Einstein Characteristic Temperatures

for Transition Metal Chlorides

Compound	θ_1	θ_2	θ_3	θ_4	a
$MnCl_2$	130	370	220	340	0.0028
$MgCl_2$	215	475	220	430	0.0029
$CoCl_2$	(173)	(422)	(220)	(369)	(0.0025)
$NiCl_2$	(194)	(448)	(220)	385	0.0027
$FeCl_2$	(163)	(410)	(220)	(365)	(0.0027)
$CuCl_2$	(153)	(406)	170	400	0.0024
$CrCl_2$	(141)	(382)	170	415	0.0020

Numbers that are in parenthesis have been estimated.

$$C_p = 2D(\theta_1/T) + D(\theta_2/T) + 3E(\theta_3/T) + 3E(\theta_4/T) + (aC_v)^2T$$

The magnetic heat capacities of $CrCl_2$, $CuCl_2$, and $CoCl_2$ are given in Tables 36, 37, and 38 respectively.

The entropy associated with the magnetic transition for $NiCl_2$ is 1.3 e.u. The spin of the nickel ion is one. Therefore,

the entropy associated with the transition should be Rln 3 (2.20 e.u.). One reason for this apparent failure of this method for calculating the magnetic heat capacity is that $NiCl_2$ has a c/a ratio which is about 20% higher than that of the other chlorides. The corresponding states method also does not work well for $NiCl_2$.[70]

Cupric Oxide

Cupric oxide is monoclinic. It is antiferromagnetic below 220°K. At very low temperatures (below 70°K), there is no appreciable magnetic contribution to the total heat capacity. The lattice heat capacity[71] of cupric oxide may be represented by

$$C_p = 2D(280/T) + D(440/T) + 3E(700/T) + (0.0024C_v)^2T \qquad (8)$$

The three characteristic temperatures are derived from the heat capacity data below 70°K. The Einstein characteristic temperature is somewhat uncertain, since it makes only a small contribution to the heat capacity at these low temperatures. The value of "a" is estimated from the values of "a" for other binary oxides. The magnetic entropy calculated using Eq. (8) to represent the lattice heat capacity is only about 0.40 e.u. The expected value of the magnetic entropy is Rln 2 (1.38 e.u.). At 300°K, the highest

temperature at which the heat capacity was measured, there is still a significant contribution to the total heat capacity by the magnetic heat capacity. However, the maximum contribution to the entropy associated with the cooperative effect above 300°K is a few tenths of an entropy unit. The lack of agreement between the expected calculated magnetic entropy is not due in this case to the parameters given in Eq. (8). This problem will be further discussed in the next chapter.

At 280°K the magnetic heat capacity begins to rise. This is apparently a Schottky effect. This rise in the heat capacity is a real effect, i.e. making small changes in the parameters in Eq. (8) will not eliminate the effect.

Summary

One of the limitations on the method presented here is the accuracy to which a sum of Debye and Einstein functions represent the heat capacity. In Table 12 the per cent error in the Debye-Einstein representation is presented in various temperature regions for the diamagnetic salts studied in this chapter. The error is always largest below 50°K. The largest error is usually less than 0.05 cal/deg/mole, but the heat capacity is quite small, making the per cent error large. Fe_2O_3 exhibits the largest percentage error

TABLE 12

Accuracy of Representing Heat Capacity Results

by Debye and Einstein Functions

Compound	Per Cent Error in Various Temperature Ranges				
	$0^{\circ}K$-$50^{\circ}K$	$50^{\circ}K$-$100^{\circ}K$	$100^{\circ}K$-$150^{\circ}K$	over $150^{\circ}K$	overall
Fe_2O_3	23.45	1.075	0.078	0.110	6.72
Al_2O_3	12.75	2.426	1.550	0.467	2.66
Ti_2O_3	-	1.167	0.105	0.315	0.45
ZnF_2	5.011	0.514	0.256	0.234	1.39
MgF_2	-	0.998	0.361	0.107	0.30
$MnCl_2$	1.116	0.296	0.164	0.181	0.43
$MgCl_2$	-	0.289	0.275	0.174	0.22
$MgTiO_3$	-	1.135	0.288	0.130	0.37

- means no heat capacity data. Representations given in chapter.

below $50^{\circ}K$. One reason for this is that its heat capacity in this temperature region is less than any of the other compounds listed in Table 12, with the exception of Al_2O_3.

In Table 13 the effect of slightly varying the characteristic temperatures of ZnF_2 is presented. The representation which best represents the heat capacity data below $50^{\circ}K$ and gives the best overall fit of the heat capacity data is chosen to represent ZnF_2.

TABLE 13

Accuracy of Various Debye-Einstein Representations for ZnF_2

Representation	Per Cent Error in Various Temperature Ranges				
	$0^{\circ}K$-$50^{\circ}K$	$50^{\circ}K$-$100^{\circ}K$	$100^{\circ}K$-$150^{\circ}K$	over $150^{\circ}K$	Overall
#1	5.011	0.514	0.256	0.234	1.385
#2	5.478	1.035	0.254	0.246	1.601
#3	7.117	0.295	0.432	0.221	1.842

#1 $C_p = 3D(245/t) + 3E(330/T) + 3E(620/T) + (0.0023C_v)^2T$

#2 $C_p = 3D(250/T) + 3E(320/T) + 3E(630/T) + (0.0024C_v)^2T$

#3 $C_p = 3D(240/T) + 3E(340/T) + 3E(610/T) + (0.0022C_v)^2T$

The Einstein characteristic temperatures varied only as a function of $\sqrt{\mu} \times V$, not $\mu \times V$. The Debye characteristic temperatures, on the other hand, varied as a function of $\sqrt{M} \times V$ sometimes and sometimes as a function of $M \times V$.

Representing the lattice heat capacity of magnetic compounds by a sum of Debye and Einstein functions that have been estimated from isomorphous diamagnetic compounds usually gives good results. One obvious advantage of this method over the other two methods mentioned earlier is that the entropy associated with the transition

is not considered as a given fact, but rather is considered an unknown. It has an advantage over the corresponding states method in that it can predict that lattice heat capacity at higher temperatures. This allows for a more complete analysis of such compounds as $CoCl_2$, CoF_2, and FeF_2. Cr_2O_3 and CuO could not be attacked by the corresponding states method, but can be undertaken using the method outlined in this chapter.

One assumption that has been made is that the density of all the isomorphous compounds behave in the same way as a function of temperature. Debye and Einstein characteristic temperatures are determined at very low temperatures, but the densities used to calculate the molar volumes have been determined at room temperature. This assumption might contribute to the failure of the Debye-Einstein method in the cases of NiF_2 and $NiCl_2$.

A disadvantage of this method is that extreme care must be exercised in examining the results of the method, e.g. in the cases of NiF_2 and $NiCl_2$. Another disadvantage is that a good deal of heat capacity data must be available in order to use the method. Such compounds as $CrCl_3$ and CrF_3 cannot be studied because no isomorphous diamagnetic compounds have had their heat capacity measured. The cubic oxides give very poor results using this method, but again a lack of experimental data might be the cause. Only in one case has the heat capacity of a cubic oxide been measured below $50^{o}K$. Analysis of heat capacity results only above $50^{o}K$ is more difficult

than when the heat capacity measurements have been carried out down to liquid hydrogen temperatures. Without data in the liquid hydrogen region, it is difficult to determine unambiguously the value of the Debye characteristic temperature.

For the transition metal fluorides and chlorides the heat capacities of only two diamagnetic salts have been measured. This presents difficulties because it is impossible to make an a priori decision as to the correct functional dependence of the characteristic temperatures. Instead, the correct functional dependence must be determined by considering which dependence gives better results with respect to the magnetic entropy.

IV. DISCUSSION OF MAGNETIC HEAT CAPACITY RESULTS

The Weiss Molecular Field Model does not predict short range order effects, so that there is no magnetic heat capacity above the Néel temperature according to it. Oguchi[25] has proposed an extended Molecular Field Theory which does predict a magnetic heat capacity above the Neel temperature. The Oguchi Theory considers the interaction of two spins exactly. The interaction of the rest of the system with these two spins is treated by an effective field approximation. The Hamiltonian of this two spin system is

$$\mathcal{H} = 2|J|(\vec{S}_i \cdot \vec{S}_j) - 2|J| \left\{ \sum_k (\vec{S}_k \cdot \vec{S}_1) + \sum_1 (\vec{S}_1 \cdot \vec{S}_j) \right\} \tag{9}$$

where J is the exchange integral and $\sum_k$ and $\sum_1$ are taken over the nearest neighbors of i-spin (except j-spin) and j-spin (except i-spin) respectively. The spin i is on the plus sublattice and j is on the minus sublattice. Though $\vec{S}_k$ and $\vec{S}_1$ are operators, they are replaced by their thermal mean expectation value $\langle S \rangle$. The z-axis is taken as the axis of the crystal, so that the expectation values of $\vec{S}^x$ and $\vec{S}^y$ vanish.

$$\mathcal{H} = 2|J| \quad (\vec{S}_i \cdot \vec{S}_j) + a\, \vec{S}_i^z + b\, \vec{S}_j^z$$

where $a = -2|J|(z-1)\langle S\rangle$

$b = 2|J|(z-1)\langle S\rangle$

where z is the number of nearest neighbors. Oguchi only considered the case where the spins are ½. The eigenfunctions for this system are

$$\psi_1^1 = \alpha_i\alpha_j$$

$$\psi_1^0 = \frac{1}{\sqrt{2}}(\alpha_i\beta_j + \beta_i\alpha_j) \qquad (11)$$

$$\psi_1^{-1} = \beta_i\beta_j$$

$$\psi_o^o = \frac{1}{\sqrt{2}}(\alpha_i\beta_j - \beta_i\alpha_j)$$

The subscript attached to ψ denotes $\vec{S}_i + \vec{S}_j$ and the superscripts attached to ψ denotes its z component and α and β represent the plus and minus spin function. The secular equation becomes

$$\mathcal{H} = \begin{vmatrix} |J| + a + b & 0 & 0 & 0 \\ 0 & |J| & 0 & a-b \\ 0 & 0 & |J| - a-b & 0 \\ 0 & a-b & 0 & -3|J| \end{vmatrix}$$

The eigenvalues are

$$E_1 = \tfrac{1}{2}|J|$$

$$E_2 = -\tfrac{1}{2}|J| + |J|\,r \qquad (12)$$

$$E_3 = \tfrac{1}{2}|J|$$

$$E_4 = \tfrac{1}{2}|J| - |J|\,r$$

where

$$r = [1 + 4(z - 1)^2 \langle S \rangle^2]^{\frac{1}{2}}$$

The thermal mean expectation value $\langle S \rangle$ is determined from the partition function Z.

$$Z = \sum_i e^{-\epsilon_i/kT}$$

$$\langle S \rangle = \frac{\partial \ln Z}{\partial H} \tag{13}$$

$$\langle S \rangle = \frac{(z - 1)\langle S \rangle \sinh\left(\frac{|J|r}{kT}\right)}{r\left[e^{-|J|kT} + \cosh\frac{|J|r}{kT}\right]}$$

Oguchi applied this theory to $CuCl_2 \cdot 2H_2O$. In the antiferromagnetic state each cupric ion has two nearest neighbors antiferromagnetically aligned and four next-nearest neighbors ferromagnetically aligned. Oguchi assumed that the short range order was due only to the antiferromagnetic interaction of nearest neighbor cupric ions. The Hamiltonian for the two nearest neighbor cupric ions i and j is

$$\mathcal{H} = 2|J|\vec{S}_i \cdot \vec{S}_j + 2|J|\left\{(\langle S_j \rangle - 4\lambda \langle S_i \rangle)\vec{S}_i^z + (\langle S_i \rangle - 4\lambda \langle S_j \rangle)\vec{S}_j^z\right\} \tag{14}$$

where $\lambda = \frac{J'}{|J|}$, J' is the ferromagnetic exchange parameter. Comparing this Hamiltonian with the one written earlier, the expression for $\langle S \rangle$ follows directly from (13)

$$\langle S \rangle = \frac{(1 + 4\lambda)\langle S \rangle}{r} \frac{\sinh (|J|r/kT)}{(e^{-|J|/kT} + \cosh|J|r/kT)} \tag{15}$$

Below the transition temperature Oguchi showed that this extended molecular field theory did little better than the Weiss molecular field model. However, above the transition temperature, the extended molecular field model did a credible job. Above the Néel temperature r = 1. The heat capacity derived from the partition function is

$$C = \frac{3Rx^2}{(e^{-x} + \cosh x)}$$
$$x = |J|/kT \tag{16}$$

Using (15), Oguchi derived a relation for J'

$$e^{|J|/kT_N} = \frac{4 + z'\lambda}{z'\lambda} \tag{17}$$

where z' is the number of second nearest neighbors.

This extended molecular field model is able to represent the heat capacity of $CuCl_2 \cdot 2H_2O$ above the Néel temperature. However, it

cannot give a good representation of the heat capacity below the Néel temperature.

For a system of two magnetic ions with a spin greater than ½, the solution of the secular equation below the Néel temperature is a formidable problem. The Hamiltonian has off-diagonal matrix elements below the transition temperature, but above the Néel temperature the Hamiltonian is diagonal. The partition function for a two spin system above the Néel temperature is

$$Z = \sum_i g_i e^{-\epsilon_i/kT} = \sum_{S'=0}^{S'=2S} (2S'+1)\, e^{-\beta[S'(S'+1)-2S(S+1)]J}$$

$$\beta = \frac{1}{kT}$$

Using the equation

$$C = -R \frac{\partial}{\partial T} \left(kT^2 \frac{\partial \ln Z}{\partial T}\right)$$

the heat capacity for the two spin system can be determined.

$$C = \frac{R\beta^2 J^2}{Z^2} \left\{ \sum_{S'=0}^{2S} (2S'+1)\, e^{-f(S')\beta J} \sum_{S'=0}^{2S} f^2(S')\, (2S'+1)\, e^{-\beta J f(S')} - \left(\sum_0^{2S} f(S')\, (2S'+1)\, e^{-\beta f(S')J} \right)^2 \right\}$$

where

$$f(S') = S'(S' + 1) - 2S(S + 1)$$

Compounds with Magnetic Transitions in the Liquid Helium Temperature Region

The magnetic heat capacity of a number of compounds with transitions in the liquid helium temperature region have been determined using the method described in the previous chapter. The Oguchi Theory has been applied to these compounds in order to determine the exchange parameters of these compounds from the heat capacity results above the Néel temperature. The exchange parameters are given in Table 14. In order to evaluate the parameters the number of nearest neighbor interactions must be known. In some cases the number of nearest neighbor interactions had to be estimated since the magnetic structure of the compound had not been determined. The exchange parameters have also been calculated using the following relationship derived from the simple molecular Weiss Molecular Field Model:

$$E = zS^2|J|/k$$

where E is the total magnetic energy.

The Oguchi Theory gives a good representation of the heat capacity above the transition temperature for compounds whose Néel temperature is in the liquid helium region.

TABLE 14

Exchange Parameters for Magnetic Compounds With Neel Temperatures Below $10^{o}K$

	$T_N(^oK)$	z	$\frac{S(\infty) - S(T_N)}{R\ln(2S+1)}$	J/k (^oK) Oguchi Theory	J/k (^oK) Weiss Model	Reference for Heat Capacity Data
$MnCl_2$	1.96	2	0.32	-0.24	-0.32	66
$MnBr_2$	2.16	2	0.50	-0.32	-0.44	46
$NiCl_2 \cdot 6H_2O$	5.27	2	0.58	-2.15	-2.76	35
$MnCl_2 \cdot 4H_2O$	1.62	2	0.86	-0.10	-0.19	37
$MnBr_2 \cdot 4H_2O$	2.14	2	0.81	-0.18	-0.28	39

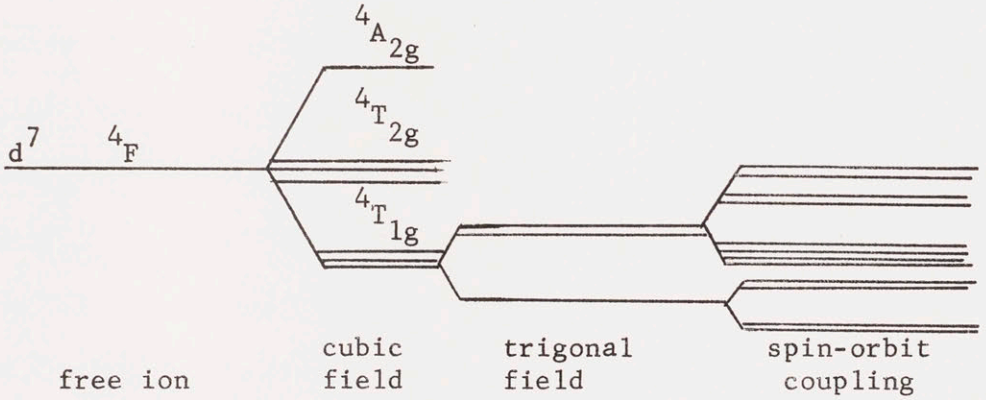
TABLE 15

Exchange Parameters for Magnetic Compounds with Spin ½

	$T_N(^oK)$	z_1	z_2	J_1/k (^oK) Oguchi Theory	J_1/k (^oK) Weiss Model	J_2/k (^oK) Oguchi Theory	Reference for Heat Capacity Data
$CoCl_2 \cdot 6H_2O$	2.25	2	4	-2.0	-4.9	0.41	35
$CoBr_2 \cdot 6H_2O$	3.08	2	4	-2.4	-5.5	0.65	33
$CuCl_2 \cdot 2H_2O$	4.3	2	4	-3.22	-	0.97	36
$LiCuCl_3 \cdot 2H_2O$	4.40	2	2	-4.1	-9.9	1.5	40
$CoCl_2$	24.7	3	9	-	24.3		63
CoF_2	37.7	8	2	-10.3	-13.0	30.7	57
$CuCl_2$	23.9	8	2	-14.	-11.5	14	62

Hydrated Cobalt Salts

In a cubic field the ^4F state of Co^{+2} splits into two orbital triplets and one orbital singlet. The lowest state is triply degenerate. The triplet splits into a doublet and singlet in a trigonal field. If the perturbation of spin-orbit coupling is taken into account the two lowest orbital levels (doublet and singlet) split into six Kramers doublets.



The splitting between the lowest Kramers doublet and the next higher one is usually large (greater than 100 cm^{-1}), so that the effective spin of Co^{+2} is ½ rather than 3/2.

The entropy associated with the magnetic transitions in $CoCl_2 \cdot 6H_2O$ [35] and $CoBr_2 \cdot 6H_2O$ [33] is about 1.4 e.u. (Rln2). The heat

capacities of these salts have been measured up to 20°K. Up to this temperature there is no indication of a Schottky effect. The two largest exchange parameters for these salts may be computed using the equations derived by Oguchi for an antiferromagnet with a spin of ½. The exchange parameters for $CoCl_2 \cdot 6H_2O$ given in Table 15 are in good agreement with the exchange parameters evaluated for this salt using the Ising model.[78]

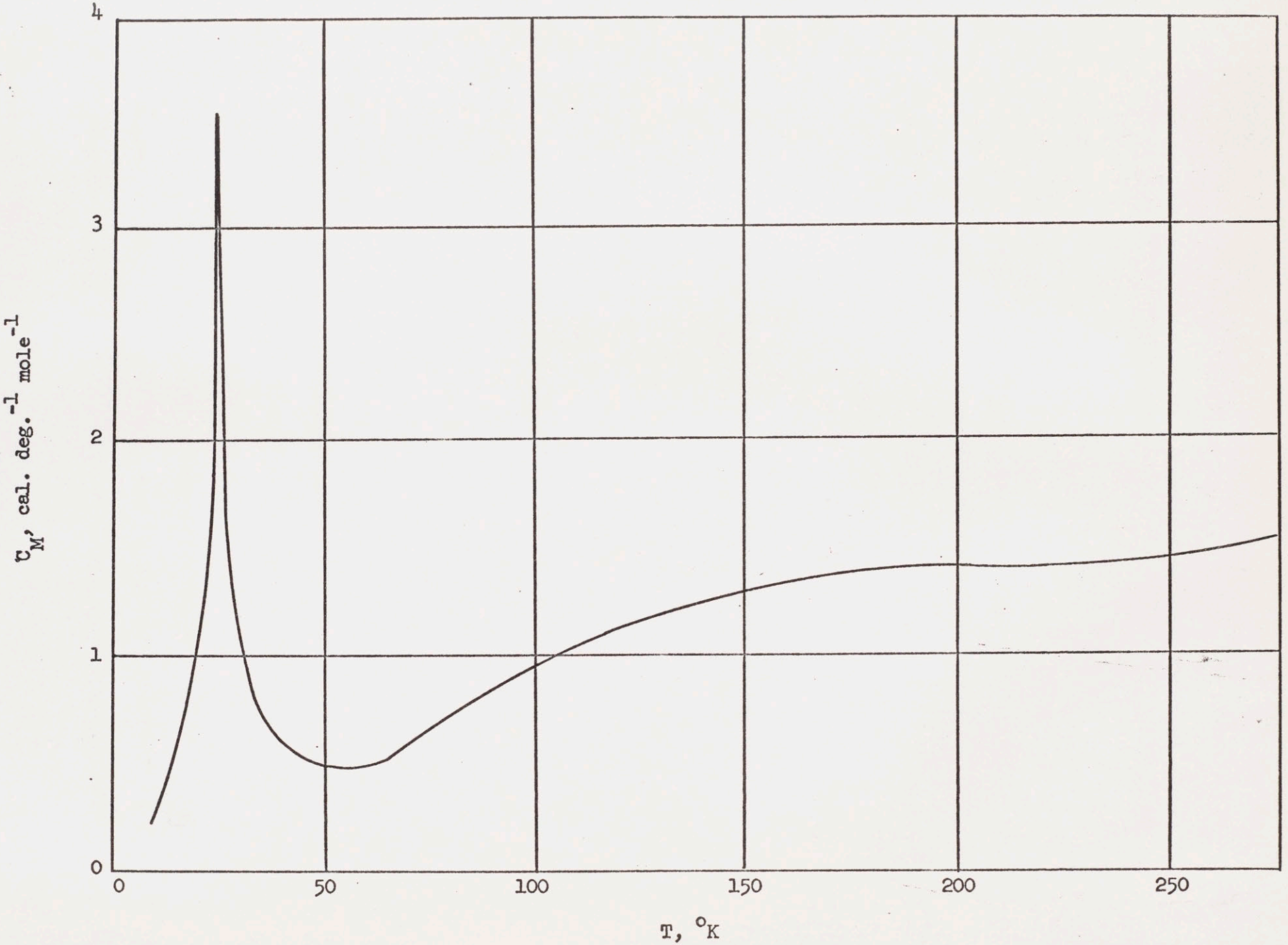
The number of nearest and next-nearest neighbors in a number of the hydrated salts listed in Table 14 and Table 15 are uncertain. An error in the number of nearest neighbors in these salts would have a different effect on the results determined from the Weiss Model and the results determined from the Oguchi Model. Therefore, it is difficult to determine whether the discrepancies between the two models in the determination of the exchange parameters are real or are due to an error in the number of nearest neighbors.

Cobalt Chloride

The magnetic heat capacity of cobalt chloride exhibits both a cooperative and a non-cooperative (Schottky) effect (Figure 10). In order to separate these two effects it is necessary to know the energy spacings of the six Kramers doublets. These energy levels may be determined from the heat capacity results above 100°K where the

Figure 10

Magnetic Heat Capacity of Cobalt Chloride


4
3
2
1
0
0
50
100
150
200
250
C_M, cal. deg.$^{-1}$ mole^{-1}
T, °K

cooperative effect makes no significant contribution to the magnetic heat capacity.

Lines[79] has been able to predict the energies of the Kramers doublest in $CoCl_2$ by using crystalline field theory. He expressed the energies of the doublets in terms of one parameter λ, which is related to the spin-orbit coupling parameter.

$$E_i = a_i\lambda \tag{18}$$

E_i is the energy of the i-th doublet and a_i is a constant determined by Lines for each doublet. Using magnetic susceptibility results for $CoCl_2$,[80] Lines was able to compute a value for λ of 158 cm^{-1}.

The magnetic heat capacity results above 100°K could not be represented by the energy levels determined by Lines. The energy spacings between the lowest three doublets may be determined unambiguously from the magnetic heat capacity results. The energies of the three lowest doublets are 0, 205, and 425 cm^{-1}, where the lowest levels has been given a value of zero. The energies of the upper three doublets cannot be determined from the heat capacity results because the energies are too close to each other. Assuming that the energies of the upper three doublets are given by (18), then the energies of the upper three levels may be determined from the heat capacity results by considering λ as an empirical parameter. Using the values of a_i for the upper three levels theoretically determined

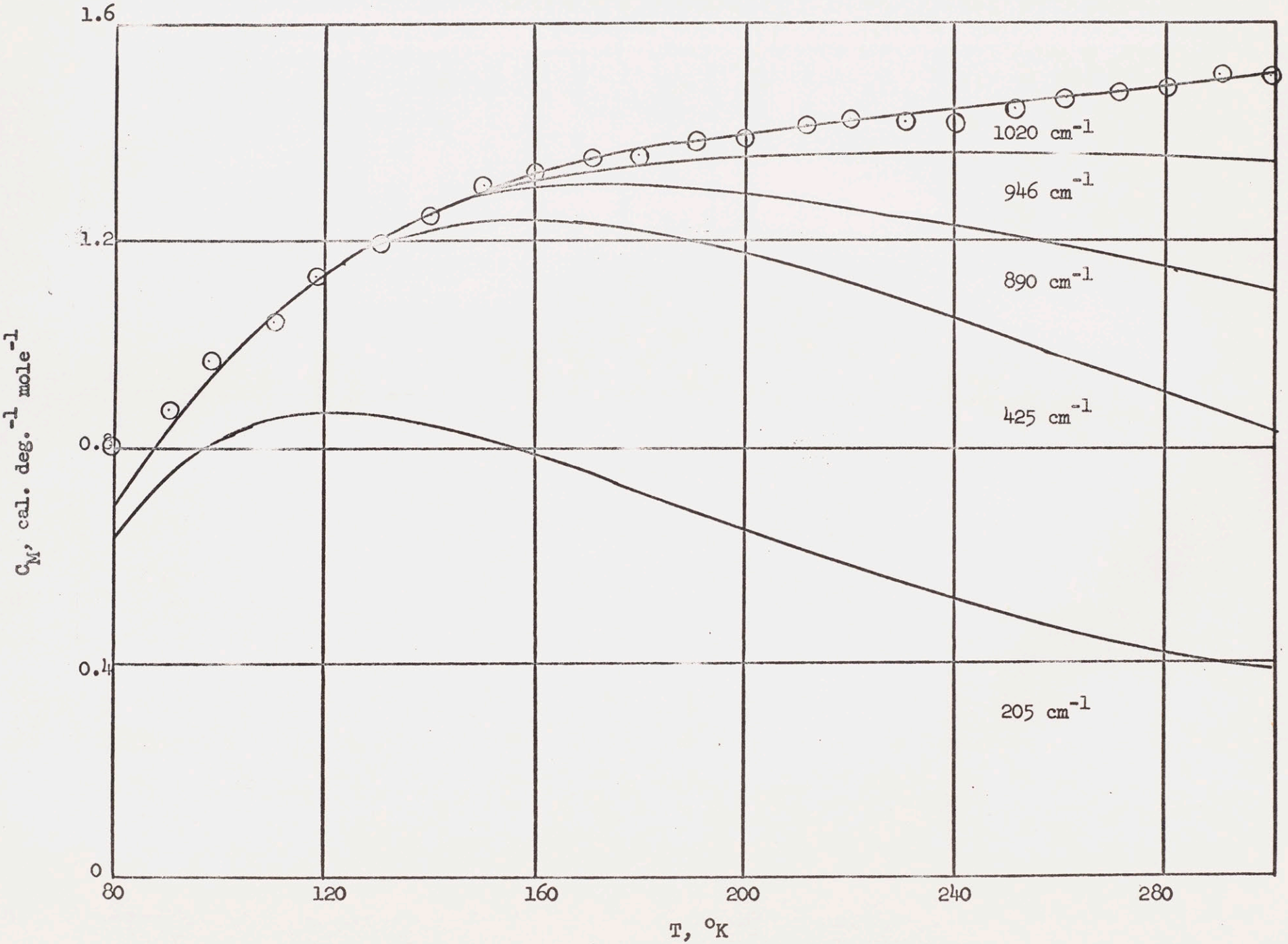
by Lines, the heat capacity results can be reproduced by the following energy levels: 0, 205, 425, 890, 946, and 1020 cm^{-1} (Figure 11). The value of λ used to determine the energies of the upper three levels which would give the best representation of the heat capacity, is 153 cm^{-1}. If a value of λ of 153 cm^{-1} were used to determine the energies of all the doublets using the values of a_i determined by Lines, the following energy levels would result: 0, 271, 432, 890, 946, and 1020 cm^{-1}. If the value of 153 cm^{-1} is assumed to be correct, the energy of the second level above the ground doublet is correctly predicted by Lines. Only the energy spacing between the lowest two doublets was incorrectly determined by the energy level scheme proposed by Lines.

The contribution of the Kramers doublets to the magnetic heat capacity of $CoCl_2$ is illustrated in Figure 11. Once the energy levels are known, the contribution to the heat capacity of the cooperative and non-cooperative effects may be separated. The individual contributions of both effects are given in Table 38 in Appendix I. The tail of the cooperative effect cannot be reproduced by the Oguchi model, because the tail is too steep. However, a small error in the energy spacing between the lowest two Kramers doublets would have a significant effect on the heat capacity of the tail of the cooperative effect. Lines evaluated the exchange parameters in $CoCl_2$ using Green function techniques. The value of J_1/k is 20.8° and J_2/k is -1.79°. The

Figure 11

The Contribution of the Six Kramers Doublets to the Magnetic Heat Capacity of $CoCl_2$ above $100^{o}K$

⊙ represent observed magnetic heat capacity


1.6
1.2
0.8
0.4
0
80
120
160
200
240
280
C_M, cal. deg.$^{-1}$ mole^{-1}
T, °K
1020 cm^{-1}
946 cm^{-1}
890 cm^{-1}
425 cm^{-1}
205 cm^{-1}

stronger of the two interactions is the superexchange interaction between magnetic ions on the same hexagonal layer. This is a ferromagnetic interaction. The weaker exchange interaction is between magnetic ions on adjacent hexagonal layers and is antiferromagnetic.

Cobalt Fluoride

The magnetic heat capacity of cobalt fluoride, like that of cobalt chloride, exhibits both a cooperative and a non-cooperative effect (Figure 12). From the magnetic heat capacity results above $100^{o}K$ it is possible to determine the energies of the Kramers doublets. The energies of the four lowest Kramers doublets are: 0, 153, 750, and 1300 cm^{-1}. The upper two Kramers doublets do not make any contribution to the heat capacity below room temperature. The individual contribution of each energy level to the magnetic heat capacity is illustrated in Figure 13. In Table 35 in Appendix I the heat capacity of the cooperative and the non-cooperative effects are given.

The Oguchi theory gives a fair representation of the magnetic heat capacity tail. The exchange parameters determined from the Oguchi model are $J_1/k = 10.3^{o}$ and $J_2/k = 30.7^{o}$. Although J_2 is greater than J_1, z_1J_1 is greater than z_2J_2.

Figure 12

Magnetic Heat Capacity of Cobalt Fluoride

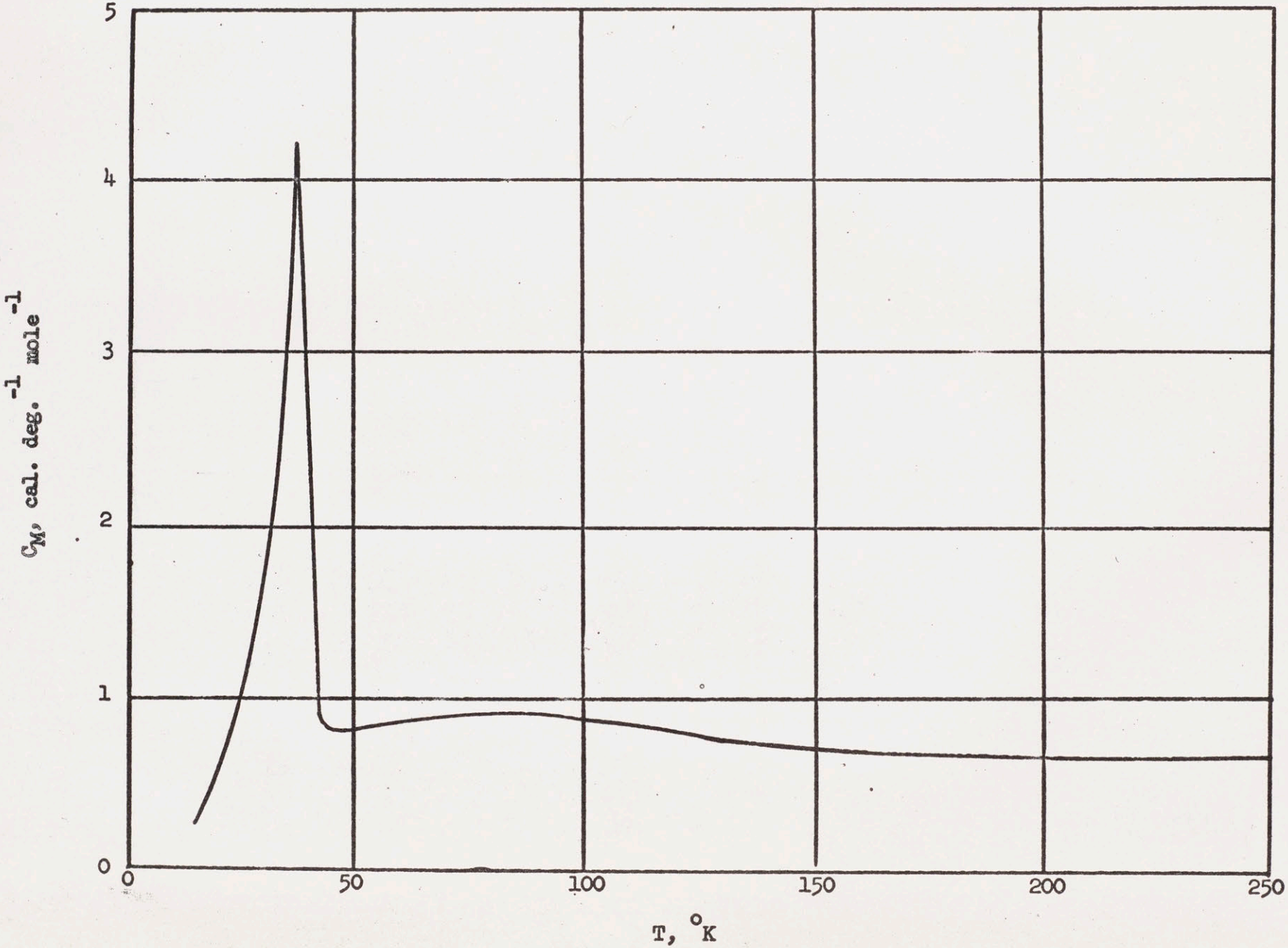
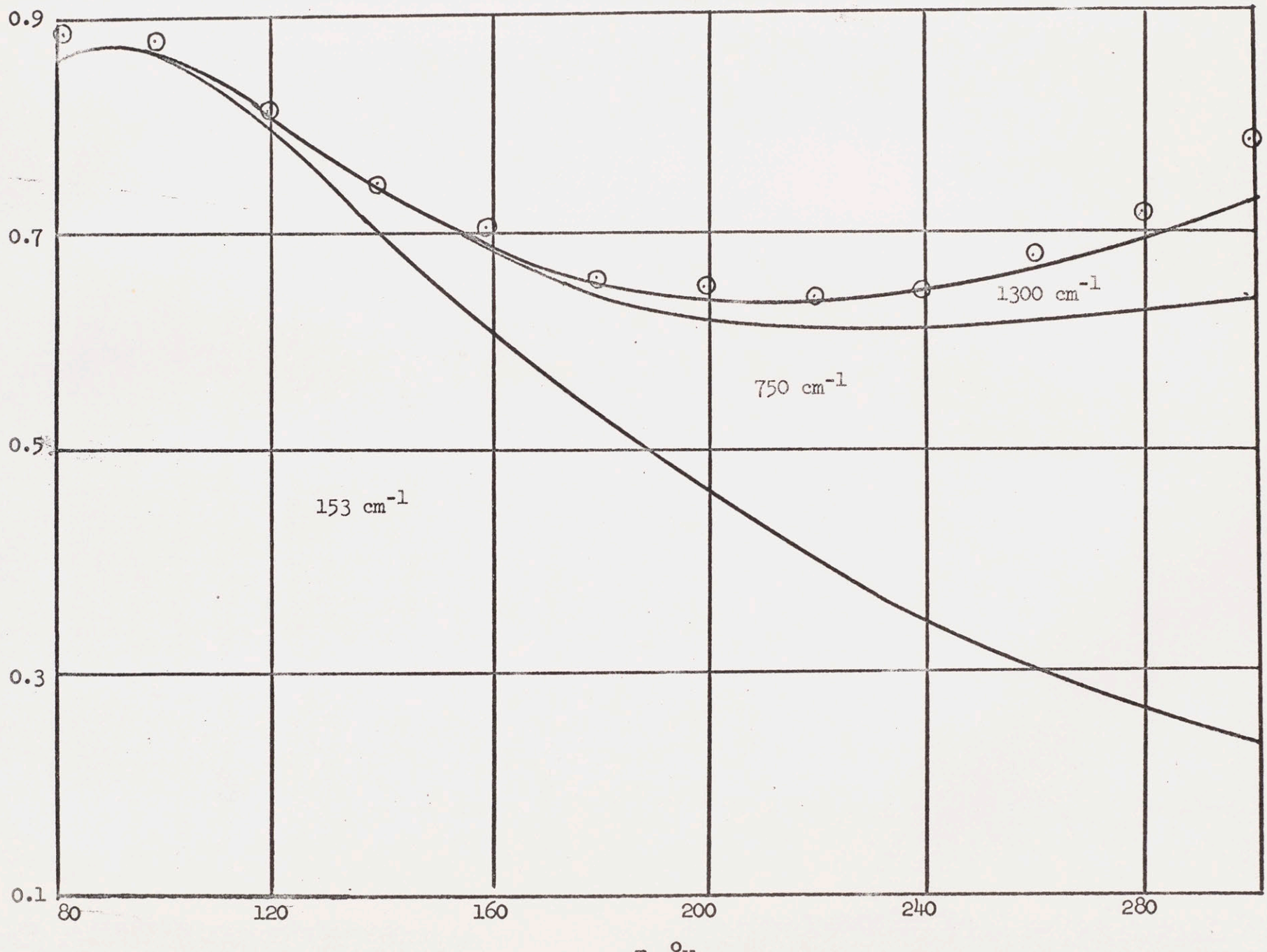

5
4
3
2
1
0
0
50
100
150
200
250
C_M, cal. deg.$^{-1}$ mole^{-1}
T, °K

Figure 13

The Contribution of the Kramers Doublets to the Magnetic Heat Capacity of CoF_2 Above $100^{o}K$

$\odot$ represents observed magnetic heat capacity


0.9
0.7
0.5
0.3
0.1
80
120
160
200
240
280
C_M, cal. deg.$^{-1}$ mole^{-1}
T, °K
153 cm^{-1}
750 cm^{-1}
1300 cm^{-1}

Cupric Chloride and Chromous Chloride

In both $CuCl_2$ and $CrCl_2$ there is a slight anomaly above the Néel temperature. This is due to the arrangement of the magnetic ions in these salts. The metal ion is surrounded by six chloride ions, which are greatly distorted from a regular octahedron. Four of the chloride ions are considerably nearer to the metal ion than the other two chloride ions. These four chloride ions link the metal ions together in linear chains, running parallel to each other. The anomaly above the transition temperature is due to the strong antiferromagnetic interactions between the metal ions in a one-dimensional chain. At lower temperatures, long-range order develops due to the interactions between neighboring chains.[62]

The Oguchi model does not reduplicate the small hump in the heat capacity above the transition temperature in these salts. However, for temperatures above the small anomaly the Oguchi model does give a fair representation of the magnetic heat capacity.

Chromic Oxide

As mentioned in the last chapter, the entropy associated with the antiferromagnetic transition is one-half the expected value. In order to explain this fact, it is necessary to assume that there are

two different important magnetic interactions in Cr_2O_3; the superexchange interaction between magnetic ions on different hexagonal layers (A_1B_1 and A_2B_1 in Figure 14) and the interaction between nearest-neighbor chromium ions along the c-axis of the rhombohedral unit cell (A_1B_2 or B_2A_1 in Figure 14b and AB in Figure 14a). Below the Néel temperature Cr_2O_3 is antiferromagnetic due to the superexchange interaction between magnetic ions on different hexagonal layers. Above the Néel temperature the long-range order has been destroyed, i.e. there is no ordering between the chromic ion pairs. However, the direct interaction between nearest-neighbor chromium ions along the c-axis is not destroyed above the Néel temperature. This interaction does not produce long-range order. The entropy associated with the transition from a completely ordered state to a state in which only the Cr ions of a Cr-Cr pair are correlated is one-half that of a transition from an ordered to a completely disordered state.

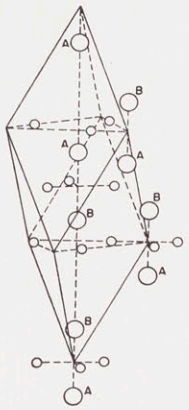
From the antiferromagnetic properties of Cr_2O_3 the nearest-neighbor pairs of chromium ions are expected to be coupled antiferromagnetically.[81] An S = 0 state is the lowest state for this pair of ions and is the only one occupied at sufficiently low temperatures. There are three states above the ground state with a total spin of S = 3, 2, and 1. There is no indication of the next lowest level being occupied below 350°K from the heat capacity results. High temperature magnetic susceptibility results show that the susceptibility

Figure 14

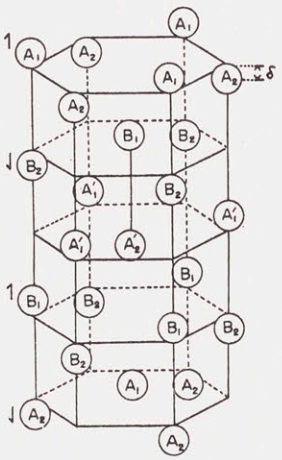
Crystal Structure of Corundum Compounds

a. Rhombohedral Unit Cell

b. Hexagonal Unit Cell


A
B
A
A
B
B
A
B
A

(a)


A1
A1
A2
A1
A2
δ
A2
B1
B2
B2
B2
A'1
A'1
A'2
A'2
B1
B1
B2
B1
B2
B2
A1
A2
A2
A2

(b)

is increasing as the temperature increases.[82] This is an indication of a Schottky anomaly. Results of electron spin resonance[83] and magnetic susceptibility[84] measurements on ruby indicate that the nearest-neighbor chromium ions in a Cr-Cr pair are strongly coupled.

Thus, the chromic oxide an entropy change of Rln 4 rather than 2Rln 4 may be explained by assuming that above the Néel temperature there is antiferromagnetic coupling between nearest-neighbor chromium ions in Cr-Cr pairs, but no coupling between different Cr-Cr pairs.

Cupric Oxide

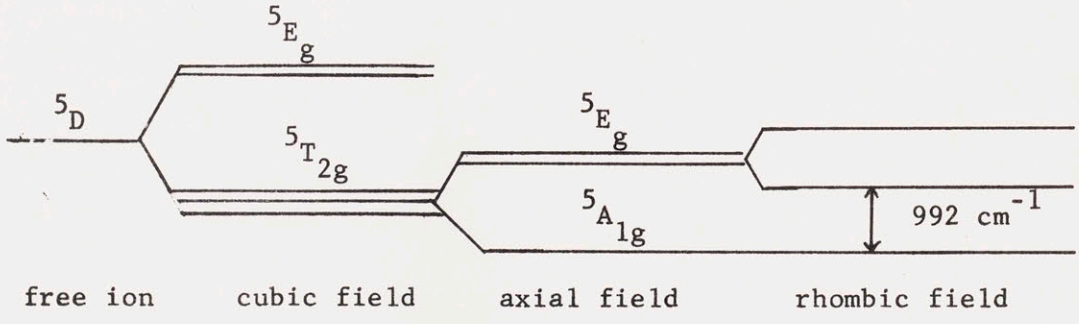
The entropy associated with the magnetic transition in cupric oxide is much less than Rln 2. The magnetic susceptibility also exhibits anomalous results.[85] At about 540°K the magnetic susceptibility exhibits a broad maximum. There is no anomaly in the magnetic susceptibility at the Néel temperature 228°K. These results were interpreted by O'Keeffe and Stone[85] in terms of antiferromagnetic superexchange, characterized by a Néel temperature of 228°K, and a direct spin coupling with an energy of 730 cm^{-1}. They assume two cupric ions, each with one unpaired electron, interact to form a singlet ground state (S = 0) and a higher triplet (S = 1). If the anomaly at 228°K is a transition from a completely ordered state to a state in which nearest-neighbor cupric ions are correlated, but no

coupling between different pairs of cupric ions, then the entropy change is $\frac{1}{2}R\ln 2$. This entropy change is in reasonable agreement with that determined in the last chapter. Therefore, the case of cupric oxide is analogous to that of chromic oxide.

Between 260°K and 300°K the magnetic heat capacity begins to rise because the S = 1 state is being occupied. The separation between the ground state (S = 0) and the triplet state is 1400 $cm^{-1} \pm 150\ cm^{-1}$ according to the magnetic heat capacity results. The energy separation determined from magnetic susceptibility data is 730 cm^{-1}.

Ferrous Fluoride and Manganous Fluoride

FeF_2 has a Néel temperature of 78.35°K. The tail of the magnetic heat capacity cannot be reproduced by the Oguchi model. Above 200°K the magnetic heat capacity of FeF_2 begins to increase. This is due to the occupation of a higher orbital state at 992 cm^{-1} above the ground state. The energy level splittings for Fe^{+2} is given below.



The energy separation between the two levels determined from heat capacity results is in good agreement with the energy separation determined from Mossbauer experiments (1028 cm^{-1},[86] 1000 cm^{-1}[87]).

The Oguchi model does not reproduce the tail of the magnetic heat capacity of MnF_2. The failure of the model for both FeF_2 and MnF_2 may be due to the fact that the model does not usually apply unless $T > 1.5\ T_N$ (T_N is Néel temperature). For magnetic compounds whose Néel temperature is in the liquid helium region, the temperature difference between T_N and $1.5\ T_N$ is small so that there is a wide temperature range above $1.5\ T_N$ where the magnetic heat capacity makes a rather large contribution to the total heat capacity. However, for those magnetic compounds with Néel temperatures in the liquid nitrogen region, the contribution of the magnetic heat capacity to the total heat capacity is quite small for temperatures greater than $1.5\ T_N$. Therefore, there is a greater uncertainty in the magnetic heat capacity above $1.5\ T_N$ for compounds with $T_N > 30^{\circ}K$ than for compounds with $T_N < 10^{\circ}K$. This is a possible explanation why the Oguchi model reproduces the tail of the magnetic heat capacity for compounds with $T_N < 10^{\circ}K$, but not for compounds with $T_N > 30^{\circ}K$.

TABLE 16

Exchange Parameters for Magnetic Compounds with Néel Temperatures Above $10^{o}K$

	$T_N(^{o}K)$	z	$\frac{S(\infty) - S(T_N)}{R\ln(2S+1)}$	J/k Weiss Model	Reference for Heat Capacity Data
NiF_2	73.2	8		-8.7	58
FeF_2	78.4	8	0.12	-3.1	57
MnF_2	66.5	8	0.10	-1.89	56
$CrCl_2$	16.1	2	0.69	4.9	62
$FeTiO_3$	56.3	-	0.48	-	32
$MnTiO_3$	62.3	-	0.45	-	This Work
Cr_2O_3	305.5	-	0.26	-	50

Manganese Titanate

Manganese titanate has the same crystal structure as the sesquioxides. In the magnetic unit cell (Figure 14) there are two intermediary oxygen atoms between each hexagonal layer of manganese ion. In Figure 14 the manganese ions are represented by A, the titanium ion by B. Since the interaction between manganese ions on different hexagonal layers is a double superexchange interaction (Mn - O - O - Mn), this interaction is weak.[167] Therefore, the interaction between manganese ions within a hexagonal layer, which is usually weak and insignificant, will be important in $MnTiO_3$. The magnetic interactions within an hexagonal layer

are antiferromagnetic and the magnetic interactions between hexagonal layers are also antiferromagnetic.[116] This magnetic structure differs from that of $FeTiO_3$ where the magnetic interactions within an hexagonal layer are ferromagnetic. The anamolous magnetic susceptibility results for $MnTiO_3$ [88] mentioned in the Introduction has been explained by assuming the intralayer and interlayer magnetic interactions have about the same strength.[89] The large amount of short range order exhibited by the heat capacity results tend to confirm the fact that both the intralayer and interlayer interactions are equally strong. The stronger the intralayer interactions the greater the short range order (illustrated by $CrCl_2$ and $CuCl_2$). However, $FeTiO_3$ has as much short range order as $MnTiO_3$ and its magnetic susceptibility behaves normally. Therefore, the heat capacity results do not help explain the anamolous magnetic susceptibility results of $MnTiO_3$.

V. MOTION OF IONIC GROUPS IN SOLIDS

The problem of rotation in solids or internal rotation in molecules has been solved only for the one dimensional problem. The potential function for three dimensional motion is a complex function for even very symmetrical groups in cubic fields, so that the general solution to Schroedinger's equation for such a potential is a formidable problem. Therefore, the only hope for attacking the problem in three dimensions is by using perturbation theory.

The one dimensional problem has been solved exactly, but in order to test the applicability of perturbation theory to rotational motion, the one dimensional problem will be solved using perturbation theory.

One Dimensional Rotation

The potential function for one dimensional rotation is

$$V(\phi) = \frac{V_o}{2} (1 - \cos n\phi) \tag{19}$$

where V_o is the height of the barrier to rotation and "n" is the

number of minima. Schroedinger's equation for this problem is

$$\frac{d^2\psi}{d\phi^2} + \frac{1}{B}\left[E - \frac{V_o}{2}(1 - \cos n\phi)\right]\psi = 0 \qquad (20)$$

where B is the rotational constant. Let $n\phi = 2y$

$$\frac{d^2\psi}{dy^2} + \frac{4}{Bn^2}\left[\left(E - \frac{V_o}{2}\right) + \frac{V_o}{2}\cos 2y\right]\psi = 0 \qquad (21)$$

This equation has the form of the Mathieu differential equation.

$$\frac{d^2\psi}{dy^2} + (a + 2\theta \cos 2y)\,\psi = 0 \qquad (22)$$

$$a = \frac{4}{Bn^2}\left(E - \frac{V_o}{2}\right) \qquad (23)$$

$$\theta = \frac{V_o}{Bn^2} \qquad (24)$$

The eigenvalues for the Mathieu differential equation have been tabulated.[90,91] The heat capacity of the one dimensional hindered rotor is tabulated as a function of Q_f and V_o, where

$$Q_f = \frac{2.7936}{n}\left(10^{38}\, I_r\, T\right)^{\frac{1}{2}}$$

I_r is the reduced moment of inertia.

If perturbation theory is to be applied to this problem the following assumptions must be made: below the barrier to rotation the zero-order wave functions are vibrational wave functions, while above the barrier they are rotational wave functions. Below the barrier the potential function given in Eq. (19) is expanded in powers of ϕ

$$V(\phi) = V_o\left(\frac{n^2\phi^2}{4} - \frac{n^4\phi^4}{48} + \ldots\right) \tag{25}$$

Using first-order perturbation theory the energy levels are given by

$$E_m = (m + \tfrac{1}{2})\,\hbar w - (2m^2 + 2m + 3)\,\frac{(\hbar w)^2}{16V_o} \tag{26}$$

$$\hbar w = n\sqrt{V_o B} \tag{27}$$

The experimentally observed frequency is

$$\begin{aligned} h\nu &= E_1 - E_o = \hbar w - \frac{(\hbar w)^2}{4} \\ V_o &= \frac{(h\nu + \frac{n^2}{4}B)^2}{n^2 B} \end{aligned} \tag{28}$$

Above the barrier, Eq. (20) is rewritten as

$$\frac{d^2\psi}{dz^2} + \frac{B}{n^2}\left[\left(E - \frac{V_o}{2}\right) + \frac{V_o}{2}\cos z\right]\psi = 0$$

$$z = n\phi \tag{29}$$

The zero-order wave function is

$$\psi = e^{\pm ikz}$$

There is no contribution to the energy from first-order perturbation theory. Using second-order theory

$$E(2) = \sum_{k'} \frac{|\langle k|V|k'\rangle|^2}{E_k - E_{k'}}$$

$$\langle k|V|k'\rangle = \frac{1}{2\pi}\int e^{\pm ikz}\cos z\, e^{\pm ik'z}\, dz$$

$$\langle k|V|k'\rangle = \frac{1}{4\pi}\int_o^{2\pi}\left[e^{i(k+k'+1)} + e^{i(k+k'-1)}\right] dz \tag{30}$$

$$= 0 \text{ unless } k' = k \pm 1$$

$$E(2) = \frac{V_o^2}{8B}\left[\frac{1}{4k^2-1}\right]$$

$$E_k = \frac{V_o}{2} + k^2 B + \frac{V_o^2}{8B}\left[\frac{1}{4k^2 - 1}\right] \qquad (31)$$

Since this problem has n-fold symmetry, only k values which are integer multiples of n are allowed. For example, if n = 3, k may have the values 0, 3, 6, 9, ...

Energy levels calculated using anharmonic levels below the barrier and perturbed rotational levels above the barrier are given in Table 17. For these levels n = 3 and B = 5.89 cm^{-1} (the rotational constant for the ammonium ion). For comparison, the energy levels determined from Mathieu's equation are also given in Table 17. For a frequency of 246 cm^{-1}, one of the vibrational levels is 7 cm^{-1} above the barrier. This level should not be included. Since these energy levels are not exact, the restriction that anharmonic levels must have energies less than the barrier height and rotational levels must have energies greater than the barrier height was relaxed.

The number of vibrational energy levels is equal to 2xi + 1, where "i" is the number of rotational energy levels not included in the energy levels scheme because they were below the barrier. Each vibrational level has a degeneracy of one, while each rotational level is two-fold degenerate except the ground state which has a

TABLE 17

Energy Levels of One-Dimensional Hindered Rotor

Three Minima, Rotational Constant = $5.89 cm^{-1}$

$\nu = 246 cm^{-1}$ Perturbed Levels	$V_o = 1270 cm^{-1}$ Tabulated Levels	$\nu = 100 cm^{-1}$ Perturbed Levels	$V_o = 246 cm^{-1}$ Tabulated Levels
0	0	0	0
246	246	100	100
479	476	187	167
698	690	295	279
904	880	295	293
1097	1060	555 (2)	555 (2)
1277	1145	925 (2)	920 (2)
1422 (2)	1422 (2)	1401 (2)	1395 (2)
1877 (2)	1875 (2)	1984 (2)	1980 (2)
2499 (2)	2440 (2)	2672 (2)	2660 (2)
3131 (2)	3120 (2)		

Horizontal line indicates transition from vibrational to rotational levels. (2) indicates level is doubly degenerate.

Tabulated levels given in reference 91.

degeneracy of one. Therefore, there is a one-to-one correspondence between the vibrational states and the rotational states that are below the barrier to rotation. If the energy levels evaluated using perturbation theory are forced to have a one-to-one correspondence between the vibrational and rotational states below the barrier, some

vibrational energy levels just above the barrier must in some cases be included in the energy levels scheme. In some problems an extra rotational energy level just below the barrier must be included in the energy level scheme. These extra levels, be they vibrational or rotational, are usually within 25 cm^{-1} of the barrier.

In Table 18 the heat capacity computed from the perturbed energy levels and from Mathieu's equation are given. The largest discrepancy between the two sets of data is 0.15cal/mole/deg.

As the number of minima in the potential function increases, the discrepancy between the calculated and the tabulated heat capacity data also increases. This is due to the fact that there are fewer energy levels and that the perturbations are larger.

Three Dimension Hindered Rotor

Ammonium chloride is an illustration of a three dimensional hindered rotor in a body-centered cubic lattice. The potential energy of the ammonium ion in such a lattice has been given by Gutowsky et. al.[93]

$$V = \frac{V_o}{2} \sum_{i=1}^{4} \left(\frac{x_i^4 + y_i^4 + z_i^4}{r^4} - \frac{3}{5} \right) \qquad (32)$$

TABLE 18

Heat Capacity of One-Dimensional Hindered Rotor

Three Minima, Rotational Constant = 5.89cm^{-1}

Temperature ^{o}K	ν = 246cm^{-1} Perturbation Theory	Tabulated Values	ν = 100cm^{-1} Perturbation Theory	Tabulated Values
20	0.000	0.000	0.078	0.079
40	0.022	0.022	0.780	0.87
60	0.191	0.192	1.376	1.46
80	0.482	0.484	1.700	1.75
100	0.781	0.799	1.824	1.819
120	1.038	1.062	1.829	1.788
140	1.245	1.262	1.776	1.708
160	1.410	1.452	1.701	1.619
180	1.543	1.588	1.623	1.548
200	1.654	1.704	1.550	1.476
220	1.747	1.806	1.484	1.424
240	1.827	1.892	1.427	1.374
260	1.896	1.971	1.378	1.335
280	1.957	2.028	1.336	1.296
300	2.009	2.079	1.299	1.265

Heat capacity expressed in cal/mole/^{o}K. Tabulated values given in reference 92.

This potential in terms of Euler's angles is

$$V = \frac{V_o}{2}\left\{-\frac{49}{8}\cos^4\theta + \frac{21}{4}\cos^2\theta - \frac{21}{40} + \frac{7}{8}\sin^4\theta(\cos4\psi - \cos4\phi)\right.$$
$$\left. + (\cos^2\theta + \frac{1}{8}\sin^4\theta)\quad \cos4\phi\ \cos4\psi - \frac{1}{2}(\cos\theta + \cos^3\theta)\sin4\phi\ \sin4\psi\right\} \tag{33}$$

Equation (33) is an expansion of Eq. (32) in terms of Euler's angles, except that the coordinate system has been rotated by $\pi/4$ around the z axis. For small oscillations, Gutowsky et. al.[43] made the following substitution into (33)

$$\begin{aligned} x &= \theta\cos\phi \\ y &= \theta\sin\phi \\ z &= \phi + \psi + \pi/4 \end{aligned} \tag{34}$$

$$V \cong \frac{V_o}{2}\left\{-\frac{12}{5} + 8(x^2+y^2+z^2) - \frac{32}{3}(x^4+y^4+z^4)\right.$$
$$\left. - 8(x^2y^2+x^2z^2+y^2z^2) + \ldots.\right\} \tag{35}$$

Using first-order perturbation theory, the energy levels of this

anharmonic oscillator becomes

$$E_{n_1 n_2 n_3} = -\frac{6}{5} V_o + (n_1 + n_2 + n_3 + \frac{3}{2}) \hbar w$$

$$- \frac{1}{16} \left[\sum_{i=1}^{3} (2n_i^2 + 2n_i + \frac{5}{4}) + n_1 n_2 + n_2 n_3 + n_1 n_3 \right] \frac{(\hbar w)^2}{V_o} \qquad (36)$$

where

$$\hbar w = 4 \sqrt{B V_o}$$

$$V_o = \frac{1}{16} \frac{(h\nu + 5B)^2}{B} \qquad (37)$$

ν is the observed torsional frequency. These energy levels of Gutowsky are good only up to the potential barrier. For energy levels above the barrier a different approach must be used.

Schroedinger's equation in terms of Euler's angles for a free rotor (spherical top) is

$$m \frac{\partial^2 U}{\partial \theta^2} + \cot\theta \frac{\partial U}{\partial \theta} + (1+\cot^2\theta) \frac{\partial^2 U}{\partial \phi^2} - \frac{2\cos\theta}{\sin^2\theta} \frac{\partial^2 U}{\partial \phi \partial \psi}$$

$$+ \frac{1}{\sin^2\theta} \frac{\partial^2 U}{\partial \psi^2} + \frac{\partial^2 U}{\partial \phi^2} + \frac{2}{B} (E - V) U = 0 \qquad (38)$$

Assuming V = 0, the zero-order wave functions are

$$U = \Theta(\theta)\,\Phi(\phi)\,\Psi(\psi) \tag{39}$$

$$\Phi(\phi) = \frac{1}{\sqrt{2\pi}}\, e^{iM\phi} \tag{40}$$

$$\Psi(\psi) = \frac{1}{\sqrt{2\pi}}\, e^{iK\psi} \tag{41}$$

$$\Theta(\theta) = N_{JKM}\,(x)^{\frac{1}{2}|K-M|}\,(1-x)^{\frac{1}{2}|K+M|}\sum_{i=0}^{n} a_i\, x^i \tag{42}$$

$$x = \frac{1}{2}(1 - \cos\theta) \qquad N_{JKM} = \text{normalization factor}$$

The left side of (42) is the hypergeometric series. It determines the energy levels of the system.

$$E(0) = J(J+1)B \tag{43}$$

Since the potential function (33) is a function of 4ψ and 4ϕ, M and K can only take on values that are integer multiples of 4. The solution of the problem of calculating the energy levels using the potential given in (33) is analogous to the calculation of the

energy levels above the barrier for the one-dimensional problem. Assuming that the potential given by Eq. (33) is a perturbation on the free rotor problem, the energy levels can be calculated above the barrier.

The hypergeometric series has matrix elements for cos θ when $J = \pm 1,0$; $K = \pm 1,0$; $M = \pm 1,0$.[94,95] Since K and M must be integer multiples of 4, only the matrix elements for $J = \pm 1,0$ must be considered. Only the first three terms in the potential given in Eq. (33) make a contribution to the energy levels. The zero-order energy levels above the barrier, assuming that the ground vibration level has an energy equal to zero are

$$E(0) = J(J + 1)\ B + \frac{15}{16} V_o - \frac{3}{2} \hbar w + \frac{15}{64} \frac{(\hbar w)^2}{V_o} \tag{44}$$

The last three terms in (44) come from adding the zero-point energy to the rotational levels and including the third term in Eq. (33) in the zero-order energy.

The perturbing potential is

$$V = \frac{V_o}{2} \left[- \frac{49}{8} \cos^4\theta + \frac{21}{4} \cos^2\theta \right] \tag{45}$$

The other terms have either been accounted for in E(0) or make no contribution to the energy levels. The matrix elements that need be

considered are

$$\left\langle J,K,M\left|\cos\theta\right|J,K,M\right\rangle = \frac{KM}{J(J+1)} = A$$

$$\left\langle J,K,M\left|\cos\theta\right|J+1,K,M\right\rangle = \frac{1}{J+1}\sqrt{\frac{(J-K+1)(J+K+1)(J+M+1)(J-M+1)}{(2J+1)(2J+3)}} = D \qquad (46)$$

$$\left\langle J,K,M\left|\cos\theta\right|J-1,K,M\right\rangle = \frac{1}{2J}\sqrt{\frac{(J^2-K^2)(J^2-M^2)}{4J^2-1}} = G$$

By matrix multiplication the matrix elements for $\cos^2\theta$ and $\cos^4\theta$ may be obtained.

The first-order energy is

$$E(1) = \langle n|V|n\rangle = \frac{V_o}{2}\left[-\frac{49}{8}\left(A^4+12A^2DG+GD^2G^2\right) + \frac{21}{4}\left(A^2+2DG\right)\right] \qquad (47)$$

The second-order energy is

$$E(2) = \sum_i \frac{\left|\langle n|V|n_i\rangle\right|^2}{E - E_i} = \frac{V_o^2}{8B}\left\{\frac{\left[-\frac{49}{2}\left(A^3D+3AD^2G\right) + \frac{21}{2}AD\right]^2}{J+1}\right.$$

$$+\frac{\left[-\frac{49}{4}\left(3A^2D^2+2D^3G\right) + \frac{21}{4}D^2\right]^2}{2J+3} + \frac{\left[-\frac{49}{2}AD^3\right]^2}{3J+6} + \frac{\left[-\frac{49}{4}D^4\right]^2}{4J+10}$$

$$-\frac{\left[-\frac{49}{2}\left(A^3G+3ADG^2\right) + \frac{21}{2}AG\right]^2}{J} - \frac{\left[-\frac{49}{4}\left(3A^2D^2+2DG^3\right) + \frac{21}{4}G^2\right]^2}{2J-1}$$

$$\left.-\frac{\left[-\frac{49}{2}AG^3\right]^2}{3J-3} - \frac{\left[-\frac{49}{8}G^4\right]^2}{4J-6}\right\} \qquad (48)$$

The energy levels for the ammonium ion are calculated using anharmonic vibrational levels below the barrier and perturbed rotational levels above the barrier. The number of rotational states below the barrier (i.e. $\sum_{n=0}^{m} g_n$, where g_n is the degeneracy of the n th level and m is the number of levels below the barrier) is greater than the number of anharmonic states. Assuming that there is a one-to-one correspondence between the rotational states that are not included in the energy levels scheme because they are below the barrier and the anharmonic states, then more anharmonic states are necessary. For example, for a torsional frequency of 350cm^{-1}, there are 38 anharmonic states below the barrier and 68 rotational states that are not included in the energy level scheme, because they are below the barrier. There should be more vibrational states below the barrier. The reason these states are missing can easily be seen by examining the energy levels of the one-dimensional hindered rotor. For the one dimensional case, the vibrational level just below the barrier was perturbed a great deal more than perturbation theory could predict, e.g. 50 cm^{-1} for a torsional frequency of 200 cm^{-1}. For a three dimensional hindered rotor, this discrepancy might well be larger, since the levels are subjected to a larger perturbation than in the one-dimensional case. For the case in which the torsional frequency is 350 cm^{-1}, the 30 anharmonic states that are missing represent a little more than one

complete vibrational energy level. The anharmonic level just above the barrier has a total quantum number $n_T (= n_1 + n_2 + n_3)$ equal to 5. The degeneracy of the energy level with $n_T = 5$ is 24. In order to correct for the discrepancy between the number of rotational states below the barrier and the number of vibrational states, an energy level is placed arbitrarily at the barrier and given a degeneracy which will correct for the difference in the number of rotational and vibrational states below the barrier. For the problem of a torsional oscillator with a frequency of 350 cm^{-1}, one energy level is placed at the barrier (1500 cm^{-1}) and given a degeneracy of 30.

Nuclear spin degeneracy is not included in the preceding discussion and does not change the method of operation even when it must be included in the total degeneracy of a given energy level. When the nuclear spin degeneracy must be considered, the degeneracies used in determining the number of rotational states below the barrier and the number of vibrational states should not include the nuclear spin degeneracy.

The method that has been described for forcing a one-to-one correspondence between the vibrational and rotational levels has assumed that the energy levels for the rotational states are perfectly correct. For some of the rotational levels, second-order perturbation theory gives a rather large negative contribution to

the energy, so that the level falls below the barrier. It is conceivable that in higher order perturbation theory a positive contribution to the energy would be large enough to put the level above the barrier. In this case, the degeneracy assigned to the level arbitrarily placed at the barrier would be incorrect. This, however, is not a serious problem, since there are not many energy levels that have a large negative second-order energy (only states which have values of K and M equal or nearly equal to J). Furthermore, even if some rotational levels were placed above the barrier, they would most likely be close to the barrier, so that the error is simply replacing a vibrational level at the barrier with a certain degeneracy with a rotational level above the barrier with the same degeneracy.

The rotational levels that are close to but below the barrier (within about 25 cm^{-1} of the barrier) are included in the energy level scheme. This is the same procedure as was followed for the one-dimensional problem.

The vibrational level that is arbitrarily placed at the barrier should undoubtedly be somewhat below the barrier. An error of about 50 cm^{-1} in the energy of this vibrational level does not cause a significant error in the heat capacity unless the height of the barrier is less than 500 cm^{-1}.

Nuclear spin must be taken into account in determining the overall degeneracy of any particular energy level. The problem of calculating the total degeneracy including the nuclear spin of energy levels for spherical top molecules has been solved by Wilson[96] using group theory. The statistical weight of a rotational level for a spherical top has a $(2J + 1)$-fold space degeneracy and a $(2J + 1)$-fold degeneracy due to the fact that all three moments of inertia are equal, i.e. both K and M may take on $(2J + 1)$ values. This does not include nuclear spin. When nuclear spin is taken into account the $(2J + 1)$-fold space degeneracy is multiplied by a factor, g_J, which is not usually equal to $2J + 1$. These factors, g_J, calculated by Wilson become approximately proportional to $2J + 1$ for large J.

Wilson solved the nuclear spin problem for an isolated spherical top molecule. This is not applicable to the problem under consideration. For the case of a tetrahedral molecule in a cubic environment it will be assumed that the nuclear spin degeneracy of all the energy levels, vibrational and rotational, does not change.

Given the energy levels for a system, together with the

degeneracies of the levels, the heat capacity may be calculated.

$$C = - R \frac{\partial}{\partial T} \left(kT^2 \frac{\partial \ln Z}{\partial T} \right)$$

$$Z = \sum_i e^{-\epsilon_i / kT}$$

$$C = \frac{R}{Z^2} \left[Z \sum_i x_i^2 \, e^{-x_i} - \left(\sum_i x_i \, e^{-x_i} \right)^2 \right]$$

$$x_i = \epsilon_i / kT$$

This theory presented in this section will be applied to the three dimensional motion of NH_4^+, ND_4^+, and BH_4^- in cubic lattices. The borohydride ion, like the ammonium ion is tetrahedral. For all the computations carried out in the chapter the rotational constant of the ammonium ion was taken as 5.89 cm^{-1}, that of the deutero-ammonium ion as 2.95 cm^{-1}, and the borohydride ion as 4.08 cm^{-1}.

Ammonium Chloride

Ammonium chloride is body-centered cubic below 456°K. There is an order-disorder transition at 242°K due to the disordering of the ammonium ions in the compound. The torsional frequency of the

ammonium ion has been calculated by representing the heat capacity results as a sum of Debye and Einstein functions.[12] The torsional motion of the ammonium ion was represented by an Einstein function with three degrees of freedom. This old analysis did not include a $C_p - C_v$ term. This analysis has been redone using a $C_p - C_v$ term determined from thermal expansion[97] and compressibility[98] data. At 300°K, $C_p - C_v = 1.24$ cal deg^{-1} mole^{-1}. This corresponds to an "a" value of 0.0034. For $C_p - C_v$ at temperatures below 300°K, $C_p - C_v$ is estimated by $(0.0034C_v)^2T$. Below 100°K the heat capacity can be represented by

$$C_p = 3D(217/T) + 3E(263/T) + 3E(560/T) + (0.0034C_v)^2T \qquad (49)$$

Below 100°K there is no anharmonic contribution to the heat capacity. The torsional frequency of the ammonium ion is equal to 560°K (389 cm^{-1}). Above 100°K the order-disorder transition begins to make a contribution to the heat capacity. By 300°K, the transition appears to make no significant contribution to the heat capacity. The contribution of the ammonium ion to the heat capacity can be calculated by subtracting from the total heat capacity 3D(217/300) + 3E(263/300) + C(int) + $(C_p - C_v)$. C(int) is the contribution of the internal frequencies of the ammonium ion to the heat capacity. The internal frequencies, taken from infrared measurements,[99] are

represented by Einstein functions. The heat capacity of the ammonium ion is 7.39 cal deg^{-1} $mole^{-1}$ at 300°K. Using the energy levels derived earlier in this chapter to compute heat capacities, the torsional frequency of the ammonium ion in NH_4Cl is determined to be 326 cm^{-1}. This corresponds to a potential barrier of 1341 cm^{-1}. The theory predicts a maximum in the rotational heat capacity at 380°K.

Deutero-Ammonium Chloride

Deutero-ammonium chloride has an order-disorder transition at 248°K. As NH_4Cl, the crystal structure of ND_4Cl is body-centered cubic both above and below the transition. The heat capacity[12] of ND_4Cl below 100°K may be represented by

$$C_p = 3D(213/T) + 3E(247/T) + 3E(413/T) + (0.0034C_v)^2T$$

The value of "a" for ND_4Cl is assumed to be equal to that of NH_4Cl. The torsional frequency is 413°K (288 cm^{-1}).

The contribution of ND_4^+ to the heat capacity above the transition is calculated in the same manner as the NH_4^+ contribution to the heat capacity of NH_4Cl. At 300°K the heat capacity of ND_4 is 7.64 cal/deg. mole. Using the theory presented earlier in this

chapter, the torsional frequency of ND_4^+ is ND_4Cl is 239 cm^{-1}. The maximum in the rotational heat capacity occurs at 390°K.

Ammonium Bromide

Ammonium bromide presents a more complicated problem than ammonium chloride. At 105°K ammonium bromide undergoes a transition from a body-centered cubic lattice to a tetragonal lattice. One of the axes of the cubic unit cell is slightly elongated to give the tetragonal structure. At 234°K ammonium bromide undergoes an order-disorder transition similar to the one in ammonium chloride. Above 234°K ammonium bromide is body-centered cubic.

Below 100°K the heat capacity[5] of NH_4Br is represented by

$$C_p = 3D(141/T) + 3E(243/T) + 3E(485/T) + (0.0034C_v)^2T$$

The value of "a" was determined at 300°K from the value of $(C_p - C_v)$ determined from thermal expansion[100] and compressibility[101] data. The torsional frequency of NH_4^+ in NH_4Br in the body-centered cubic lattice is 485°K (337 cm^{-1}).

The transition to the tetragonal phase exhibits a large region of hysterisis. The tetragonal phase can be supercooled to

$85^{o}K$. The heat capacity of both the cubic and tetragonal phases have been measured between $85^{o}K$ and $105^{o}K$. Taking this data together with the fact that there is an entropy change of 0.3 e.u. at the transition allows one to calculate the torsional frequency of NH_4^+ in the tetragonal phase. The order-disorder transition begins to make a contribution to the heat capacity even at these low temperatures. In order to by-pass this difficulty, it is necessary to assume that the contribution of the order-disorder transition to the heat capacity of both phases, cubic and tetragonal, is the same at a given temperature. The heat capacity of NH_4Br in the cubic phase is subtracted from the heat capacity of NH_4Br in the tetragonal phase. This difference is represented by

$$C_p(\text{tetragonal}) - C_p(\text{cubic}) = \left[3D(\theta_1/T) + 3E(\theta_2/T) + 3E(\theta_3/T) \right] - \left[3D(141/T) + 3E(243/T) + 3E(485/T) \right]$$

Using the difference between the heat capacity of the two phases between $85^{o}K$ and $105^{o}K$ together with the fact that the left hand side of the above equation must yield an entropy of 0.30 e.u. allows for the calculation of θ_1, θ_2, and θ_3.

$$C_p(\text{tetragonal}) = 3D(136/T) + 3E(237/T) + 3E(497/T) + (0.0034C_v)^2T$$

The torsional frequency of NH_4^+ in the tetragonal phase is 497°K (345 cm^{-1}).

The heat capacity of NH_4^+ at 300°K is 7.82 cal/deg mole. This corresponds to a torsional frequency of 308 cm^{-1} for NH_4^+. The maximum in the rotational heat capacity occurs at 350°K.

Deutero-Ammonium Bromide

Deutero-ammonium bromide undergoes a transition from a body-centered cubic structure to a tetragonal structure at 167°K. At 215°K it undergoes an order-disorder transition. Above the transition ND_4Br is body-centered cubic.

Below 100°K the heat capacity[102] of ND_4Br may be represented by

$$C_p = 3D(141/T) + 3E(225/T) + 3E(350/T) + (0.0034C_v)^2T$$

The value of "a" is assumed to be equal to that of NH_4Br. The torsional frequency of ND_4^+ in the cubic form of ND_4Br is 350°K (243 cm^{-1}). The torsional frequency of ND_4^+ in the tetragonal phase of ND_4Br cannot be determined as it was for NH_4Br since the cubic-tetragonal transition temperature is too close to the order-disorder transition temperature.

The heat capacity of ND_4^+ in ND_4Br at 300°K is 8.42 cal deg^{-1} $mole^{-1}$. According to the theory presented earlier, this

corresponds to a torsional frequency for ND_4^+ of 214 cm^{-1}. The maximum in the rotational heat capacity occurs at 320°K.

Ammonium Iodide (tetragonal)

At low temperatures ammonium iodide has a tetragonal structure. Below 100°K the heat capacity[5,103] of ammonium iodide may be represented by

$$C_p = 3D(101/T) + 3E(219/T) + 3E(406/T) + (0.0036C_v)^2T$$

The value of "a" has been estimated. The torsional frequency of the ammonium ion is 406°K (282 cm^{-1}).

Ammonium iodide undergoes an order-disorder transition at 230°K. At 255°K, it undergoes a first-order transition to a face-centered cubic structure. At 255°K the heat capacity of NH_4^+ is 7.66 cal deg^{-1} $mole^{-1}$. This, however, assumes that the order-disorder transition is making no contribution to the heat capacity. Undoubtedly, the transition is making a small contribution to the heat capacity. Since there is no way to estimate this contribution, the torsional frequency for NH_4^+ in NH_4I was calculated using the value for the heat capacity of NH_4^+ given above. The torsional frequency calculated using the theory given earlier is 282 cm^{-1}.

Sodium Borohydride

The heat capacity of sodium borohydride exhibits an order-disorder transition at 190°K.[104] Sodium borohydride has a face-centered cubic structure above the transition and tetragonal (slight distortion of face-centered cubic structure) below the transition. The B-H bond is not directed at one of the nearest-neighbor sodium ions. The hydrogen atoms, instead, lie on the cube diagonals.[108] There are two possible orientations of the tetrahedra in the lattice which accounts for the order-disorder transition in the heat capcity. Below 100°K the heat capacity is represented by

$$C_p = 3D(205/T) + 3E(255/T) + 3E(525/T) + (0.0041C_v)^2T$$

The value of "a" for $NaBH_4$ is assumed to be equal to the value of "a" for NaBr, since the size of BH_4^- is about the same as Br^-. The frequency of torsional oscillation is 525°K (365 cm^{-1}).

The borohydride ion in $NaBH_4$ undergoes three-dimensional hindered rotation similar to that of the ammonium ion in NH_4Cl. The heat capacity of BH_4^- may be evaluated above 220°K assuming that the order-disorder transition is not contributing to the

total heat capacity.

$$C(BH_4^-) = C_p(\text{observed}) - 3D(205/T) - 3E(255/T) - C(\text{int}) - (C_p - C_v) \quad (50)$$

C(int) is the contribution of the internal frequencies[105,106] of BH_4^- to the heat capacity. The heat capacity contributions of these internal frequencies are represented by Einstein functions.

The $(C_p - C_v)$ term may be determined by using

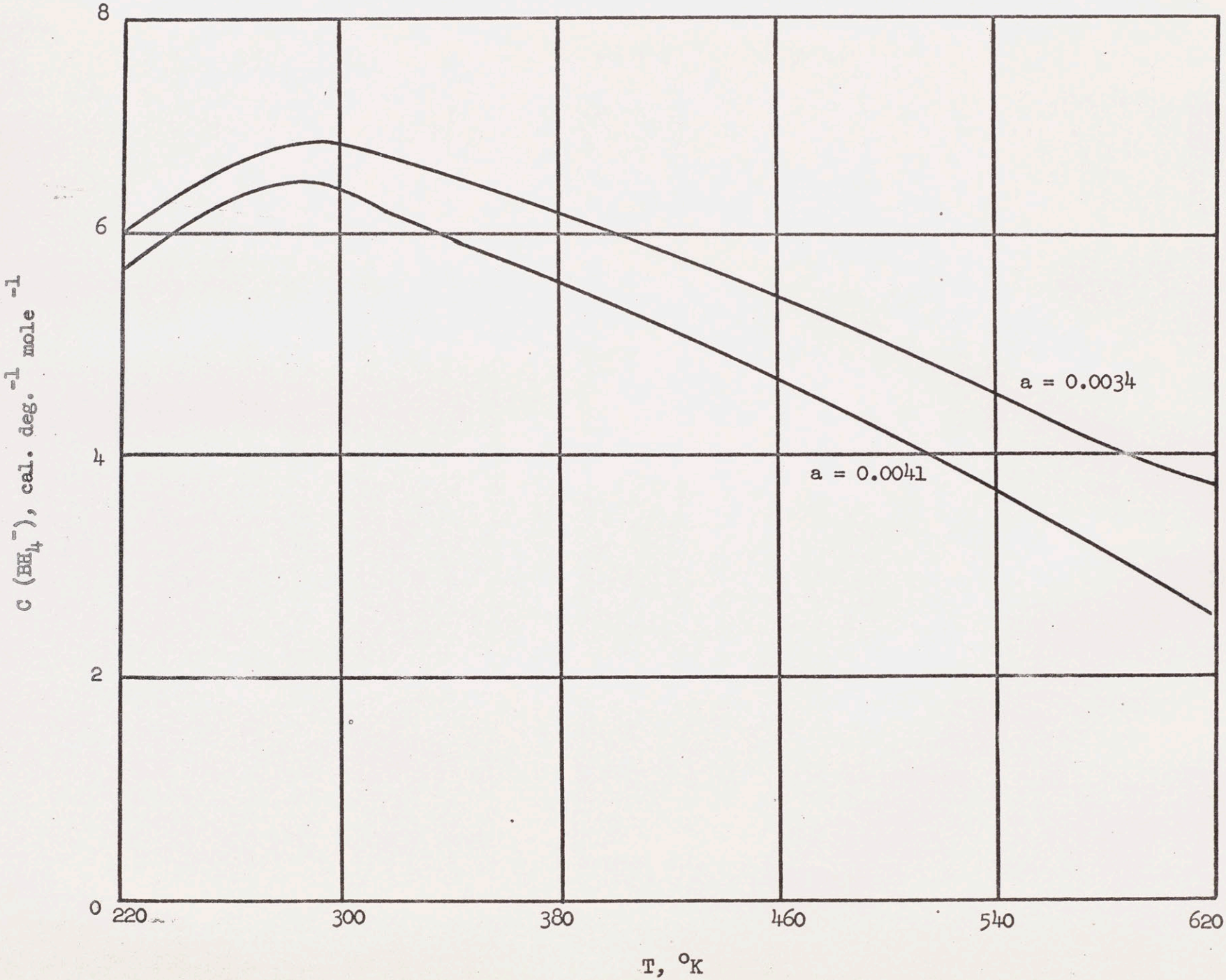
$$C_p - C_v = (aC_v)^2 T$$

Since C_p is known, C_v may be calculated. This is the same procedure that was used for $CoCl_2$ and CoF_2. The value of "a" for $NaBH_4$ must be estimated. The value of "a" is assumed to lie between the values of "a" for NaBr (0.0043) and NH_4Cl (0.0034).

The heat capacity of BH_4^- in $NaBH_4$ is illustrated in Fig. 15. Below 300°K the heat capacity of $NaBH_4$ has been measured by Johnston.[104] Above 300°K high temperature heat capacity measurements have been performed by Douglas.[107] These high temperature measurements have an accuracy of about one percent. The heat capacity of BH_4^- passes through a maximum at about 290°K. The general features of the heat capacity curve is independent of the

Figure 15

Rotational Heat Capacity of BH_4^- in $NaBH_4$


8
6
4
2
0
220
300
380
460
540
620
a = 0.0034
a = 0.0041
c (BH_4^-), cal. deg.$^{-1}$ mole^{-1}
T, °K

value of "a" chosen for $NaBH_4$. The motion of the borohydride ion in $NaBH_4$ will be further discussed in the next section.

Potassium Borohydride

Potassium borohydride has a face-centered cubic unit cell at room temperature. In the unit cell the hydrogen atoms point away from the potassium ions. As in $NaBH_4$ there are two possible orientations of BH_4^-.[108] The heat capacity of KBH_4 exhibits a lambda point at 77°K and a broad transition between 200°K and 450°K.[109] The entropy associated with the transition at 77°K is 0.80 e.u. or about ½Rln 2, rather than the expected Rln 2 that is associated with the transition in $NaBH_4$. Furukawa et. al.[109] explained their results by assuming that half the entropy associated with the disordering of BH_4^- occurs at 77°K and the other half occurs between 200°K and 450°K.

The heat capacity of potassium borohydride may be represented below 60°K by

$$C_p = 3D(185/T) + 3E(263/T)$$

Below 60°K the torsional frequency of the borohydride ion and the $(C_p - C_v)$ term make only a very small contributions to the total heat capacity. In order to study the motion of BH_4^-, the heat

capacity of BH_4^- is determined above 100°K. The heat capacity of BH_4^- is

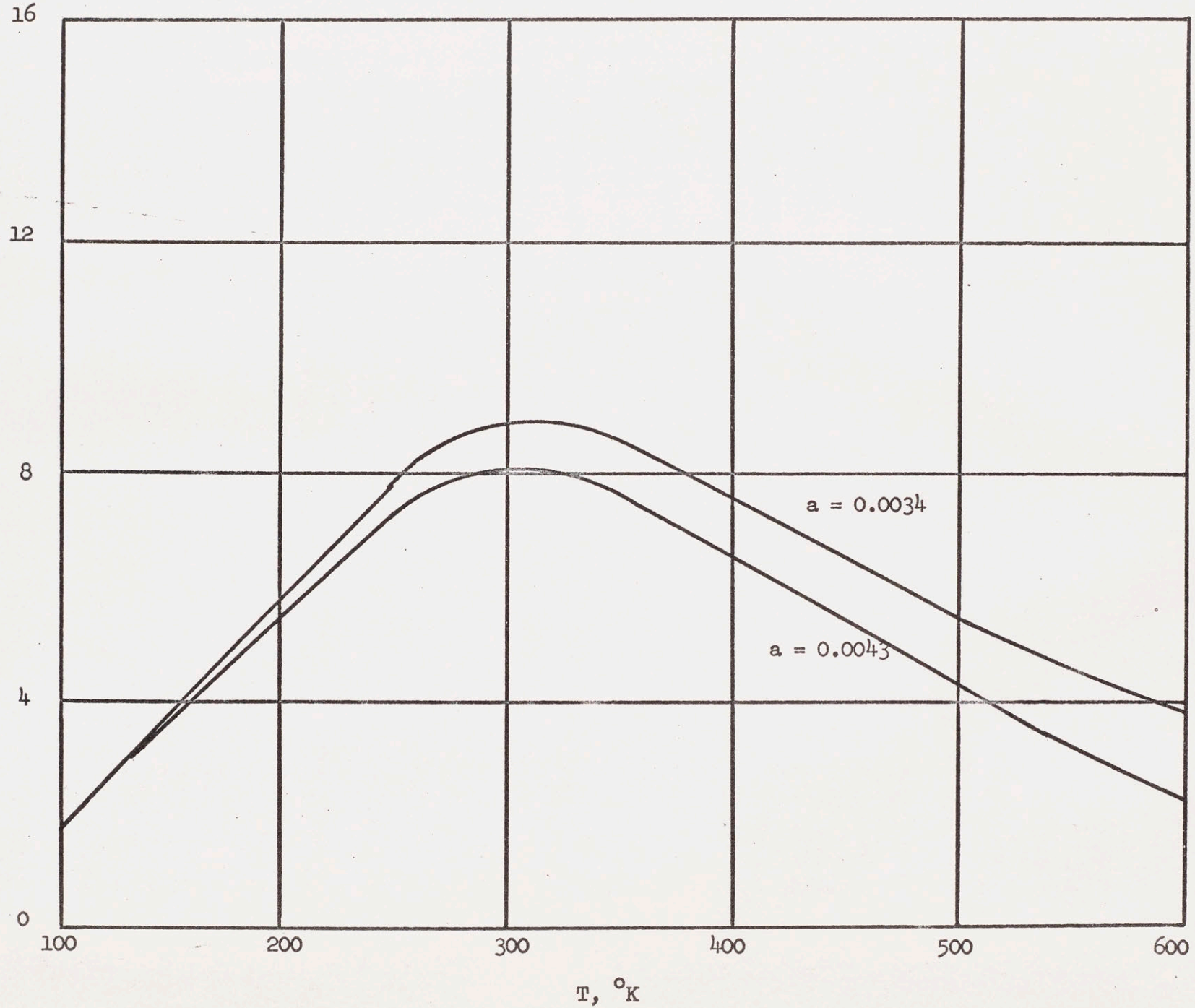
$$C(BH_4^-) = C_p(\text{observed}) - (C_p - C_v) - 3D(185/T) - 3E(263/T) - C(\text{int}) \quad (51)$$

Two of the four internal frequencies of the borohydride ion in KBH_4 have been measured by infrared spectroscopy.[110] The other two frequencies are taken from the values of these frequencies in $NaBH_4$.[105,106] The heat capacity contributions of these internal frequencies are represented by Einstein functions. The value of "a" for KBH_4, as for $NaBH_4$, must be estimated. The value of "a" is assumed to lie between the values of "a" for KBr (0.0043) and NH_4Cl (0.0034).

The heat capacity of the borohydride ion is illustrated in Fig. 16. The experimental heat capacity was measured below 370°K using an adiabatic calorimeter and above 370°K using a drop calorimeter method. The latter measurements are much less accurate than the former measurements. The curve illustrated in Fig. 16 is a perfect example of the heat capacity of a three-dimension hindered rotor. The maximum in the heat capacity occurs at about 300°K. Therefore, the broad transition observed by Furukawa et. al.[109] is not due to an order-disorder phenomena, but rather to the hindered

Figure 16

Rotational Heat Capacity of BH_4^- in KBH_4


16
12
8
4
0
100
200
300
400
500
600
a = 0.0034
a = 0.0043
C (BH_4^-), cal. deg.$^{-1}$ mole^{-1}
T, °K

rotation of the borohydride ion. This leaves unexplained the nature of the transition at 77°K. It is possible that it is due to a change in crystal structure. The crystal structure of KBH_4 at liquid helium temperatures has been studied by Welsh[111] using X-ray diffraction techniques. He decided that KBH_4 was face-centered cubic below the transition at 77°K. However, Welsh had difficulty observing the crystal structure change in $NaBH_4$ below its transition temperature. He only observed the crystal structure change in $NaBH_4$ when his samples had been annealed at 175°C. Therefore, there is a distinct possibility that he would miss a crystal structure change in KBH_4 if one did occur. Welsh did not compute lattice parameters from his X-ray patterns.

If the transition at 77°K is not in any way due to an order-disorder phenomena, what are the orientations of BH_4^- in KBH_4? $NaBH_4$ has an order-disorder transition at 190°K. Since the lattice parameters of KBH_4 are larger than the corresponding parameters of $NaBH_4$ at room temperature,[112,113] one would expect the order-disorder transition to occur at a lower temperature in KBH_4 than in $NaBH_4$ due to weaker interactions between neighboring borohydride ions. However, if the transition temperature were to be much lower in KBH_4 than in $NaBH_4$, the borohydride ions would not have enough freedom of motion in the lattice to change their orientation, i.e. the transition would be frozen out so that there

would be a zero-point entropy. In the ammonium halides an order-disorder transition appears only because at the transition temperature some of the ammonium ions are in their rotational states and therefore have enough freedom of motion to reorientate themselves. On the other hand, in KBH_4 the borohydride ions may not have enough freedom of motion to reorientate themselves, so that even at very low temperatures the borohydride ions will be disordered.

Another explanation of the absence of an order-disorder transition is that the borohydride ions are undergoing "violent" motions at the expected transition temperature, so that there are no longer two different orientations of the borohydride ions. For example, if the borohydride ions were freely rotating there is obviously not two different orientations of the borohydride ions. This explanation is less likely to be true than the one given earlier.

The heat capacity of the borohydride ion in KBH_4 between $100^{o}K$ and $120^{o}K$ can be represented by an Einstein function with three degrees of freedom whose frequency is $420^{o}K$ ($290\ cm^{-1}$). It is possible, however, that the lattice frequencies (Debye and Einstein characteristic temperatures given in (51)) change going through the transition at $77^{o}K$. For the ammonium halides, this is no problem because the transition occurs at higher temperatures where these frequencies are nearly classically excited. For KBH_4 this difficulty introduces an uncertainty in the evaluation of the

torsional frequency. The overall rotational heat capacity of BH_4^- can best be represented by a torsional frequency of 250 cm^{-1} when the theory presented earlier in this chapter is used. The potential function for a tetrahedron in an octahedral environment (6-fold coordination) is the same as that for a tetrahedron in a cubic environment (8-fold coordination). Therefore, the theory presented earlier in this chapter should apply to the motion of BH_4^-. A torsional frequency of 250 cm^{-1} gives the correct temperature for the maximum in the heat capacity curve of the borohydride ion in KBH_4. In Fig. 17 the theoretical heat capacity curve of the borohydride ion is compared to the heat capacity of the borohydride ion in KBH_4 and $NaBH_4$ evaluated from Eqs. (50) and (51) respectively. A value of "a" of 0.0034 was used for both $NaBH_4$ and KBH_4, when the heat capacities of the borohydride ion were being calculated. The comparison between the theoretical and observed rotational heat capacity of BH_4^- is poor in the case of $NaBH_4$ and fair in the case of KBH_4.

The lower limit of the value of "a" is used in determining the observed heat capacity of the borohydride ion in both $NaBH_4$ and KBH_4. The total heat capacity from which $(C_p - C_v)$ is computed includes at high temperatures a large contribution from the internal frequencies. As pointed out in the Introduction a more satisfactory equation for $(C_p - C_v)$ than the one that has

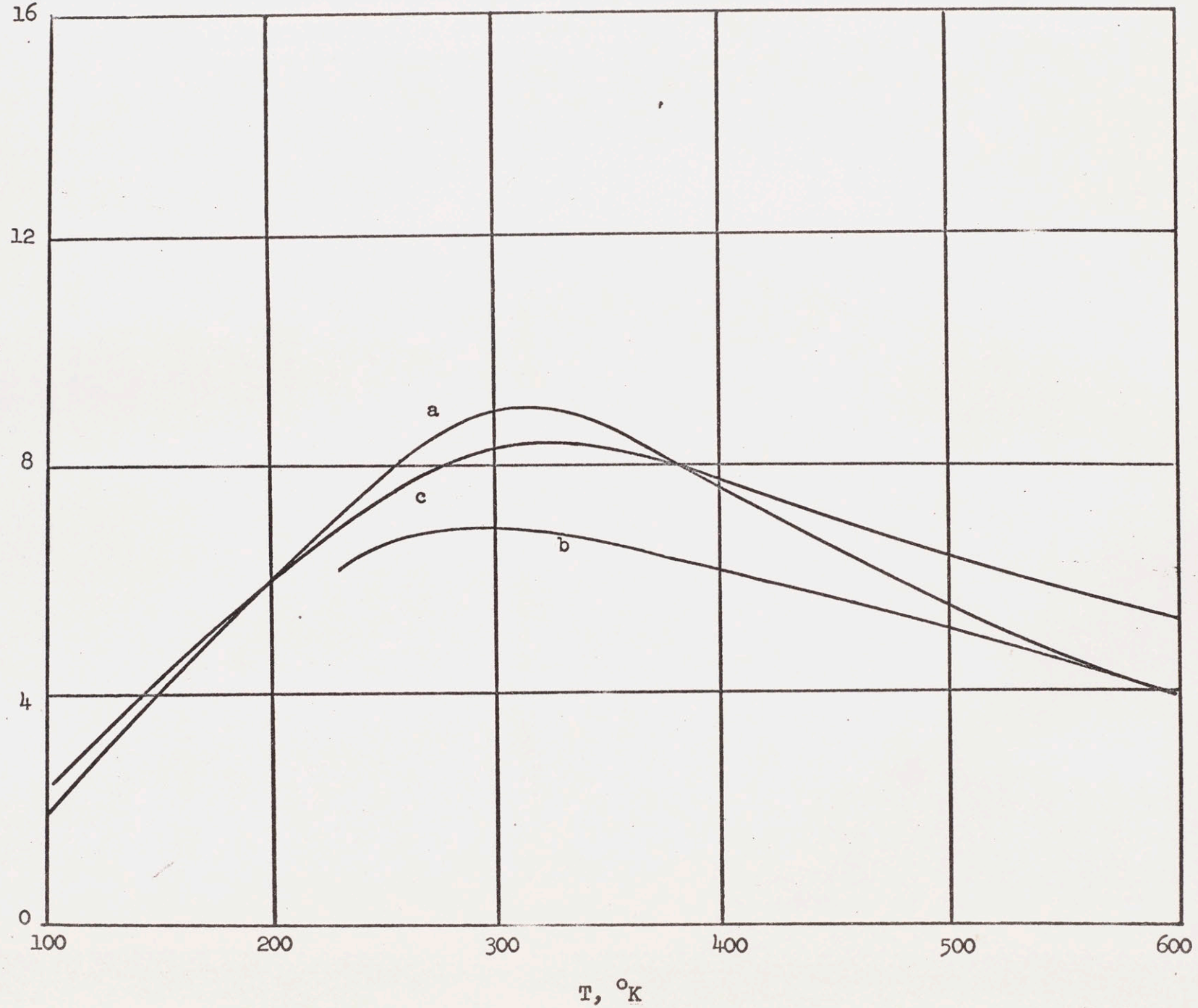
Figure 17

Comparison of Observed and Theoretical Heat Capacity of BH_4^- in $NaBH_4$ and KBH_4

a - KBH_4 observed

b - $NaBH_4$ observed

c - theory


16
12
8
4
0
100
200
300
400
500
600
a
b
c
C (BH_4^-), cal. deg.$^{-1}$ mole^{-1}
T, °K

been used is

$$C_p - C_v = \left[(aC_{v1}) + (bC_{v2}) \right]^2 T$$

where the first term in the brackets is the contribution of the intermolecular vibrations to $C_p - C_v$ and the second term in the brackets is the contribution of the intramolecular vibrations to $C_p - C_v$. Usually the assumption is made that a = b. However, Wulff[114] has shown that in some cases "b" is less than "a". If this is true for the borohydrides, then $C_p - C_v$ is overestimated and therefore the heat capacity of the borohydride ion is underestimated. Also, above room temperature the formula given above tends to overestimate $C_p - C_v$. For these two reasons the lower value of "a" was used in comparing the theoretical with the observed heat capacity of BH_4^-.

The torsional frequency of the borohydride ion in KBH_4 above 77°K is given a value of 270 cm^{-1} ± 30 cm^{-1}. This corresponds to a barrier to rotation of 1300 cm^{-1} ± 260 cm^{-1}. The torsional frequency of the borohydride ion in $NaBH_4$ above the transition at 190°K is given a value of 280 cm^{-1} ± 40 cm^{-1}. This corresponds to a barrier to rotation of 1380 cm^{-1} ± 400 cm^{-1}. The torsional frequency of the borohydride ion in $NaBH_4$ decreases by between 45 cm^{-1} to 125 cm^{-1} going through the order-disorder

transition. In the ammonium halides the decrease is only about 30 cm^{-1}. The much larger decrease in $NaBH_4$ is most likely due to a 3% increase in volume going through the transition compared to a less than 1% change in volume for the ammonium halides.

Ammonium Fluoborate

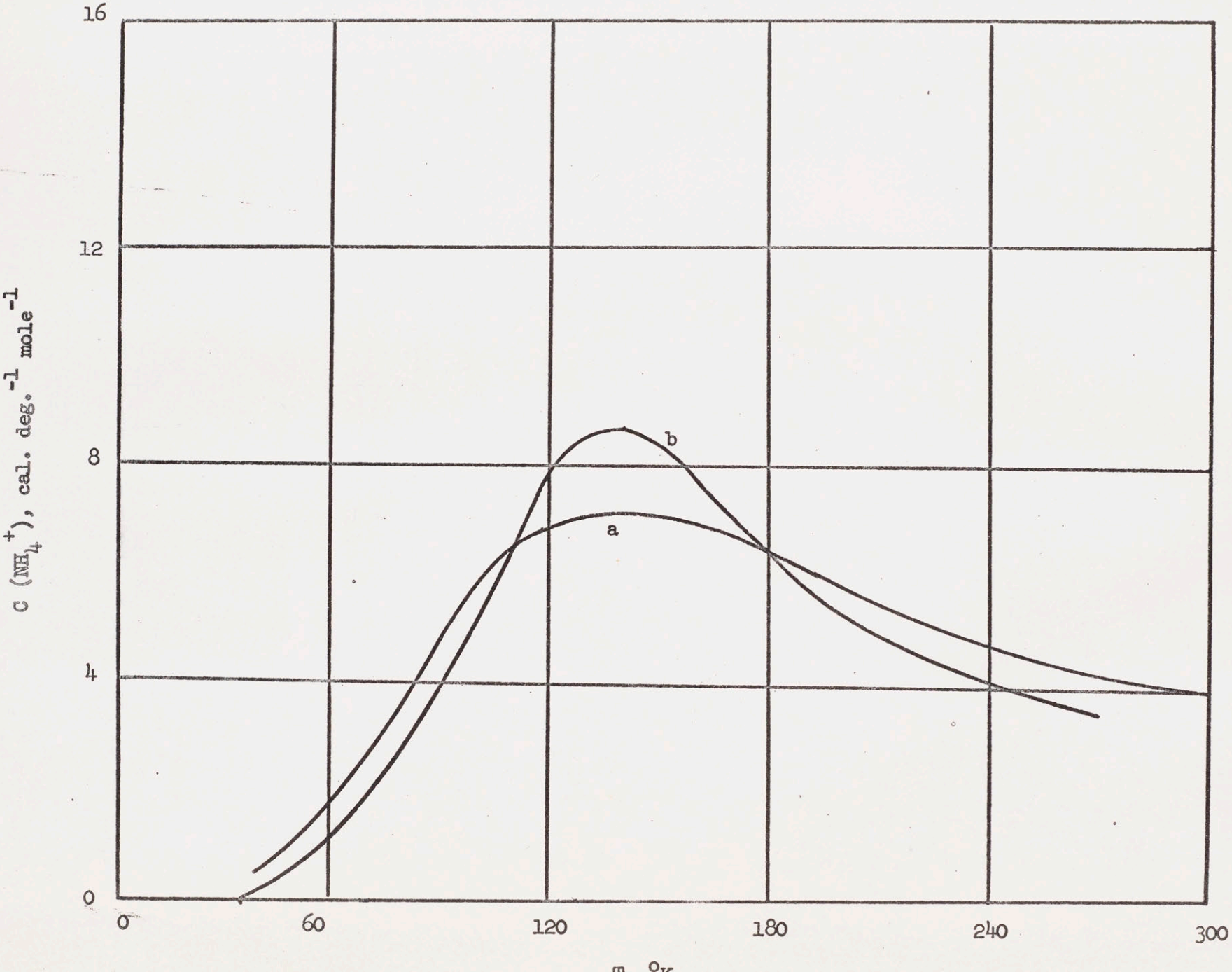
Ammonium fluoborate has an orthorhombic crystal structure belonging to the space group V_h^{16}-Pnma.[121] Orehotsky analyzed the heat capacity results of NH_4BF_4 and ND_4BF_4.[21] By comparing the heat capacity results of the two compounds he was able to determine the torsional frequencies of NH_4^+ (201 cm^{-1}) and ND_4^+ (147 cm^{-1}). The rotational heat capacities of both NH_4^+ and ND_4^+ pass through a maximum at about 135°K. In Fig. 18 the heat capacity computed using the three-dimensional hindered rotor theory is compared to the heat capacity of NH_4^+ in NH_4BF_4 determined by Orehotsky. The theoretical heat capacity was forced to have a maximum at the same temperature as the observed heat capacity. The frequency of torsional oscillation of the theoretical heat capacity is 173 cm^{-1}. Since NH_4BF_4 is orthorhombic it is not surprising that the theoretical and observed heat capacity of NH_4^+ do not match well. The results for the heat capacity of ND_4^+ in ND_4BF_4 are similar to those of NH_4^+ in NH_4BF_4. The frequency of

Figure 18

Rotation Heat Capacity of NH_4^+ in NH_4BF_4

a - theory

b - observed


16
12
8
4
0
0
60
120
180
240
300
b
a
C (NH_4^+), cal. deg.$^{-1}$ mole^{-1}
T, °K

torsional oscillation of the theoretical heat capacity for ND_4^+ in ND_4BF_4 is 135 cm^{-1}.

Lithium Borohydride

Lithium borohydride has an orthorhombic crystal structure.[119] The heat capacity measurements in $LiBH_4$ show no order-disorder transition.[120] The heat capacity may be represented below 200°K by

$$C_p = 3D(255/T) + 3E(400/T) + 3E(530/T) + C(int) + (0.0046C_v)^2T$$

The value of "a" for $LiBH_4$ was assumed to be equal to that of LiBr. Two of the four internal frequencies of BH_4^- in $LiBH_4$ have been determined from infrared studies.[110] The other two frequencies were assumed to be equal to those in $NaBH_4$.[105,106] The torsional frequency, 530°K, is relatively close to the lattice frequency at 400°K. Therefore, there is a large uncertainty in the torsional frequency of BH_4^- in $LiBH_4$. The frequency assigned to the torsional oscillation is 350 cm^{-1} ± 50 cm^{-1}.

Above 200°K the anharmonic motion of BH_4^- make significant contributions to the heat capacity so that the sum of Debye and Einstein functions will not represent the heat capacity. Since $LiBH_4$ is orthorhombic, the theory given earlier in this chapter does not apply.

Ammonium Fluoride

Ammonium fluoride is unique among the ammonium halides since it exits in a hexagonal or wurtzite phase, rather than a cubic phase. In the hexagonal lattice there are not two equally probable orientations for the ammonium ions, so there is no order-disorder transition. The heat capacity[117] of NH_4F is represented by

$$C_p = 2D(150/T) + D(390/T) + 3E(380/T) + 3E(790/T) + C(int) + C(anh) + (0.0036C_v)^2T$$

The internal frequencies have been determined by Hornig.[118] The contribution of the torsional motion of the ammonium ion to the heat capacity is given by an Einstein function with a characteristic temperature of 790^oK (548 cm^{-1}). C(anh) represents the anharmonic contribution of the motion of the ammonium ion to the heat capacity. The barrier to rotation (6013 cm^{-1}) is high so that the rotational levels make no contribution to the heat capacity below room temperature. The anharmonic energy levels computed using the theory presented earlier in this chpater were used to evaluate the heat capacity of NH_4^+ even though NH_4F is hexagonal rather than cubic.

C(anh) is very small, amounting to only 0.08 cal $deg.^{-1}$ $mole^{-1}$ at 300°K. The hindered-rotor theory is only for cubic compounds, but it should be a good approximation in this case because of the high barrier to rotation.

Ammonium Nitrate

Ammonium nitrate exists in five crystalline phases at normal pressures.[122]

V - tetragonal	-	below 256.2°K
IV - rhombic	-	256.2°K - 305.4°K
III - rhombic	-	305.4°K - 356.4°K
II - tetragonal	-	356.4°K - 398.2°K
I - cubic	-	398.2°K - 442.8°K
liquid	-	above 442.8°K

Stephenson et. al.[3] have measured the heat capacity of NH_4NO_3 from 15°K to 315°K. There are two isothermal (first-order) transitions in this temperature range. The heat capacity at the 256.2°K transition decreases by 1.63 cal/deg. mole. At the transition at 305.4°K the heat capacity decreases by 5.3 cal/deg mole. This large decrease in the heat capacity was attributed to the free rotation of the ammonium ion in phase III, but torsional oscillation in phase IV.

The torsional frequency of the ammonium ion in the low temperature phase has been calculated by Stephenson et. al. by representing the heat capacity of NH_4NO_3 by a sum of Debye and Einstein functions. However, in their analysis no $(C_p - C_v)$ term was included. The value of $(C_p - C_v)$ at different temperatures may be estimated from the values of $(C_p - C_v)$ for other nitrates. The Debye and Einstein characteristic temperatures together with the value of "a" for some other nitrates are given in Table 19.

TABLE 19

Debye and Einstein Characteristic Temperatures for Some Nitrates

$$C_p = 3D(\theta_1/T) + 3E(\theta_2/T) + 3E(\theta_3/T) + (aC_v)^2T$$

	θ_1	θ_2	θ_3	a	Reference for Heat Capacity Results
$NaNO_3$	160	205	330	0.0047	123
KNO_3	140	173	235	0.0048	123
$AgNO_3$	92	170	260	0.00435	124
$TlNO_3$	67	135	210	0.0044	125

All characteristic temperatures are given in ^oK. θ_3 represents the torsional frequency of the nitrate ion.

The value of "a" for NH_4NO_3 is assumed to be equal to 0.0038. The heat capacity of NH_4NO_3 is represented by

$$C_p = 3D(150/T) + 3E(178/T) + 3E(320/T) + 3E(455/T) + (0.0038C_v)^2T$$

The Einstein characteristic temperature of 320°K (222 cm^{-1}) is the torsional frequency of the nitrate ion while the Einstein characteristic temperature of 455°K (316 cm^{-1}) is the torsional frequency of the ammonium ion.

Discussion on Three-Dimension Hindered Rotation

The torsional frequencies determined in this chapter for the ammonium ion in ammonium compounds are compared with the results of infrared and inelastic neutron scattering measurements in Table 20. The barriers to rotation for the ammonium ion in ammonium salts are given in Table 21. The torsional frequencies of the ammonium ion evaluated using the three-dimensional hindered rotor theory are in good agreement with the infrared and inelastic neutron scattering measurements. The rotational energy levels need not necessarily be accurate in order to evaluate accurate torsional frequencies, since the rotational heat capacity is a sensitive function of the torsional frequency. A stricter test of the model is a comparison of the rotational heat capacity over a large temperature range predicted by the theory and that determined by experiment. Unfortunately, order-disorder transitions in the ammonium halides do not allow for the experimental determination of the heat capacity of the ammonium ion. The only ammonium salts

TABLE 20

Torsional Frequencies for the Ammonium Halides

Frequencies Expressed in cm^{-1}

	Heat Capacity This Work	Infrared Freq.	Ref.	Neutron Scattering Freq.	Ref.
NH_4F (IV)	548	523	118	560	128
ND_4F (IV)		376	118		
NH_4Cl (I)	389	391	99	393	129
NH_4Cl (II)	326	359	99	350	129
ND_4Cl (I)	288	281	99	285	129
ND_4Cl (II)	239	269	99	264	129
NH_4Br (I)	337				
NH_4Br (III)	345	319	130	340	128
				331	129
NH_4Br (II)	308	311	130	315	128
				324	129
ND_4Br (I)	243	248	130		
ND_4Br (III)		230	130		
ND_4Br (II)	214	217	130		
NH_4I (III)	282	285	131	295	128
NH_4I (II)	282			270	128

I - ordered body-centered cubic

II - disordered body-centered cubic

III - tetragonal

IV - hexagonal

TABLE 21

Heights of Barriers to Rotation for Ammonium Halides

	Barrier Height calories	Torsional Frequency cm^{-1}
NH_4F (IV)	17,200	548
NH_4Cl (I)	5,340	389
NH_4Cl (II)	3,830	326
ND_4Cl (I)	5,560	288
ND_4Cl (II)	3,900	239
NH_4Br (I)	4,070	337
NH_4Br (III)	4,250	345
NH_4Br (II)	3,450	308
ND_4Br (I)	4,020	243
ND_4Br (II)	3,170	214
NH_4I (III)	2,940	282
NH_4I (II)	2,940	282

I - ordered body-centered cubic

II - disordered body-centered cubic

III - tetragonal

IV - hexagonal

TABLE 22

Debye and Einstein Characteristic Temperatures for the Ammonium Halides in their Low Temperatures Phases

$$C_p = 3D(\theta_1/T) + 3E(\theta_2/T) + 3E(\theta_3/T) + (aC_v)^2 T$$

	θ_1	θ_2	θ_3	a
NH_4F	150(2) 390(1)	380	790	0.0035
NH_4Cl	217	263	560	0.0034
ND_4Cl	213	247	413	0.0034
NH_4Br (bcc)	141	243	485	0.0034
NH_4Br (tetra.)	136	237	497	0.0034
ND_4Br	141	225	350	0.0034
NH_4I	101	219	406	0.0036

which have low barriers to rotation and no order-disorder transition are not cubic. However, in KBH_4 and $NaBH_4$ the rotational heat capacity of the borohydride ion may be determined from the experimental heat capacity over a large temperature range. For the hindered rotation of the borohydride ion in KBH_4 the three-dimensional hindered rotor theory gives good semiquantitative agreement with experiment. For rotation of the borohydride ion in $NaBH_4$ the theory gives reasonable qualitative results. Since the rotational heat capacity of the borohydride ion in KBH_4 and $NaBH_4$ have a maximum at about the same temperature, the torsional frequencies of BH_4^- in both KBH_4 and $NaBH_4$ should be about equal. Therefore, the rotational heat capacity of both these salts should be about the same. However, this is not the case. The reason for the difference in the rotational heat capacity of both salts is unclear.

For a given torsional frequency the rotational heat capacity computed from the energy levels of a three-dimensional hindered rotor is too small below the maximum in the heat capacity. The temperature of the maximum is too high in the cases where a comparison is possible. In part, these two errors are due to the inability of the theory to predict the vibrational energy levels just below the barrier to rotation. There are other major assumptions which limit the theory; only the nearest neighbor interactions are considered, the use of perturbation theory for the calculation of the energy levels

above the barrier, and the nuclear spin approximation.

The nuclear spin approximation does not effect the qualitative features of the rotational heat capacity. If, for example, the rotational energy levels had a nuclear spin degeneracy 30% higher than the vibrational levels, the temperature of the maximum in the rotational heat capacity would be the same as if both vibrational and rotational levels has the same nuclear spin degeneracy. The height of the maximum, however, would change by about 15%.

The energy levels used to calculate the heat capacity of BH_4^- in KBH_4 from 0^oK to 450^oK (ν = 250 cm^{-1}), the ammonium ion in the ordered state of NH_4Cl from 0^oK to 300^oK (ν = 389 cm^{-1}), and the deutero-ammonium ion in ND_4Cl from 0^oK to 300^oK (ν = 288 cm^{-1}) are given in Appendix II.

Ammonium Iodide (face-centered cubic)

At 255^oK ammonium iodide undergoes a first-order transition. There is about a 3.8 cal/deg mole decrease in the heat capacity at the transition. This cannot be accounted for by the crystal structure change from a body-centered cubic to a face-centered cubic lattice. Stephenson et. al.[20] proposed that in the face-centered cubic phase the ammonium ion was rotating, while in the body-centered lattice it was behaving as a torsional oscillator.

Since the classical value of the heat capacity of a three dimensional torsional oscillator is 3R and that of a three dimensional free rotor is 3R/2, 3 cal/deg mole can be explained.

The heat capacity of solid solutions of KI and NH_4I have been measured.[103] The face-centered cubic form of NH_4I may be supercooled when KI is present. A 80.2% NH_4I solid solution may be supercooled down to 110°K, while a 45.8% NH_4I solid solution exists only in the face-centered cubic lattice.

The heat capacity of the 45.8% NH_4I - 54.2% KI solid solution exhibited an anomolously high heat capacity at liquid hydrogen temperatures. This was explained by assuming that the barrier to rotation is very low. No definite conclusion was reached as to the number of degrees of freedom for nearly free rotation of the ammonium ion.[103]

In order to study the motion of the ammonium ion in the solid solutions it is necessary to know the lattice heat capacities of the solid solutions. The lattice heat capacities of face-centered cubic alkali halides, as mentioned in the Introduction, may be represented by

$$C_p = 3D(\theta_1/T) + 3E(\theta_2/T) + (aC_v)^2T \qquad (52)$$

The values of θ_1, θ_2, and "a" for NaI,[14] RbI,[115] and KI[14] have been determined from their respective heat capacity results. The lattice

heat capacities of face-centered cubic NH_4I and that of the solid solutions may be determined by the same method as that used for magnetic compounds. The value of θ_1 for NaI, KI, and RbI is nearly a linear function of $\sqrt{M} \times V$, while θ_2 is nearly a linear function of $\mu \times V$. θ_2 is not a linear function of $\sqrt{\mu} \times V$. The value of "a" for the solid solutions may be estimated from those of the alkali halides. The molar volumes of the solid solutions were determined by assuming the additivity of densities for NH_4I and KI. The values for the parameters in (52) are given in Table 23. Using these parameters it is possible to evaluate the heat capacity of the ammonium ion in the solid solutions. For the solid solution containing 45.8% NH_4I, these values are given in Table 24. Also in this table is the heat capacity of the ammonium ion assuming that the ammonium ion is a one-dimensional rotor, i.e. the ammonium ion is rotating freely around a N-H bond. The ammonium ion in this case is a symmetric top with a symmetry number of 3. The nuclear spin degeneracy makes no contribution to the heat capacity for this case. The heat capacity of a one-dimensional free rotor resembles that of the ammonium ion in the solid solution. Both have a maximum at about $30^{\circ}K$. This data illustrates that the ammonium ion behaves as a one-dimensional rotor with a very low barrier to rotation and does not behave as a three-dimensional rotor. A three dimensional free rotor would make a much larger contribution to the heat capacity.

TABLE 23

Debye and Einstein Characteristic Temperatures for Solid Solutions of Ammonium Iodide and Potassium Iodide

Percentage NH_4I	KI	θ_1	θ_2	a
100	0	89	184	0.0036
80.2	19.8	90	179	0.0038
45.8	54.2	90	171	0.0040
0	100	90	161	0.0044

Parameters are for face-centered structures. The parameters for the first three compositions have been estimated.

$$C_p = 3D(\theta_1/T) + 3E(\theta_2/T) + (aC_v)^2T$$

TABLE 24

The Heat Capacity of the Ammonium Ion in a Solid Solution 45.8% NH_4I and 54.2% KI between 15°K and 60°K.

Heat Capacity expressed in cal. $deg.^{-1}$ $mole^{-1}$		
Temperature	$C(NH_4^+)$	C(free rotation)
15	1.27	0.62
20	1.54	1.17
25	1.69	1.46
26	1.71	1.49
27	1.71	1.51
28	1.71	1.519
29	1.73	1.523
30	1.73	1.522
32	1.68	1.50
34	1.64	1.47
36	1.57	1.44
38	1.49	1.39
40	1.49	1.35
45	1.45	1.25
50	1.45	1.17
55	1.47	1.11
60	1.58	1.06

$C(NH_4^+)$ is the heat capacity of the ammonium ion in the solid solution assuming that the lattice heat capacity of the solid solution can be represented by the Debye and Einstein characteristic temperatures given in Table 23. C(free rotation) is the heat capacity of a free rotor (one dimension) which has a symmetry number of three.

If the Debye characteristic temperature is lowered by $3^{o}K$ to $87^{o}K$, the resulting heat capacity of the ammonium ion in the solid solution (45.8% NH_4I) corresponds nearly exactly to the heat capacity of a one-dimensional free rotor below $50^{o}K$. Between $50^{o}K$ and $130^{o}K$ the difference between the heat capacity of the ammonium ion and that of a one-dimensional free rotor can be represented by an Einstein function ($350^{o}K$) with two degrees of freedom. Above $130^{o}K$ the heat capacity of the ammonium ion is less than the sum of the heat capacities of a one-dimensional free rotor and a two dimensional torsional oscillator with a frequency of $350^{o}K$ ($243\ cm^{-1}$) (see Table 25). The Einstein function cannot represent the two degrees of freedom of hindered rotation above $130^{o}K$ because the rotational levels of the ammonium ion begin to contribute to the heat capacity.

In the face-centered cubic lattice only one of the N-H bonds may have close approach to an iodide ion. In the 45.8% NH_4I solid solution, the ammonium ion is freely rotating around this N-H bond. For the other two degrees of freedom the ammonium ion acts as a torsional oscillator. For the 80.2% NH_4I solid solution the frequency of torsional oscillation for the ammonium ion is lowered to $290^{o}K$ ($200\ cm^{-1}$). Between $100^{o}K$ and $300^{o}K$ the heat capacity of the ammonium ion in the 80.2% NH_4I solid solution is greater than that of the ammonium ion in the 45.8% NH_4I solid solution. Between $235^{o}K$ and $300^{o}K$ the heat capacity of the ammonium ion in the face-

TABLE 25

The Heat Capacity of the Ammonium Ion in a Solid Solution

45.8% NH_4I and 54.2% KI between 15°K and 300°K

Temperature °K	Heat Capacity expressed in cal. $deg.^{-1}$ $mole^{-1}$			
	C_1	C_2	$C_1 + C_2$	$C(NH_4^+)$
15	0.62	0.00	0.62	1.03
20	1.17	0.00	1.17	1.24
25	1.46	0.00	1.46	1.40
26	1.49	0.00	1.49	1.44
27	1.51	0.00	1.51	1.47
28	1.519	0.00	1.519	1.49
29	1.523	0.00	1.523	1.47
30	1.522	0.00	1.522	1.49
32	1.50	0.00	1.50	1.49
34	1.47	0.00	1.47	1.44
36	1.44	0.00	1.44	1.33
38	1.39	0.02	1.41	1.31
40	1.35	0.04	1.39	1.33
45	1.25	0.10	1.35	1.30
50	1.17	0.17	1.34	1.33
55	1.11	0.27	1.38	1.38
60	1.06	0.40	1.46	1.46
65	1.04	0.54	1.58	1.62
70	1.02	0.68	1.70	1.75
80	1.00	0.99	1.99	1.97

TABLE 25 (continued)

Temperature °K	Heat Capacity expressed in cal. deg.$^{-1}$ mole^{-1} C_1	C_2	$C_1 + C_2$	$C(NH_4^+)$
90	1.00	1.28	2.28	2.23
100	1.00	1.56	2.56	2.49
110	1.00	1.82	2.82	2.80
120	1.00	2.05	3.05	2.97
130	1.00	2.24	3.24	3.14
140	1.00	2.42	3.42	3.26
150	1.00	2.58	3.58	3.44
160	1.00	2.71	3.71	3.54
170	1.00	2.82	3.82	3.65
180	1.00	2.92	3.92	3.72
190	1.00	3.02	4.02	3.80
200	1.00	3.10	4.10	3.85
220	1.00	3.23	4.23	3.89
240	1.00	3.34	4.34	3.96
260	1.00	3.42	4.42	4.06
280	1.00	3.49	4.49	4.17
300	1.00	3.55	4.55	4.15

C_1 represents heat capacity of one dimension free rotor which has a symmetry number of three. $C_2 = 2E(350/T)$. $C(NH_4^+)$ is the heat capacity of the ammonium ion in the solid solution assuming the lattice heat capacity is given by $C_p = 3D(87/T) + 3E(170/T) + C(int) + (0.0040C_v)^2T$.

centered cubic NH_4I is about the same as that in the 80.2% solid solution. It is not surprising that the torsional frequency is greater as the percentage of NH_4^+ decreases, since as the percentage decreases the volume of the unit cell decreases. This makes it more difficult for the ammonium ion to move.

The conclusion that the ammonium ion acts as a one-dimensional pseudo-free rotor has also been reached by Hornig and Veeder[127] from infrared studies of solid solutions of NH_4I and KI. They also proposed that the barrier to rotation for the other two degrees of freedom is relatively high. From the heat capacity results the barrier to rotation of the ammonium ion around an N-H bond is less than 50 cm^{-1}. A barrier higher than this will produce significant discrepancies between the observed and calculated values of the heat capacity.

Hydroxides

The hydroxyl ion undergoes torsional oscillations in NaOH, LiOH, $Mg(OH)_2$, and $Ca(OH)_2$. The frequency of the torsional oscillation has not been determined conclusively from spectroscopic data.

LiOH possesses tetragonal symmetry, belonging to the space group D^7_{4h}-P4/nmm.[132,133] There are two lithium ions and two hydroxyl

ions per unit cell. It is impossible to represent the heat capacity results of LiOH to a Debye function with three degrees of freedom and an Einstein function with three degrees of freedom. Instead, a Debye function with 1.5 degrees of freedom and an Einstein function with 4.5 degrees of freedom must be used. In the unit cell of LiOH, there are three translatory vibrations and nine vibrations of one ion with respect to the others. Since there are two molecular units per unit cell it is reasonable to fit the lattice heat capacity to a Debye function with 3/2 degrees of freedom and an Einstein function with 9/2 degrees of freedom. The contribution of the librational motion of the hydroxyl ion to the heat capacity of LiOH is represented by an Einstein function with two degrees of freedom.

The sodium hydroxide unit cell is orthorhombic.[32] The lattice heat capacity may be prepresented by a Debye function with three degrees of freedom and an Einstein function with three degrees of freedom. As with LiOH, the torsional motion of the hydroxyl ion is represented by an Einstein function with two degrees of freedom.

Both $Mg(OH)_2$ and $Ca(OH)_2$ are hexagonal, belonging to the space group $D^3_{3d}(P\bar{3}m)$.[134-136] The lattice heat capacity of these hydroxides may be represented by a Debye function with three degrees of freedom and an Einstein function with six degrees of freedom. The

heat capacity due to the torsional oscillation of the hydroxide ion is represented by an Einstein function with four degrees of freedom.

The heat capacity results of the hydroxides may be represented by the following functions:

$$\text{LiOH} \quad C_p = 3/2D(240/T) + 9/2E(540/T) + 2E(1010/T) + (0.0034C_v)^2T$$

$$\text{NaOH} \quad C_p = 3D(290/T) + 3E(370/T) + 2E(700/T) + (0.0036C_v)^2T$$

$$\text{Mg(OH)}_2 \quad C_p = 3D(357/T) + 6E(529/T) + 4E(960/T) + (0.0010C_v)^2T$$

$$\text{Ca(OH)}_2 \quad C_p = 3D(260/T) + 6E(420/T) + 4E(800/T) + (0.0019C_v)^2T$$

TABLE 26

Torsional Frequencies for the Hydroxides

	Torsional Frequency cm^{-1}	Reference for Heat Capacity Data
LiOH	700	138
NaOH	486	139
$Mg(OH)_2$	666	140
$Ca(OH)_2$	555	141

The torsional frequencies evaluated from heat capacity data bear little resemblance to the frequencies obtained by infrared and Raman spectra.[142]

Ice

There has been a great amount of speculation as to the torsional frequency of the water molecule in ice.[143,144] Spectroscopic studies indicate a torsional frequency of 800 cm^{-1} in ice, while inelastic neutron scattering experiments yield a lower value. Heat capacity measurements have been carried out for both heavy and regular ice.[165,166]

There are two different moments of inertia for the water molecule,[145] so there should be two different torsional frequencies.

$$I_z = I_y = 1.908 \times 10^{-40} \text{ g. cm}^2$$

$$I_x = 0.996 \times 10^{-40} \text{ g. cm}^2$$

Since the torsional frequency depends on the square root of the moment of inertia, the two torsional frequencies should differ by about a factor of $\sqrt{2}$. If the environment of the water molecule in ice is also considered, the difference in the frequencies should decrease.[146]

The lattice heat capacity of H_2O and D_2O could not be represented by a Debye function with three degrees of freedom and an Einstein function with three degrees of freedom. Ice possesses hexagonal symmetry, so it is not surprising that the Debye function

must be split.

$$H_2O \quad C_p = D(132/T) + 2D(430/T) + 3E(960/T) + E(2380/T) + (0.0080C_v)^2T$$

$$D_2O \quad C_p = D(126/T) + 2D(418/T) + 3E(730/T) + E(1696/T) + (0.0080C_v)^2T$$

The Einstein function with three degrees of freedom represents the torsional frequency. No evidence for two different torsional frequencies was found. The Einstein function with one degree of freedom represents the bending frequency, which has been determined from spectroscopic results.

TABLE 27

Torsional Frequency of Water Molecule in H_2O and D_2O Lattices

	This Work cm^{-1}	Spectroscopy cm^{-1}	Neutron Scattering cm^{-1}
H_2O	666	800	630(2) 849(1)
D_2O	507	600	-

Number in parenthesis indicates degeneracy.

Blue[146] has calculated the torsional frequencies in H_2O and D_2O by subtracting the heat capacity of H_2O from that of D_2O and representing the resulting curve by a difference of two Einstein functions. He found the torsional frequency of H_2O to be 660 cm^{-1} and D_2O to be 475 cm^{-1}.

Hydrogen Peroxide

In the solid state H_2O_2 is tetragonal belonging to the space group D_4^4-$P4_12_1$.[147] Two of the three moments of inertia are about equal and are about ten times as large as the third moment of inertia. The heat capacity[148] of hydrogen peroxide may be represented by

$$C_p = 3D(235/T) + 2E(384/T) + 2E(1080/T) + C(int) + (0.0080C_v)^2T$$

The internal frequencies are given by Giguere.[149] The characteristic temperature of 384°K (267 cm^{-1}) represents two of the three hindered rotations of the H_2O_2 molecule as a whole. These two frequencies are infrared inactive, but have been estimated by Giguere to be 290 cm^{-1}.[149] Raman spectra indicates that the frequencies are 245 cm^{-1} and 289 cm^{-1}.[150]

The third hindered motion of the molecule as a whole and the internal motion of the hydroxyl groups have about the same frequency. According to the heat capacity analysis these frequencies are both 1080°K (750 cm^{-1}). Infrared measurements on the solid yield frequencies of 661 cm^{-1} and 695 cm^{-1}.[149]

Ferrocene

The ferrocene molecule (bis-cyclopentadenyl iron-II) has a "sandwich" structure, possessing symmetry of the point group D_{5d}. X-ray diffraction studies have determined that the ferrocene crystal is monoclinic with two molecules per unit cell.[160,161]

The torsional frequency has not been observed by infrared studies of solid ferrocene.[162] The heat capacity results[163] have therefore been examined in order to study the motion of the cyclopentadienyl rings. Ferrocene undergoes a second order phase transition at 164°K. The entropy associated with this transition is about R ln2. Edwards et. al.[163,164] have explained the transition in terms of the relative positions of the cyclopentadienyl rings. Due to this transition the heat capacity could be represented by a sum of Debye and Einstein functions only up to 50°K and near room temperature.

There is one degree of freedom for the torsional motion of the cyclopentadienyl rings. The potential function for this motion is given by

$$V(\theta) = \frac{V_o}{2} (1 - \cos 5\theta)$$

where V_o is the height of the barrier to rotation. No anharmonic contribution is made to the heat capacity below 50°K for frequencies

greater than $60^{o}K$, so that the heat capacity may be determined using tabulated Einstein functions. For frequencies less than $60^{o}K$, the heat capacity was determined from the tables of Pitzer et. al.[92] The rotational constant for ferrocene is 0.152 cm^{-1}.[126]

The heat capacity of solid ferrocene may be represented by

$$C_p = 3D(85/T) + 3E(123/T) + E(63/T) + C(int) + (0.0034C_v)^2T$$

The frequencies of the internal vibrations have been determined by Winter et. al.[162] The one degree of torsional freedom has a frequency of $63^{o}K$ (44 cm^{-1}) in the above representation of the heat capacity. Unfortunately, this frequency cannot be given an upper limit, since if the value of this frequency is increased and the value of the lattice frequency ($123^{o}K$) is decreased, the heat capacity data can be represented equally well. For example, the following function also can represent the heat capacity data:

$$C_p = 3D(73/T) + 3E(107/T) + E(140/T) + C(int) + (0.0034C_v)^2T$$

A lower limit can be set to the torsional frequency. No torsional frequency less than $55^{o}K$ (38 cm^{-1}) is allowed by the heat capacity data. This frequency corresponds to a barrier to rotation of 1150 cal. From nuclear magnetic resonance line width data, Mulay and Attalla[158] estimated the value of the barrier to rotation to be 2300 cal.

Quartic Oscillator

Bell has suggested that the out-of-plane bending motion of four-membered rings may be quartic in nature.[151] Infrared studies[152] and microwave work[153] have shown that this motion in trimethylene oxide is quartic in nature. Heat capacity measurements have been reported for cyclobutane[154] and trimethylene sulfide.[155] These results have been analyzed to determine whether the out-of-plane bending motion in the solid is quartic in nature in these compounds.

For the potential function $V(x) = ax^4$, Schroedinger's equation is

$$\frac{d^2\Psi}{dy^2} + (\lambda - \xi^4)\Psi = 0$$

$$\xi = \left[\frac{2ma}{\hbar^2}\right]^{1/6} x \qquad \lambda = 4E\left[\frac{m^2}{16\hbar^4 a}\right]^{1/3}$$

E is the total energy. The eigenvalues of λ have been given by Chan, Stelman, and Thompson.[156] The energy of the n th level is

$$E_n = h\nu_o\left[\frac{\lambda_n}{\lambda_1 - \lambda_o}\right]$$

where

$$\nu_o = \frac{1}{4}(\lambda_1 - \lambda_o)\left[\frac{2\pi a}{\pi^3 m^2}\right]^{1/3}$$

The heat capacity of a quartic oscillator can be found by using the relations

$$C_v = \frac{R}{Q}\left[\sum_n x_n^2 \exp(-x_n) - \left\{\sum_n x_n \exp(-x_n)\right\}^2 \frac{1}{Q}\right]$$

$$Q = \sum_n \exp(-x_n)$$

$$x_n = E_n/kT$$

The classical value of the heat capacity of a quartic oscillator is 3/4R.

The heat capacity of cyclobutane may be represented by the following function:

$$C_p = 3D(130/T) + 3E(165/T) + E(386/T) + C(\text{int}) + (0.0125C_v)^2 T$$

C(int) is the heat capacity due to the internal vibrations. The frequencies of the internal vibrations were taken from Lord and Nakagawa.[157] The out-of-plane bending motion has a frequency of

386°K (268 cm^{-1}). No determination could be made of the nature of the motion. When $h\nu/kT$ is large, the quartic and quadratic oscillator make the same contribution to the heat capacity. It is only when the vibration becomes close to fully excited, i.e. $h\nu/kT$ is small, that the contributions of the quartic and quadratic oscillators to the heat capacity differ. Cyclobutane melts at 192°K. The heat capacity of the solid can be represented by (1) only up to 100°K, because above this temperature pre-melting effects contribute to an anomalously high heat capacity. At 100°K the difference between the contribution of the quartic and the quadratic oscillators to the heat capacity in cyclobutane is too small to differentiate between the two types of motion.

Lord and Nakagawa[157] have estimated the frequency of the out-of-plane motion in gaseous cyclobutane to be 200 cm^{-1}. The heat capacity result is significantly higher. This is not surprising since this motion should be more restricted in the solid phase. The significant increase in the frequency of a vibration going from the gaseous to the solid phase has also been found in iodine.[12]

The heat capacity results of trimethylene sulfide could not be reproduced by a sum of Debye and Einstein functions, if the out-of-plane bending motion was assumed to be quadratic in nature.

The heat capacity may be represented by:

$$C_p = 3D(125/T) + 3E(167/T) + E_{qt}(110/T) + C(int) + (0.0098C_v)^2T \quad (53)$$

$E_{qt}(x)$ is the contribution of the quartic oscillator to the heat capacity. The internal vibrations were taken from Scott et. al.[155] The frequency of the out-of-plane bending motion is $110^oK \pm 30^oK$ ($75\ cm^{-1} \pm 20\ cm^{-1}$). The large uncertainty in the value of the frequency is due to the fact that the value of the frequency is low. By changing the lattice frequency and the frequency of the quartic oscillator, functions different from (53) can reproduce the heat capacity results. For example, the following two functions were found to give good representations of the heat capacity:

$$C_p = 3D(138/T) + 3E(163/T) + E_{qt}(80/T) + C(int) + (0.0098C_v)^2T$$

$$C_p = 3D(118/T) + 3E(168/T) + E_{qt}(130/T) + C(int) + (0.0098C_v)^2T$$

Infrared studies have indicated that there is a small quadratic term in addition to the quartic term in the potential for the out-of-plane bending motion in trimethylene sulfide.[159] The heat capacity data is not sufficiently sensitive to the contribution of the out-of-plane bending motion to determine the amount of quadratic nature, if any, to the potential function.

Summary

In this past chapter torsional frequencies have been determined from heat capacity results for a number of compounds. Usually the results are in excellent agreement with spectroscopic results. There are some limitations on the evaluation of torsional frequencies from heat capacity results. The torsional frequency must be about 120-170 cm^{-1} above the lattice frequencies. If the torsional frequency is not much larger than the lattice frequencies, then it is impossible to determine unambiguously the value of the torsional frequency. This difficulty was encountered in the analysis of the heat capacity results of $LiBH_4$, ferrocene, and trimethylene sulfide.

The torsional frequency must have a value less than 800 cm^{-1}. If the frequency of oscillation is higher than 800 cm^{-1}, the contribution to the heat capacity of this vibration is too small to allow for its evaluation. For high frequencies the contribution of both the torsional oscillation and $(C_p - C_v)$ are about the same. Therefore, neither of these values, the torsional frequency and the value of "a" used to determine $(C_p - C_v)$ are known well. The results of varying the torsional frequency and the value of "a" for NaOH and LiOH are given in Tables 28 and 29. The torsional frequency of OH^- in NaOH is between 680°K and 700°K. Therefore, in NaOH the range of the torsional frequency is quite small. For LiOH

TABLE 28

Accuracy of the Torsional Frequency of OH^- in NaOH

$$C_p = 3D(290/T) + 3E(370/T) + 2E(\theta/T) + (aC_v)^2 T$$

$\theta(^oK)$	a	Per Cent Error in Various Temperature Ranges				
		0^oK-50^oK	50^oK-100^oK	100^oK-150^oK	over 150^oK	Overall
640	0.0030	2.783	0.725	0.886	0.743	1.156
660	0.0032	2.783	0.627	0.526	0.480	0.956
670	0.0034	2.783	0.650	0.423	0.521	0.969
680	0.00345	2.783	0.678	0.450	0.360	0.891
690	0.00355	2.783	0.703	0.632	0.320	0.895
700	0.0036	2.783	0.729	0.900	0.219	0.877
710	0.0037	2.783	0.753	1.115	0.266	0.932
720	0.0038	2.783	0.776	1.317	0.345	1.003

TABLE 29

Accuracy of the Torsional Frequency of OH^- in LiOH

$$C_p = 1.5D(240/T) + 4.5E(540/T) + 2E(\theta/T) + (aC_v)^2T$$

$\theta(^oK)$	a	Per Cent Error in Various Temperature Ranges				
		0^oK-50^oK	50^oK-100^oK	100^oK-150^oK	over 150^oK	Overall
940	0.0027	8.700	0.444	0.513	0.860	1.810
960	0.0029	8.700	0.457	0.297	0.609	1.645
980	0.0031	8.700	0.470	0.142	0.406	1.516
990	0.0032	8.701	0.474	0.110	0.323	1.468
1000	0.0032	8.701	0.488	0.115	0.255	1.436
1010	0.0034	8.701	0.477	0.124	0.194	1.404
1020	0.0035	8.701	0.476	0.174	0.191	1.411
1030	0.0037	8.702	0.461	0.181	0.138	1.382
1040	0.0038	8.703	0.458	0.228	0.160	1.401
1060	0.0041	8.704	0.433	0.251	0.143	1.292
1080	0.0043	8.704	0.417	0.301	0.224	1.440
1100	0.0045	8.705	0.398	0.330	0.296	1.479
1120	0.0047	8.706	0.375	0.341	0.347	1.504
1140	0.0049	8.706	0.350	0.334	0.382	1.516
1160	0.0051	8.708	0.321	0.314	0.406	1.521
1200	0.0054	8.709	0.288	0.304	0.500	1.562

the range is much larger, about 200°K.

In some problems, it is possible to represent the lattice heat capacity of compounds by two different types of representations. For NH_4Cl the lattice heat capacity can be represented by a Debye function with six degrees of freedom, instead of a Debye function with three degrees of freedom and an Einstein function with three degrees of freedom. As shown in Table 30, the torsional frequency is only 10°K different from one representation to the other.

TABLE 30

Accuracy of the Torsional Frequency of NH_4^+ in NH_4Cl

Representation of Heat Capacity	Average Deviation 0°K - 100°K
$6D(282/T)+3E(570/T)+(0.0034C_v)^2T$	0.026
$6D(282/T)+3E(560/T)+(0.0034C_v)^2T$	0.040
$3D(217/T)+3E(263/T)+3E(580/T)+(0.0034C_v)^2T$	0.029
$3D(217/T)+3E(263/T)+3E(560/T)+(0.0034C_v)^2T$	0.019
$3D(217/T)+3E(263/T)+3E(550/T)+(0.0034C_v)^2T$	0.029

Average deviations expressed in calories $degree^{-1}$ $mole^{-1}$

APPENDIX I

MAGNETIC HEAT CAPACITIES OF SOME ANTIFERROMAGNETIC COMPOUNDS

TABLE 31

Magnetic Heat Capacity and Entropy of Chromic Oxide

Temperature ^{o}K	Magnetic Heat Capacity	Magnetic Entropy e.u.	$S_m/R\ln(2S + 1)$
110	0.14	0.02	0.007
120	0.28	0.03	0.01
130	0.46	0.06	0.02
140	0.64	0.10	0.04
150	0.80	0.15	0.05
160	0.98	0.21	0.08
170	1.19	0.28	0.10
180	1.39	0.35	0.13
190	1.63	0.43	0.16
200	1.88	0.52	0.19
210	2.15	0.62	0.22
220	2.44	0.73	0.26
230	2.75	0.84	0.30
240	3.05	0.97	0.35
250	3.38	1.10	0.40
260	3.77	1.24	0.45
270	4.23	1.39	0.50
280	4.78	1.55	0.56
290	5.51	1.73	0.63
300	6.55	1.93	0.70
305.5	7.33	2.03	0.74
310	4.25	2.16	0.78
315	3.02	2.22	0.80
320	2.30	2.26	0.82
330	1.62	2.32	0.84
335	1.40	2.34	0.85

TABLE 32

Magnetic Heat Capacity and Entropy of Manganese Titanate

Temperature ^{o}K	Magnetic Heat Capacity	Magnetic Entropy e.u.	$S_m/R\ln(2S + 1)$
31	1.18	0.50	0.14
32	1.24	0.54	0.15
34	1.34	0.61	0.17
36	1.46	0.69	0.19
38	1.57	0.78	0.22
40	1.68	0.86	0.24
42	1.83	0.94	0.26
44	1.95	1.03	0.29
46	2.08	1.12	0.31
48	2.22	1.21	0.34
50	2.38	1.30	0.37
52	2.57	1.40	0.39
54	2.77	1.51	0.42
56	2.99	1.60	0.45
58	3.24	1.72	0.48
60	3.51	1.83	0.51
61	3.65	1.90	0.53
62	3.81	1.93	0.54
62.3	3.85	1.97	0.55
63	3.41	2.01	0.57
64	3.20	2.06	0.58
66	2.85	2.15	0.61
68	2.68	2.24	0.63
70	2.59	2.32	0.65

TABLE 32 (Continued)

Temperature ^{o}K	Magnetic Heat Capacity	Magnetic Entropy e.u.	$S_m/R\ln(2S + 1)$
72	2.47	2.38	0.67
74	2.39	2.45	0.69
76	2.28	2.51	0.71
78	2.20	2.57	0.72
80	2.14	2.62	0.74
85	1.93	2.75	0.77
90	1.76	2.85	0.80
95	1.60	2.94	0.83
100	1.47	3.03	0.85
110	1.24	3.16	0.89
120	1.02	3.25	0.91
130	0.79	3.33	0.94
140	0.61	3.38	0.95
150	0.49	3.41	0.96
160	0.41	3.44	0.97
170	0.35	3.47	0.98
180	0.24	3.49	0.98
190	0.15	3.50	0.98
200	0.08	3.50	0.98
210	0.01	3.51	0.99

TABLE 33

Magnetic Heat Capacity and Entropy of Manganese Fluoride

Temperature ^{o}K	Magnetic Heat Capacity	Magnetic Entropy e.u.	$E_m/R\ln(2S + 1)$
15	0.53	0.19	0.053
20	0.94	0.40	0.11
25	1.35	0.65	0.18
30	1.74	0.93	0.26
35	2.07	1.22	0.34
40	2.35	1.52	0.43
45	2.63	1.81	0.51
50	2.95	2.10	0.59
55	3.34	2.40	0.67
60	3.88	2.72	0.76
65	4.85	3.06	0.86
66.5	5.23	3.19	0.90
70	1.81	3.28	0.92
75	1.18	3.39	0.95
80	0.84	3.44	0.97
90	0.49	3.52	0.99
100	0.32	3.56	1.00
110	0.21	3.59	1.01
120	0.15	3.60	1.01
130	0.10	3.61	1.01
140	0.06	3.62	1.02
150	0.04	3.62	1.02

TABLE 34

Magnetic Heat Capacity of Ferrous Fluoride

Temperature ^{o}K	Magnetic Heat Capacity	C(Schottky) cal/deg/mole	C(coop)	S(coop) e.u.	S(coop)/ Rln(2S + 1)
15	0.07	0	0.07	0.010	0.003
20	0.28	0	0.28	0.056	0.018
25	0.58	0	0.58	0.15	0.047
30	0.94	0	0.94	0.28	0.087
35	1.30	0	1.30	0.46	0.14
40	1.66	0	1.66	0.65	0.20
45	2.03	0	2.03	0.87	0.27
50	2.40	0	2.40	1.10	0.34
55	2.81	0	2.81	1.35	0.42
60	3.28	0	3.28	1.62	0.51
65	3.85	0	3.85	1.90	0.59
70	4.61	0	4.61	2.21	0.69
75	5.97	0	5.97	2.57	0.80
78.35	12.6	0	12.6	2.81	0.88
80	1.84	0	1.84	2.95	0.92
85	1.04	0	1.04	3.03	0.95
90	0.77	0	0.77	3.08	0.96
100	0.49	0	0.49	3.14	0.98
110	0.34	0	0.34	3.19	0.99
120	0.25	0	0.25	3.21	1.00
130	0.19	0	0.19	3.23	1.01
140	0.17	0.01	0.16	3.25	1.02
150	0.15	0.01	0.14	3.26	1.02
160	0.14	0.02	0.12	3.26	1.02
170	0.12	0.03	0.09	3.27	1.02

TABLE 34 (Continued)

Temperature ^{o}K	Magnetic Heat Capacity	C(Schottky) cal/deg/mole	C(coop)	S(coop) e.u.	S(coop)/ Rln(2S + 1)
180	0.10	0.04	0.06	3.28	1.03
190	0.11	0.06	0.05	3.28	1.03
200	0.11	0.08	0.03	3.28	1.03
210	0.12	0.10	0.02	3.28	1.03
220	0.13	0.13	-	-	-
230	0.15	0.15	-	-	-
240	0.18	0.18	-	-	-
250	0.22	0.21	-	-	-
260	0.25	0.24	-	-	-
270	0.28	0.28	-	-	-
280	0.30	0.31	-	-	-
290	0.33	0.34	-	-	-
300	0.38	0.38	-	-	-

C(Schottky) is the heat capacity of a two energy level system; the energy levels being $1430^{o}K$ (992 cm^{-1}) apart. C(coop) is the heat capacity associated with the cooperative phenomena. S(coop) is the entropy associated with the cooperative phenomena.

TABLE 35

Magnetic Heat Capacity of Cobalt Fluoride

Temperature ^{o}K	Magnetic Heat Capacity	C(Schottky)	C(coop)	S(coop) e.u.	S(coop)/ Rln(2S + 1)
15	0.23	0.00	0.23	0.04	0.03
20	0.60	0.00	0.60	0.16	0.12
25	1.10	0.02	1.08	0.34	0.24
30	1.73	0.07	1.67	0.59	0.43
35	2.66	0.15	2.51	0.90	0.65
37.7	4.17	0.19	3.98	1.13	0.82
40	0.99	0.24	0.75	1.21	0.88
45	0.81	0.35	0.46	1.28	0.93
50	0.80	0.46	0.34	1.33	0.96
55	0.82	0.56	0.26	1.35	0.98
60	0.85	0.65	0.20	1.37	0.99
65	0.88	0.72	0.16	1.39	1.01
70	0.90	0.78	0.12	1.40	1.01
75	0.93	0.82	0.11	1.41	1.02
80	0.91	0.85	0.06	1.42	1.03
90	0.90	0.87	0.03	1.42	1.03
100	0.87	0.87	0.00	1.42	1.03
110	0.84	0.84	-	-	-
120	0.80	0.81	-	-	-
130	0.78	0.77	-	-	-
140	0.79	0.74	-	-	-
150	0.72	0.71	-	-	-
160	0.70	0.68	-	-	-

TABLE 35 (Continued)

Temperature ^{o}K	Magnetic Heat Capacity	C(Schottky)	C(coop)	S(coop) e.u.	S(coop)/ Rln(2S + 1)
170	0.67	0.66	-	-	-
180	0.66	0.65	-	-	-
190	0.65	0.64	-	-	-
200	0.64	0.64	-	-	-
210	0.63	0.64	-	-	-
220	0.63	0.64	-	-	-
230	0.63	0.64	-	-	-
240	0.64	0.65	-	-	-
250	0.65	0.66	-	-	-
260	0.66	0.67	-	-	-
270	0.68	0.68	-	-	-
280	0.71	0.69	-	-	-
290	0.73	0.71	-	-	-
300	0.77	0.72	-	-	-

C(Schottky) is the heat capacity of a system comprised of four energy levels; the energy of these levels given in cm^{-1} are 0, 153, 750, and 1300. The lowest energy level is defined as 0. C(coop) is the heat capacity associated with the cooperative effect. S(coop) is the entropy associated with the cooperative effect.

TABLE 36

Magnetic Heat Capacity and Entropy of Chromous Chloride

Temperature °K	Magnetic Heat Capacity	Magnetic Entropy e.u.	$S_m/R\ln(2S+1)$
10	0.72	0.30	0.08
11	0.90	0.38	0.12
12	1.12	0.46	0.14
13	1.45	0.57	0.18
14	1.76	0.69	0.22
15	2.25	0.82	0.25
16	2.92	0.99	0.31
16.06	2.97	1.00	0.31
17	1.91	1.13	0.35
18	1.70	1.23	0.38
19	1.67	1.32	0.41
20	1.68	1.40	0.44
21	1.69	1.48	0.46
22	1.70	1.56	0.49
23	1.70	1.64	0.51
24	1.70	1.71	0.53
25	1.69	1.78	0.56
30	1.59	2.09	0.65
35	1.43	2.32	0.73
40	1.23	2.50	0.78
45	1.04	2.63	0.82
50	0.86	2 .73	0.85
55	0.72	2.81	0.88
60	0.59	2.87	0.90
65	0.48	2.90	0.91

TABLE 36 (Continued)

Temperature °K	Magnetic Heat Capacity	Magnetic Entropy e.u.	$S_m/R\ln(2S+1)$
70	0.39	2.94	0.92
75	0.31	2.96	0.93
80	0.25	2.98	0.93
90	0.14	3.00	0.94
100	0.05	3.02	0.95

TABLE 37

Magnetic Heat Capacity and Entropy of Cupric Chloride

Temperature °K	Magnetic Heat Capacity	Magnetic Entropy e.u.	$S_m/R\ln(2S+1)$
10	0.19	0.08	0.06
15	0.41	0.20	0.14
20	0.77	0.36	0.26
21	0.87	0.40	0.29
22	1.00	0.44	0.32
23	1.18	0.49	0.35
23.92	1.36	0.53	0.38
24	1.33	0.55	0.40
25	1.03	0.59	0.43
30	0.97	0.77	0.56
35	0.92	0.91	0.66
40	0.83	1.04	0.75
45	0.68	1.12	0.81
50	0.62	1.20	0.87
55	0.53	1.25	0.91
60	0.46	1.29	0.94
65	0.38	1.32	0.96
70	0.30	1.35	0.98
75	0.25	1.37	0.99
80	0.21	1.39	1.01
90	0.14	1.41	1.02
100	0.05	1.42	1.03

TABLE 38

Magnetic Heat Capacity of Cobalt Chloride

Temperature °K	Magnetic Heat Capacity	C(Schottky)	C(coop)	S(coop) e.u.	S(coop)/ Rln(2S+1)
10	0.21	0.00	0.21	0.08	0.006
15	0.58	0.00	0.58	0.23	0.17
20	1.30	0.00	1.30	0.48	0.35
24.71	3.52	0.00	3.52	0.91	0.66
25	1.99	0.00	1.99	0.93	0.68
30	0.97	0.01	0.96	1.16	0.84
35	0.73	0.03	0.70	1.29	0.94
40	0.58	0.07	0.51	1.37	0.99
45	0.47	0.12	0.35	1.42	1.03
50	0.42	0.19	0.23	1.45	1.05
60	0.44	0.35	0.09	1.48	1.07
70	0.58	0.53	0.05	1.49	1.08
80	0.70	0.70	-	-	-
90	0.87	0.84	-	-	-
100	0.95	0.97	-	-	-
110	1.03	1.06	-	-	-
120	1.12	1.14	-	-	-
130	1.18	1.20	-	-	-
140	1.23	1.25	-	-	-
150	1.28	1.28	-	-	-
160	1.32	1.31	-	-	-
170	1.34	1.33	-	-	-
180	1.36	1.35	-	-	-
190	1.37	1.37	-	-	-

TABLE 38 (Continued)

Temperature °K	Magnetic Heat Capacity	C(Schottky)	C(coop)	S(coop) e.u.	S(coop)/ Rln(2S+1)
200	1.39	1.39	-	-	-
210	1.40	1.40	-	-	-
220	1.42	1.42	-	-	-
230	1.41	1.43	-	-	-
240	1.41	1.44	-	-	-
250	1.43	1.46	-	-	-
260	1.46	1.47	-	-	-
270	1.47	1.48	-	-	-
280	1.48	1.49	-	-	-
290	1.50	1.50	-	-	-
300	1.50	1.50	-	-	-

C(Schottky) is the heat capacity of a system comprised of six energy levels; the energy of these levels given in cm^{-1} are 0, 205, 425, 890, 946, and 1020. The lowest energy level is defined as 0. C(coop) is the heat capacity associated with the cooperative phenomena. S(coop) is the entropy associated with the cooperative phenomena.

APPENDIX II

ENERGY LEVELS OF THREE-DIMENSION HINDERED ROTOR

Symbols

N(1), N(2), N(3) quantum numbers for vibrational energy levels

E - energy of level

G - degeneracy

J,K,M - quantum numbers for rotational energy levels

E(0), E(1), E(2) zero-order energy, first-order energy, and second-order energy respectively

NH_4Cl page 192

ND_4Cl page 196

KBH_4 page 204

AMMONIUM CHLORIDE
BODY CENTERED CUBIC (ORDERED)
POTENTIAL BARRIER = 1858.026 RECIPROCAL CM.

ANHARMONIC ENERGY LEVELS

N(1)	N(2)	N(3)	E	G
00	00	00	0.	1
1	00	00	389.00	3
2	00	00	754.44	3
1	1	00	772.11	3
3	00	00	1096.32	3
2	1	00	1131.66	6
1	1	1	1149.33	1
4	00	00	1414.64	3
3	1	00	1467.65	6
2	2	00	1485.32	3
2	1	1	1502.99	3
5	00	00	1709.40	3
4	1	00	1780.08	6
3	2	00	1815.42	6
3	1	1	1833.09	3
2	2	1	1850.76	3
			1858.02	24

ROTATIONAL ENERGY LEVELS

J	K	M	E(0)	E(1)	E(2)	E	G
4	00	00	1254.11	280.73	941.69	2476.53	1
5	00	00	1313.01	289.05	569.62	2171.68	1
6	4	00	1383.69	692.64	-28.92	2047.40	4
6	00	00	1383.69	293.67	385.63	2063.00	1
7	4	00	1466.15	653.43	18.36	2137.94	4
7	00	00	1466.15	296.51	279.88	2042.55	1
8	4	4	1560.39	412.34	-20.11	1952.63	4
8	4	00	1560.39	605.25	29.32	2194.96	4
8	00	00	1560.39	298.39	213.03	2071.81	1
9	8	00	1666.41	510.07	-212.10	1964.39	4
9	4	4	1666.41	457.21	19.19	2142.82	4
9	4	00	1666.41	561.37	33.73	2261.52	4
9	00	00	1666.41	299.69	167.88	2133.99	1
10	8	4	1784.21	457.30	-95.27	2146.25	8
10	8	00	1784.21	643.03	-101.42	2325.83	4
10	4	4	1784.21	479.48	36.34	2300.03	4
10	4	00	1784.21	524.29	36.03	2344.54	4
10	00	00	1784.21	300.64	135.88	2220.72	1
11	8	8	1913.79	272.61	-232.31	1954.09	4
11	8	4	1913.79	480.75	-40.36	2354.19	8
11	8	00	1913.79	689.36	-41.31	2561.85	4
11	4	4	1913.79	486.82	41.52	2442.13	4
11	4	00	1913.79	493.67	36.94	2444.39	4
11	00	00	1913.79	301.34	112.31	2327.45	1
12	12	8	2055.15	1030.99	-186.11	2900.03	8
12	12	00	2055.15	-0.	-102.68	1952.47	4
12	8	8	2055.15	254.45	-116.18	2193.42	4

12	8	4	2055.15	508.69	-21.54	2542.31	8
12	8	00	2055.15	696.14	-14.06	2737.24	4
12	4	4	2055.15	485.26	41.11	2581.52	4
12	4	00	2055.15	468.47	36.80	2560.42	4
12	00	00	2055.15	301.88	94.45	2451.48	1
13	12	8	2208.29	584.85	-187.59	2605.55	8
13	12	4	2208.29	468.24	-299.29	2377.25	8
13	12	00	2208.29	399.81	-116.71	2491.39	4
13	8	8	2208.29	278.81	-60.94	2426.16	4
13	8	4	2208.29	529.62	-9.84	2728.08	8
13	8	00	2208.29	684.33	-2.28	2890.34	4
13	4	4	2208.29	478.76	38.52	2725.58	4
13	4	00	2208.29	447.69	35.92	2691.89	4
13	00	00	2208.29	302.31	80.56	2591.16	1
14	12	12	2373.21	481.42	-513.66	2340.96	4
14	12	8	2373.21	429.86	-127.09	2675.98	8
14	12	4	2373.21	507.06	-105.84	2774.43	8
14	12	00	2373.21	550.27	-82.92	2840.57	4
14	8	8	2373.21	318.81	-33.90	2658.12	4
14	8	4	2373.21	541.89	-1.34	2913.76	8
14	8	00	2373.21	664.16	2.86	3040.24	4
14	4	4	2373.21	469.77	35.36	2878.34	4
14	4	00	2373.21	430.43	34.56	2838.20	4
14	00	00	2373.21	302.64	69.55	2745.40	1
15	12	12	2549.91	380.92	-248.79	2682.04	4
15	12	8	2549.91	368.79	-73.24	2845.47	8
15	12	4	2549.91	543.65	-45.52	3048.04	8
15	12	00	2549.91	632.04	-50.70	3131.26	4
15	8	8	2549.91	360.18	-18.74	2891.35	4
15	8	4	2549.91	546.78	4.49	3101.18	8
15	8	00	2549.91	640.82	5.26	3195.99	4
15	4	4	2549.91	459.74	32.27	3041.92	4
15	4	00	2549.91	416.00	32.93	2998.85	4
15	00	00	2549.91	302.92	60.66	2913.49	1
16	16	12	2738.39	1017.50	-164.35	3591.54	8
16	16	8	2738.39	801.04	-557.29	2982.14	8
16	16	4	2738.39	252.58	-555.07	2435.91	8
16	16	00	2738.39	-0.	-47.12	2691.27	4
16	12	12	2738.39	301.60	-147.59	2892.40	4
16	12	8	2738.39	357.14	-42.18	3053.35	8
16	12	4	2738.39	572.40	-23.80	3286.99	8
16	12	00	2738.39	674.35	-28.78	3383.96	4
16	8	8	2738.39	396.63	-8.89	3126.13	4
16	8	4	2738.39	546.16	8.17	3292.72	8
16	8	00	2738.39	616.93	6.53	3361.85	4
16	4	4	2738.39	449.50	29.48	3217.38	4
16	4	00	2738.39	403.85	31.17	3173.41	4
16	00	00	2738.39	303.14	53.39	3094.92	1
17	16	16	2938.65	396.93	-1175.88	2159.70	4
17	16	12	2938.65	673.68	-132.02	3480.32	8
17	16	8	2938.65	580.05	-225.31	3293.40	8
17	16	4	2938.65	404.87	-200.68	3142.85	8
17	16	00	2938.65	326.61	-67.71	3197.55	4

17	12	12	2938.65	260.70	-91.93	3107.42	4
17	12	8	2938.65	369.51	-26.07	3282.08	8
17	12	4	2938.65	592.34	-13.96	3517.03	8
17	12	00	2938.65	692.81	-15.38	3616.08	4
17	8	8	2938.65	426.13	-2.03	3362.75	4
17	8	4	2938.65	541.71	10.28	3490.65	8
17	8	00	2938.65	593.82	7.31	3539.79	4
17	4	4	2938.65	439.53	27.04	3405.22	4
17	4	00	2938.65	393.53	29.37	3361.55	4
17	00	00	2938.65	303.33	47.35	3289.34	1
18	16	16	3150.69	503.09	-537.99	3115.79	4
18	16	12	3150.69	508.11	-107.22	3551.58	8
18	16	8	3150.69	494.96	-111.88	3533.77	8
18	16	4	3150.69	479.14	-94.16	3535.68	8
18	16	00	3150.69	472.52	-58.88	3564.33	4
18	12	12	3150.69	251.11	-57.82	3343.98	4
18	12	8	3150.69	391.71	-17.24	3525.15	8
18	12	4	3150.69	604.40	-8.26	3746.83	8
18	12	00	3150.69	696.66	-7.55	3839.80	4
18	8	8	3150.69	448.62	2.79	3602.10	4
18	8	4	3150.69	534.75	11.36	3696.80	8
18	8	00	3150.69	572.11	7.86	3730.66	4
18	4	4	3150.69	430.06	24.92	3605.68	4
18	4	00	3150.69	384.71	27.60	3563.00	4
18	00	00	3150.69	303.49	42.29	3496.47	1
19	16	16	3374.51	461.83	-260.93	3575.41	4
19	16	12	3374.51	402.75	-82.02	3695.23	8
19	16	8	3374.51	460.60	-56.42	3778.69	8
19	16	4	3374.51	534.68	-49.25	3859.94	8
19	16	00	3374.51	565.92	-43.77	3896.65	4
19	12	12	3374.51	261.93	-37.07	3599.38	4
19	12	8	3374.51	416.16	-11.61	3779.07	8
19	12	4	3374.51	610.07	-4.42	3980.17	8
19	12	00	3374.51	691.59	-3.06	4063.04	4
19	8	8	3374.51	464.89	6.05	3845.45	4
19	8	4	3374.51	526.24	11.79	3912.54	8
19	8	00	3374.51	552.03	8.27	3934.82	4
19	4	4	3374.51	421.22	23.07	3818.80	4
19	4	00	3374.51	377.11	25.90	3777.52	4
19	00	00	3374.51	303.63	38.00	3716.14	1
20	20	20	3610.11	-257.47	-946.44	2406.20	4
20	20	16	3610.11	913.80	-316.05	4207.86	8
20	20	12	3610.11	985.89	-131.40	4464.61	8
20	20	8	3610.11	587.98	-486.20	3711.89	8
20	20	4	3610.11	169.46	-275.46	3504.11	8
20	20	00	3610.11	-0.	-25.41	3584.70	4
20	16	16	3610.11	388.05	-151.51	3846.65	4
20	16	12	3610.11	343.54	-58.33	3895.32	8
20	16	8	3610.11	453.35	-30.19	4033.27	8
20	16	4	3610.11	575.53	-28.39	4157.25	8
20	16	00	3610.11	625.63	-30.27	4205.47	4
20	12	12	3610.11	284.12	-24.48	3869.75	4
20	12	8	3610.11	439.11	-7.46	4041.77	8

20	12	4	3610.11	610.82	-1.67	4219.27	8
20	12	00	3610.11	681.17	-.50	4290.78	4
20	8	8	3610.11	475.97	8.14	4094.22	4
20	8	4	3610.11	516.88	11.83	4138.82	8
20	8	00	3610.11	533.65	8.57	4152.33	4
20	4	4	3610.11	413.05	21.44	4044.60	4
20	4	00	3610.11	370.53	24.28	4004.93	4
20	00	00	3610.11	303.74	34.34	3948.19	1

DEUTERO-AMMONIUM CHLORIDE
BODY CENTERED CUBIC (ORDERED)
POTENTIAL BARRIER = 1941.897 RECIPROCAL CM.

ANHARMONIC ENERGY LEVELS

N(1)	N(2)	N(3)	E	G
00	00	00	0.	1
1	00	00	288.00	3
2	00	00	564.20	3
1	1	00	573.05	3
3	00	00	828.60	3
2	1	00	846.30	6
1	1	1	855.15	1
4	00	00	1081.20	3
3	1	00	1107.75	6
2	2	00	1116.60	3
2	1	1	1125.45	3
5	00	00	1322.00	3
4	1	00	1357.40	6
3	2	00	1375.10	6
3	1	1	1383.95	3
2	2	1	1392.80	3
6	00	00	1551.00	3
5	1	00	1595.25	6
4	2	00	1621.80	6
4	1	1	1630.65	3
3	3	00	1630.65	3
3	2	1	1648.35	6
2	2	2	1657.20	1
7	00	00	1768.20	3
6	1	00	1821.30	6
5	2	00	1856.70	6
5	1	1	1865.55	3
4	3	00	1874.40	6
4	2	1	1892.10	6
3	3	1	1900.95	3
3	2	2	1909.80	3
			1941.90	25

ROTATIONAL ENERGY LEVELS

J	K	M	E(0)	E(1)	E(2)	E	G
5	00	00	1465.97	302.09	1242.30	3010.36	1
6	4	00	1501.37	723.90	-63.08	2162.19	4
6	00	00	1501.37	306.93	841.04	2649.33	1
7	4	00	1542.67	682.93	40.04	2265.63	4
7	00	00	1542.67	309.90	610.40	2462.97	1
8	4	4	1589.87	430.96	-43.86	1976.96	4
8	4	00	1589.87	632.57	63.94	2286.38	4
8	00	00	1589.87	311.86	464.60	2366.32	1
9	4	4	1642.97	477.85	41.85	2162.67	4
9	4	00	1642.97	586.71	73.57	2303.25	4
9	00	00	1642.97	313.22	366.14	2322.33	1
10	8	4	1701.97	477.95	-207.77	1972.14	8

10	8	00	1701.97	672.06	-221.18	2152.85	4
10	4	4	1701.97	501.13	79.26	2282.35	4
10	4	00	1701.97	547.96	78.58	2328.50	4
10	00	00	1701.97	314.21	296.33	2312.51	1
11	8	4	1766.87	502.45	-88.02	2181.30	8
11	8	00	1766.87	720.48	-90.08	2397.26	4
11	4	4	1766.87	508.79	90.56	2366.22	4
11	4	00	1766.87	515.95	80.55	2363.37	4
11	00	00	1766.87	314.94	244.95	2326.76	1
12	12	8	1837.67	1077.52	-405.88	2509.31	8
12	8	4	1837.67	531.65	-46.97	2322.35	8
12	8	00	1837.67	727.56	-30.66	2534.57	4
12	4	4	1837.67	507.16	89.66	2434.49	4
12	4	00	1837.67	489.62	80.25	2407.54	4
12	00	00	1837.67	315.51	205.98	2359.16	1
13	12	8	1914.37	611.25	-409.12	2116.49	8
13	12	00	1914.37	417.85	-254.53	2077.69	4
13	8	8	1914.37	291.40	-132.91	2072.86	4
13	8	4	1914.37	553.53	-21.45	2446.44	8
13	8	00	1914.37	715.22	-4.97	2624.62	4
13	4	4	1914.37	500.37	84.02	2498.76	4
13	4	00	1914.37	467.89	78.33	2460.59	4
13	00	00	1914.37	315.95	175.70	2406.02	1
14	12	8	1996.97	449.26	-277.18	2169.05	8
14	12	4	1996.97	529.95	-230.83	2296.08	8
14	12	00	1996.97	575.11	-180.83	2391.24	4
14	8	8	1996.97	333.21	-73.94	2256.23	4
14	8	4	1996.97	566.35	-2.93	2560.38	8
14	8	00	1996.97	694.14	6.24	2697.35	4
14	4	4	1996.97	490.98	77.11	2565.05	4
14	4	00	1996.97	449.86	75.37	2522.20	4
14	00	00	1996.97	316.31	151.68	2464.95	1
15	12	12	2085.47	398.11	-542.59	1940.99	4
15	12	8	2085.47	385.44	-159.73	2311.18	8
15	12	4	2085.47	568.20	-99.28	2554.38	8
15	12	00	2085.47	660.57	-110.57	2635.47	4
15	8	8	2085.47	376.43	-40.86	2421.04	4
15	8	4	2085.47	571.46	9.79	2666.72	8
15	8	00	2085.47	669.75	11.47	2766.68	4
15	4	4	2085.47	480.49	70.37	2636.33	4
15	4	00	2085.47	434.78	71.82	2592.07	4
15	00	00	2085.47	316.59	132.30	2534.36	1
16	16	12	2179.87	1063.43	-358.43	2884.87	8
16	16	00	2179.87	-0.	-102.77	2077.09	4
16	12	12	2179.87	315.21	-321.88	2173.19	4
16	12	8	2179.87	373.26	-92.00	2461.13	8
16	12	4	2179.87	598.24	-51.92	2726.19	8
16	12	00	2179.87	704.79	-62.77	2821.89	4
16	8	8	2179.87	414.53	-19.39	2575.00	4
16	8	4	2179.87	570.82	17.81	2768.49	8
16	8	00	2179.87	644.78	14.24	2838.89	4
16	4	4	2179.87	469.79	64.30	2713.96	4
16	4	00	2179.87	422.08	67.97	2669.92	4

16	00	00	2179.87	316.83	116.43	2613.13	1
17	16	12	2280.17	704.09	-287.93	2696.33	8
17	16	8	2280.17	606.24	-491.38	2395.02	8
17	16	4	2280.17	423.15	-437.66	2265.66	8
17	16	00	2280.17	341.35	-147.67	2473.84	4
17	12	12	2280.17	272.46	-200.49	2352.14	4
17	12	8	2280.17	386.19	-56.87	2609.49	8
17	12	4	2280.17	619.07	-30.45	2868.79	8
17	12	00	2280.17	724.08	-33.54	2970.70	4
17	8	8	2280.17	445.36	-4.42	2721.11	4
17	8	4	2280.17	566.16	22.43	2868.76	8
17	8	00	2280.17	620.63	15.95	2916.75	4
17	4	4	2280.17	459.37	58.98	2798.51	4
17	4	00	2280.17	411.29	64.06	2755.52	4
17	00	00	2280.17	317.03	103.27	2700.47	1
18	16	12	2386.37	531.04	-233.83	2683.58	8
18	16	8	2386.37	517.30	-244.01	2659.66	8
18	16	4	2386.37	500.77	-205.35	2681.78	8
18	16	00	2386.37	493.85	-128.42	2751.79	4
18	12	12	2386.37	262.44	-126.09	2522.71	4
18	12	8	2386.37	409.39	-37.61	2758.15	8
18	12	4	2386.37	631.69	-18.02	3000.03	8
18	12	00	2386.37	728.11	-16.47	3098.00	4
18	8	8	2386.37	468.87	6.08	2861.32	4
18	8	4	2386.37	558.88	24.79	2970.04	8
18	8	00	2386.37	597.93	17.15	3001.45	4
18	4	4	2386.37	449.48	54.35	2890.19	4
18	4	00	2386.37	402.07	60.20	2848.64	4
18	00	00	2386.37	317.19	92.23	2795.79	1
19	16	16	2498.47	482.67	-569.07	2412.06	4
19	16	12	2498.47	420.93	-178.89	2740.50	8
19	16	8	2498.47	481.39	-123.04	2856.81	8
19	16	4	2498.47	558.81	-107.41	2949.87	8
19	16	00	2498.47	591.46	-95.47	2994.46	4
19	12	12	2498.47	273.76	-80.84	2691.38	4
19	12	8	2498.47	434.95	-25.32	2908.10	8
19	12	4	2498.47	637.61	-9.63	3126.44	8
19	12	00	2498.47	722.81	-6.68	3214.59	4
19	8	8	2498.47	485.88	13.19	2997.54	4
19	8	4	2498.47	549.99	25.72	3074.17	8
19	8	00	2498.47	576.95	18.04	3093.46	4
19	4	4	2498.47	440.24	50.31	2989.01	4
19	4	00	2498.47	394.14	56.48	2949.09	4
19	00	00	2498.47	317.33	82.88	2898.68	1
20	20	16	2616.47	955.05	-689.29	2882.22	8
20	20	12	2616.47	1030.39	-286.56	3360.30	8
20	20	8	2616.47	614.52	-1060.38	2170.61	8
20	20	4	2616.47	177.11	-600.76	2192.82	8
20	20	00	2616.47	-0.	-55.41	2561.05	4
20	16	16	2616.47	405.57	-330.44	2691.59	4
20	16	12	2616.47	359.05	-127.22	2848.29	8
20	16	8	2616.47	473.82	-65.84	3024.44	8
20	16	4	2616.47	601.51	-61.92	3156.05	8

20	16	00	2616.47	653.87	-66.01	3204.32	4
20	12	12	2616.47	296.95	-53.39	2860.02	4
20	12	8	2616.47	458.93	-16.26	3059.14	8
20	12	4	2616.47	638.39	-3.64	3251.22	8
20	12	00	2616.47	711.91	-1.09	3327.29	4
20	8	8	2616.47	497.45	17.76	3131.67	4
20	8	4	2616.47	540.21	25.80	3182.47	8
20	8	00	2616.47	557.73	18.70	3192.90	4
20	4	4	2616.47	431.69	46.76	3094.92	4
20	4	00	2616.47	387.26	52.96	3056.68	4
20	00	00	2616.47	317.45	74.89	3008.81	1
21	20	16	2740.37	730.03	-372.70	3097.70	8
21	20	12	2740.37	727.39	-216.34	3251.42	8
21	20	8	2740.37	543.87	-459.58	2824.66	8
21	20	4	2740.37	361.00	-279.56	2821.80	8
21	20	00	2740.37	287.91	-91.86	2936.42	4
21	16	16	2740.37	338.12	-218.26	2860.22	4
21	16	12	2740.37	331.32	-87.30	2984.39	8
21	16	8	2740.37	480.71	-39.03	3182.05	8
21	16	4	2740.37	631.83	-38.41	3333.79	8
21	16	00	2740.37	692.44	-43.71	3389.10	4
21	12	12	2740.37	325.40	-36.16	3029.60	4
21	12	8	2740.37	479.60	-9.07	3210.89	8
21	12	4	2740.37	635.35	.69	3376.41	8
21	12	00	2740.37	697.81	2.15	3440.32	4
21	8	8	2740.37	504.66	20.45	3265.48	4
21	8	4	2740.37	530.04	25.39	3295.80	8
21	8	00	2740.37	540.22	19.16	3299.75	4
21	4	4	2740.37	423.83	43.62	3207.82	4
21	4	00	2740.37	381.27	49.65	3171.28	4
21	00	00	2740.37	317.56	68.00	3125.93	1
22	20	20	2870.17	494.89	-1125.85	2239.21	4
22	20	16	2870.17	599.00	-233.39	3235.77	8
22	20	12	2870.17	581.89	-168.47	3283.58	8
22	20	8	2870.17	515.65	-236.53	3149.29	8
22	20	4	2870.17	454.22	-159.06	3165.33	8
22	20	00	2870.17	430.12	-90.42	3209.86	4
22	16	16	2870.17	292.38	-151.49	3011.06	4
22	16	12	2870.17	326.13	-59.84	3136.45	8
22	16	8	2870.17	494.09	-25.86	3338.40	8
22	16	4	2870.17	652.30	-24.83	3497.63	8
22	16	00	2870.17	714.60	-27.98	3556.79	4
22	12	12	2870.17	354.94	-24.62	3200.48	4
22	12	8	2870.17	496.40	-3.29	3363.28	8
22	12	4	2870.17	629.57	3.79	3503.52	8
22	12	00	2870.17	682.00	4.09	3556.25	4
22	8	8	2870.17	508.43	21.83	3400.43	4
22	8	4	2870.17	519.82	24.73	3414.71	8
22	8	00	2870.17	524.30	19.45	3413.92	4
22	4	4	2870.17	416.63	40.82	3327.62	4
22	4	00	2870.17	376.02	46.56	3292.74	4
22	00	00	2870.17	317.65	62.03	3249.84	1
23	20	20	3005.87	516.14	-596.72	2925.28	4

23	20	16	3005.87	489.69	-172.48	3323.08	8
23	20	12	3005.87	494.08	-118.46	3381.48	8
23	20	8	3005.87	509.75	-125.39	3390.23	8
23	20	4	3005.87	524.11	-97.07	3432.91	8
23	20	00	3005.87	529.72	-75.72	3459.87	4
23	16	16	3005.87	268.18	-106.39	3167.65	4
23	16	12	3005.87	334.79	-41.90	3298.76	8
23	16	8	3005.87	509.47	-18.54	3496.80	8
23	16	4	3005.87	665.05	-16.23	3654.69	8
23	16	00	3005.87	725.36	-17.28	3713.95	4
23	12	12	3005.87	383.11	-16.32	3372.66	4
23	12	8	3005.87	509.41	1.27	3516.55	8
23	12	4	3005.87	621.88	5.96	3633.71	8
23	12	00	3005.87	665.48	5.29	3676.64	4
23	8	8	3005.87	509.58	22.31	3537.75	4
23	8	4	3005.87	509.77	23.94	3539.57	8
23	8	00	3005.87	509.85	19.59	3535.30	4
23	4	4	3005.87	410.04	38.30	3454.20	4
23	4	00	3005.87	371.39	43.68	3420.94	4
23	00	00	3005.87	317.73	56.81	3380.40	1
24	24	20	3147.47	826.47	-827.15	3146.78	8
24	24	16	3147.47	1090.18	-47.68	4189.97	8
24	24	12	3147.47	858.76	-532.19	3474.04	8
24	24	8	3147.47	459.62	-738.43	2868.66	8
24	24	4	3147.47	126.60	-326.18	2947.89	8
24	24	00	3147.47	-0.	-33.21	3114.26	4
24	20	20	3147.47	471.69	-343.11	3276.05	4
24	20	16	3147.47	408.23	-133.01	3422.68	8
24	20	12	3147.47	444.54	-79.68	3512.33	8
24	20	8	3147.47	515.89	-69.51	3593.85	8
24	20	4	3147.47	576.83	-62.64	3661.65	8
24	20	00	3147.47	600.15	-58.83	3688.79	4
24	16	16	3147.47	261.34	-75.10	3333.70	4
24	16	12	3147.47	351.25	-30.18	3468.53	8
24	16	8	3147.47	524.40	-13.67	3658.19	8
24	16	4	3147.47	671.82	-10.38	3808.90	8
24	16	00	3147.47	728.21	-10.16	3865.52	4
24	12	12	3147.47	408.61	-9.99	3546.08	4
24	12	8	3147.47	518.97	4.77	3671.20	8
24	12	4	3147.47	612.92	7.47	3767.86	8
24	12	00	3147.47	648.86	6.10	3802.43	4
24	8	8	3147.47	508.73	22.20	3678.40	4
24	8	4	3147.47	500.04	23.10	3670.61	8
24	8	00	3147.47	496.73	19.59	3663.78	4
24	4	4	3147.47	404.02	36.01	3587.50	4
24	4	00	3147.47	367.29	41.02	3555.78	4
24	00	00	3147.47	317.79	52.23	3517.49	1
25	24	24	3294.97	202.38	-1544.81	1952.53	4
25	24	20	3294.97	710.87	-461.72	3544.11	8
25	24	16	3294.97	805.19	-91.06	4009.10	8
25	24	12	3294.97	675.87	-294.84	3676.00	8
25	24	8	3294.97	474.80	-360.69	3409.07	8
25	24	4	3294.97	310.66	-181.44	3424.19	8

25	24	00	3294.97	248.70	-60.62	3483.05	4
25	20	20	3294.97	410.62	-222.13	3483.45	4
25	20	16	3294.97	353.39	-101.53	3546.83	8
25	20	12	3294.97	420.48	-53.27	3662.18	8
25	20	8	3294.97	527.90	-41.15	3781.71	8
25	20	4	3294.97	616.11	-42.15	3868.92	8
25	20	00	3294.97	649.47	-43.80	3900.64	4
25	16	16	3294.97	267.05	-53.55	3508.47	4
25	16	12	3294.97	371.43	-22.22	3644.17	8
25	16	8	3294.97	537.64	-9.92	3822.69	8
25	16	4	3294.97	674.00	-6.25	3962.73	8
25	16	00	3294.97	725.56	-5.46	4015.07	4
25	12	12	3294.97	430.88	-5.03	3720.82	4
25	12	8	3294.97	525.53	7.36	3827.86	8
25	12	4	3294.97	603.18	8.49	3906.64	8
25	12	00	3294.97	632.55	6.68	3934.20	4
25	8	8	3294.97	506.39	21.73	3823.09	4
25	8	4	3294.97	490.72	22.25	3807.94	8
25	8	00	3294.97	484.80	19.48	3799.25	4
25	4	4	3294.97	398.51	33.93	3727.41	4
25	4	00	3294.97	363.65	38.55	3697.17	4
25	00	00	3294.97	317.86	48.18	3661.00	1
26	24	24	3448.37	440.26	-1016.83	2871.80	4
26	24	20	3448.37	632.25	-267.39	3813.22	8
26	24	16	3448.37	652.68	-102.14	3998.90	8
26	24	12	3448.37	582.12	-188.36	3842.12	8
26	24	8	3448.37	485.30	-203.22	3730.45	8
26	24	4	3448.37	408.62	-118.29	3738.69	8
26	24	00	3448.37	379.96	-64.90	3763.43	4
26	20	20	3448.37	354.43	-157.12	3645.68	4
26	20	16	3448.37	320.81	-76.16	3693.02	8
26	20	12	3448.37	413.00	-36.41	3824.96	8
26	20	8	3448.37	542.07	-26.38	3964.06	8
26	20	4	3448.37	644.78	-29.16	4063.99	8
26	20	00	3448.37	683.23	-31.68	4099.91	4
26	16	16	3448.37	281.07	-38.78	3690.65	4
26	16	12	3448.37	392.70	-16.45	3824.61	8
26	16	8	3448.37	548.67	-6.77	3990.27	8
26	16	4	3448.37	672.73	-3.25	4117.85	8
26	16	00	3448.37	719.16	-2.37	4165.16	4
26	12	12	3448.37	449.79	-1.09	3897.06	4
26	12	8	3448.37	529.56	9.21	3987.14	8
26	12	4	3448.37	593.02	9.16	4050.55	8
26	12	00	3448.37	616.77	7.13	4072.26	4
26	8	8	3448.37	502.97	21.05	3972.39	4
26	8	4	3448.37	481.85	21.42	3951.64	8
26	8	00	3448.37	473.95	19.28	3941.59	4
26	4	4	3448.37	393.47	32.03	3873.87	4
26	4	00	3448.37	360.40	36.28	3845.04	4
26	00	00	3448.37	317.91	44.58	3810.86	1
27	24	24	3607.67	513.22	-599.14	3521.75	4
27	24	20	3607.67	545.67	-178.43	3974.90	8
27	24	16	3607.67	544.45	-93.22	4058.90	8

27	24	12	3607.67	525.39	-119.22	4013.84	8
27	24	8	3607.67	501.98	-117.96	3991.69	8
27	24	4	3607.67	484.01	-80.80	4010.87	8
27	24	00	3607.67	477.36	-58.93	4026.10	4
27	20	20	3607.67	311.09	-116.12	3802.63	4
27	20	16	3607.67	305.44	-56.59	3856.52	8
27	20	12	3607.67	415.93	-25.91	3997.70	8
27	20	8	3607.67	556.29	-18.26	4145.70	8
27	20	4	3607.67	665.06	-20.47	4252.26	8
27	20	00	3607.67	705.41	-22.41	4290.66	4
27	16	16	3607.67	300.05	-28.57	3879.15	4
27	16	12	3607.67	413.45	-12.00	4009.11	8
27	16	8	3607.67	557.36	-4.07	4160.96	8
27	16	4	3607.67	668.86	-1.04	4275.48	8
27	16	00	3607.67	710.22	-.33	4317.55	4
27	12	12	3607.67	465.47	2.01	4075.14	4
27	12	8	3607.67	531.51	10.47	4149.65	8
27	12	4	3607.67	582.68	9.59	4199.94	8
27	12	00	3607.67	601.67	7.48	4216.82	4
27	8	8	3607.67	498.79	20.25	4126.71	4
27	8	4	3607.67	473.46	20.62	4101.75	8
27	8	00	3607.67	464.06	19.00	4090.73	4
27	4	4	3607.67	388.86	30.28	4026.81	4
27	4	00	3607.67	357.49	34.17	3999.32	4
27	00	00	3607.67	317.96	41.37	3967.00	1
28	28	28	3772.87	-416.25	-901.44	2455.18	4
28	28	24	3772.87	701.57	-825.62	3648.82	8
28	28	20	3772.87	1079.15	-63.30	4788.71	8
28	28	16	3772.87	1000.62	-196.81	4576.68	8
28	28	12	3772.87	698.46	-527.91	3943.42	8
28	28	8	3772.87	353.48	-493.95	3632.39	8
28	28	4	3772.87	94.83	-191.08	3676.62	8
28	28	00	3772.87	-0.	-21.45	3751.42	4
28	24	24	3772.87	506.01	-357.67	3921.20	4
28	24	20	3772.87	466.94	-132.69	4107.11	8
28	24	16	3772.87	469.86	-76.81	4165.92	8
28	24	12	3772.87	493.33	-75.43	4190.77	8
28	24	8	3772.87	521.39	-70.90	4223.36	8
28	24	4	3772.87	542.74	-57.09	4258.51	8
28	24	00	3772.87	550.60	-49.53	4273.94	4
28	20	20	3772.87	282.09	-87.18	3967.78	4
28	20	16	3772.87	302.67	-42.11	4033.43	8
28	20	12	3772.87	425.04	-19.27	4178.63	8
28	20	8	3772.87	569.36	-13.38	4328.84	8
28	20	4	3772.87	678.70	-14.42	4437.15	8
28	20	00	3772.87	718.94	-15.52	4476.28	4
28	16	16	3772.87	321.55	-21.34	4073.07	4
28	16	12	3772.87	432.73	-8.40	4197.20	8
28	16	8	3772.87	563.79	-1.77	4334.89	8
28	16	4	3772.87	663.08	.59	4436.54	8
28	16	00	3772.87	699.62	1.02	4473.51	4
28	12	12	3772.87	478.17	4.41	4255.45	4
28	12	8	3772.87	531.77	11.27	4315.90	8

28	12	4	3772.87	572.37	9.85	4355.09	8
28	12	00	3772.87	587.32	7.77	4367.96	4
28	8	8	3772.87	494.08	19.41	4286.35	4
28	8	4	3772.87	465.54	19.86	4258.26	8
28	8	00	3772.87	455.04	18.67	4246.57	4
28	4	4	3772.87	384.63	28.67	4186.17	4
28	4	00	3772.87	354.86	32.22	4159.95	4
28	00	00	3772.87	318.00	38.50	4129.37	1

POTASSIUM BOROHYDRIDE
FACE-CENTERED CUBIC
POTENTIAL BARRIER = 1120.039 RECIPROCAL CM.

ANHARMONIC ENERGY LEVELS

N(1)	N(2)	N(3)	E	G
00	00	00	0.	1
1	00	00	250.00	3
2	00	00	483.68	3
1	1	00	495.92	3
3	00	00	701.04	3
2	1	00	725.52	6
1	1	1	737.76	1
4	00	00	902.08	3
3	1	00	938.80	6
2	2	00	951.04	3
2	1	1	963.28	3
5	00	00	1086.80	3
			1120.04	34

ROTATIONAL ENERGY LEVELS

J	K	M	E(0)	E(1)	E(2)	E	G
4	00	00	741.34	169.23	494.00	1404.56	1
5	00	00	782.14	174.24	298.81	1255.19	1
6	4	00	831.10	417.53	-15.17	1233.45	4
6	00	00	831.10	177.03	202.30	1210.42	1
7	4	00	888.22	393.90	9.63	1291.74	4
7	00	00	888.22	178.74	146.82	1213.78	1
8	4	4	953.50	248.56	-10.55	1191.51	4
8	4	00	953.50	364.85	15.38	1333.73	4
8	00	00	953.50	179.87	111.75	1245.12	1
9	8	4	1026.94	289.27	-181.76	1134.44	8
9	8	00	1026.94	307.48	-111.26	1223.15	4
9	4	4	1026.94	275.61	10.07	1312.62	4
9	4	00	1026.94	338.40	17.70	1383.03	4
9	00	00	1026.94	180.66	88.07	1295.66	1
10	8	4	1108.54	275.67	-49.98	1334.23	8
10	8	00	1108. 4	387.63	-53.20	1442. 6	4
10	4	4	1108.54	289.04	19.06	1416.64	4
10	4	00	1108.54	316.05	18.90	1443.49	4
10	00	00	1108.54	181.23	71.28	1361.04	1
11	8	8	1198.30	164.33	-121.87	1240.76	4
11	8	4	1198.30	289.80	-21.17	1466.93	8
11	8	00	1198.30	415.56	-21.67	1592.18	4
11	4	4	1198.30	293.46	21.78	1513.54	4
11	4	00	1198.30	297.59	19.38	1515.26	4
11	00	00	1198.30	181.65	58.92	1438.87	1
12	12	8	1296.22	621.49	-97.63	1820.08	8
12	12	00	1296.22	-0.	-53.87	1242.35	4
12	8	8	1296.22	153.38	-60.95	1388.65	4
12	8	4	1296.22	306.64	-11.30	1591.56	8
12	8	00	1296.22	419.64	-7.37	1708.48	4
12	4	4	1296.22	292.52	21.57	1610.30	4

12	4	00	1296.22	282.40	19.30	1597.92	4
12	00	00	1296.22	181.98	49.55	1527.74	1
13	12	8	1402.30	352.55	-98.41	1656.44	8
13	12	4	1402.30	282.26	-157.00	1527.56	8
13	12	00	1402.30	241.01	-61.22	1582.08	4
13	8	8	1402.30	168.07	-31.97	1538.40	4
13	8	4	1402.30	319.26	-5.16	1716.40	8
13	8	00	1402.30	412.52	-1.20	1813.62	4
13	4	4	1402.30	288.60	20.21	1711.11	4
13	4	00	1402.30	269.87	18.84	1691.01	4
13	00	00	1402.30	182.23	42.26	1626.79	1
14	12	12	1516.54	290.20	-269.46	1537.28	4
14	12	8	1516.54	259.12	-66.67	1708.99	8
14	12	4	1516.54	305.66	-55.52	1766.68	8
14	12	00	1516.54	331.71	-43.50	1804.75	4
14	8	8	1516.54	192.18	-17.79	1690.94	4
14	8	4	1516.54	326.66	-.70	1842.49	8
14	8	00	1516.54	400.37	1.50	1918.40	4
14	4	4	1516.54	283.18	18.55	1818.27	4
14	4	00	1516.54	259.47	18.13	1794.14	4
14	00	00	1516.54	182.44	36.48	1735.46	1
15	12	12	1638.94	229.62	-130.51	1738.05	4
15	12	8	1638.94	222.31	-38.42	1822.83	8
15	12	4	1638.94	327.72	-23.88	1942.78	8
15	12	00	1638.94	381.00	-26.60	1993.34	4
15	8	8	1638.94	217.12	-9.83	1846.23	4
15	8	4	1638.94	329.61	2.35	1970.90	8
15	8	00	1638.94	386.29	2.76	2027.99	4
15	4	4	1638.94	277.14	16.93	1933.00	4
15	4	00	1638.94	250.77	17.27	1906.98	4
15	00	00	1638.94	182.60	31.82	1853.36	1
16	16	12	1769.50	613.36	-86.21	2296.64	8
16	16	8	1769.50	482.88	-292.35	1960.02	8
16	16	4	1769.50	152.26	-291.18	1630.58	8
16	16	00	1769.50	-0.	-24.72	1744.78	4
16	12	12	1769.50	181.81	-77.42	1873.88	4
16	12	8	1769.50	215.29	-22.13	1962.65	8
16	12	4	1769.50	345.05	-12.49	2102.06	8
16	12	00	1769.50	406.51	-15.10	2160.90	4
16	8	8	1769.50	239.09	-4.66	2003.92	4
16	8	4	1769.50	329.23	4.28	2103.01	8
16	8	00	1769.50	371.89	3.42	2144.82	4
16	4	4	1769.50	270.96	15.47	2055.93	4
16	4	00	1769.50	243.44	16.35	2029.29	4
16	00	00	1769.50	182.74	28.01	1980.24	1
17	16	16	1908.22	239.27	-616.85	1530.64	4
17	16	12	1908.22	406.10	-69.26	2245.07	8
17	16	8	1908.22	349.66	-118.19	2139.69	8
17	16	4	1908.22	244.06	-105.27	2047.01	8
17	16	00	1908.22	196.88	-35.52	2069.58	4
17	12	12	1908.22	157.15	-48.23	2017.14	4
17	12	8	1908.22	222.74	-13.68	2117.28	8
17	12	4	1908.22	357.07	-7.32	2257.96	8

17	12	00	1908.22	417.63	-8.07	2317.78	4
17	8	8	1908.22	256.87	-1.06	2164.03	4
17	8	4	1908.22	326.55	5.40	2240.16	8
17	8	00	1908.22	357.96	3.84	2270.02	4
17	4	4	1908.22	264.95	14.19	2187.36	4
17	4	00	1908.22	237.22	15.41	2160.85	4
17	00	00	1908.22	182.85	24.84	2115.91	1
18	16	16	2055.10	303.27	-282.22	2076.14	4
18	16	12	2055.10	306.29	-56.24	2305.15	8
18	16	8	2055.10	298.37	-58.69	2294.77	8
18	16	4	2055.10	288.83	-49.39	2294.53	8
18	16	00	2055.10	284.84	-30.89	2309.05	4
18	12	12	2055.10	151.37	-30.33	2176.14	4
18	12	8	2055.10	236.12	-9.05	2282.18	8
18	12	4	2055.10	364.34	-4.33	2415.10	8
18	12	00	2055.10	419.95	-3.96	2471.09	4
18	8	8	2055.10	270.43	1.46	2326.99	4
18	8	4	2055.10	322.35	5.96	2383.41	8
18	8	00	2055.10	344.87	4.13	2404.10	4
18	4	4	2055.10	259.25	13.07	2327.42	4
18	4	00	2055.10	231.91	14.48	2301.48	4
18	00	00	2055.10	182.95	22.19	2260.23	1
19	16	16	2210.14	278.39	-136.88	2351.65	4
19	16	12	2210.14	242.78	-43.03	2409.89	8
19	16	8	2210.14	277.65	-29.60	2458.19	8
19	16	4	2210.14	322.31	-25.84	2506.61	8
19	16	00	2210.14	341.14	-22.96	2528.31	4
19	12	12	2210.14	157.90	-19.45	2348.59	4
19	12	8	2210.14	250.87	-6.09	2454.92	8
19	12	4	2210.14	367.76	-2.32	2575.58	8
19	12	00	2210.14	416.90	-1.61	2625.43	4
19	8	8	2210.14	280.24	3.17	2493.55	4
19	8	4	2210.14	317.22	6.19	2533.54	8
19	8	00	2210.14	332.77	4.34	2547.25	4
19	4	4	2210.14	253.92	12.10	2476.16	4
19	4	00	2210.14	227.33	13.59	2451.05	4
19	00	00	2210.14	183.03	19.94	2413.10	1
20	20	20	2373.34	-155.21	-496.49	1721.64	4
20	20	16	2373.34	550.85	-165.80	2758.39	8
20	20	12	2373.34	594.31	-68.93	2898.71	8
20	20	8	2373.34	354.44	-255.06	2472.72	8
20	20	4	2373.34	102.16	-144.50	2330.99	8
20	20	00	2373.34	-0.	-13.33	2360.01	4
20	16	16	2373.34	233.92	-79.48	2527.78	4
20	16	12	2373.34	207.09	-30.60	2549.83	8
20	16	8	2373.34	273.29	-15.84	2630.79	8
20	16	4	2373.34	346.94	-14.89	2705.38	8
20	16	00	2373.34	377.13	-15.88	2734.59	4
20	12	12	2373.34	171.27	-12.84	2531.77	4
20	12	8	2373.34	264.70	-3.91	2634.13	8
20	12	4	2373.34	368.21	-.87	2740.67	8
20	12	00	2373.34	410.62	-.26	2783.69	4
20	8	8	2373.34	286.92	4.27	2664.53	4

20	8	4	2373.34	311.58	6.21	2691.12	8
20	8	00	2373.34	321.69	4.50	2699.52	4
20	4	4	2373.34	248.99	11.25	2633.57	4
20	4	00	2373.34	223.36	12.74	2609.44	4
20	00	00	2373.34	183.10	18.01	2574.45	1
21	20	20	2544.70	175.36	-481.92	2238.13	4
21	20	16	2544.70	421.06	-89.65	2876.12	8
21	20	12	2544.70	419.54	-52.04	2912.20	8
21	20	8	2544.70	313.69	-110.54	2747.84	8
21	20	4	2544.70	208.21	-67.24	2685.67	8
21	20	00	2544.70	166.06	-22.09	2688.66	4
21	16	16	2544.70	195.02	-52.50	2687.22	4
21	16	12	2544.70	191.10	-21.00	2714.80	8
21	16	8	2544.70	277.26	-9.39	2812.57	8
21	16	4	2544.70	364.42	-9.24	2899.88	8
21	16	00	2544.70	399.38	-10.51	2933.57	4
21	12	12	2544.70	187.68	-8.70	2723.68	4
21	12	8	2544.70	276.62	-2.18	2819.14	8
21	12	4	2544.70	366.46	.17	2911.32	8
21	12	00	2544.70	402.48	.52	2947.69	4
21	8	8	2544.70	291.07	4.92	2840.69	4
21	8	4	2544.70	305.71	6.11	2856.52	8
21	8	00	2544.70	311.59	4.61	2860.89	4
21	4	4	2544.70	244.46	10.49	2799.65	4
21	4	00	2544.70	219.91	11.94	2776.54	4
21	00	00	2544.70	183.16	16.36	2744.21	1
22	20	20	2724.22	285.44	-270.80	2738.85	4
22	20	16	2724.22	345.49	-56.14	3013.56	8
22	20	12	2724.22	335.62	-40.52	3019.31	8
22	20	8	2724.22	297.42	-56.89	2964.74	8
22	20	4	2724.22	261.98	-38.26	2947.94	8
22	20	00	2724.22	248.08	-21.75	2950.55	4
22	16	16	2724.22	168.64	-36.44	2856.42	4
22	16	12	2724.22	188.10	-14.39	2897.93	8
22	16	8	2724.22	284.98	-6.22	3002.98	8
22	16	4	2724.22	376.23	-5.97	3094.47	8
22	16	00	2724.22	412.16	-6.73	3129.65	4
22	12	12	2724.22	204.72	-5.92	2923.01	4
22	12	8	2724.22	286.31	-.79	3009.74	8
22	12	4	2724.22	363.12	.91	3088.25	8
22	12	00	2724.22	393.36	.98	3118.56	4
22	8	8	2724.22	293.25	5.25	3022.72	4
22	8	4	2724.22	299.82	5.95	3029.98	8
22	8	00	2724.22	302.41	4.68	3031.30	4
22	4	4	2724.22	240.30	9.82	2974.34	4
22	4	00	2724.22	216.88	11.20	2952.29	4
22	00	00	2724.22	183.21	14.92	2922.35	1
23	20	20	2911.90	297.70	-143.53	3066.06	4
23	20	16	2911.90	282.44	-41.49	3152.85	8
23	20	12	2911.90	284.97	-28.49	3168.37	8
23	20	8	2911.90	294.01	-30.16	3175.75	8
23	20	4	2911.90	302.29	-23.35	3190.84	8
23	20	00	2911.90	305.53	-18.21	3199.21	4

23	16	16	2911.90	154.68	-25.59	3040.98	4
23	16	12	2911.90	193.10	-10.08	3094.92	8
23	16	8	2911.90	293.85	-4.46	3201.29	8
23	16	4	2911.90	383.58	-3.90	3291.58	8
23	16	00	2911.90	418.37	-4.16	3326.11	4
23	12	12	2911.90	220.97	-3.92	3128.94	4
23	12	8	2911.90	293.82	.31	3206.02	8
23	12	4	2911.90	358.68	1.43	3272.02	8
23	12	00	2911.90	383.83	1.27	3297.00	4
23	8	8	2911.90	293.91	5.37	3211.17	4
23	8	4	2911.90	294.02	5.76	3211.68	8
23	8	00	2911.90	294.07	4.71	3210.68	4
23	4	4	2911.90	236.50	9.21	3157.61	4
23	4	00	2911.90	214.21	10.51	3136.61	4
23	00	00	2911.90	183.26	13.66	3108.82	1
24	24	24	3107.74	-203.76	-319.25	2584.72	4
24	24	20	3107.74	476.69	-198.96	3385.47	8
24	24	16	3107.74	628.79	-11.47	3725.06	8
24	24	12	3107.74	495.31	-128.01	3475.04	8
24	24	8	3107.74	265.10	-177.62	3195.22	8
24	24	4	3107.74	73.02	-78.46	3102.30	8
24	24	00	3107.74	-0.	-7.99	3099.75	4
24	20	20	3107.74	272.06	-82.53	3297.27	4
24	20	16	3107.74	235.46	-31.99	3311.20	8
24	20	12	3107.74	256.40	-19.16	3344.97	8
24	20	8	3107.74	297.55	-16.72	3388.57	8
24	20	4	3107.74	332.70	-15.07	3425.37	8
24	20	00	3107.74	346.15	-14.15	3439.74	4
24	16	16	3107.74	150.73	-18.06	3240.41	4
24	16	12	3107.74	202.59	-7.26	3303.07	8
24	16	8	3107.74	302.46	-3.29	3406.91	8
24	16	4	3107.74	387.49	-2.50	3492.73	8
24	16	00	3107.74	420.01	-2.44	3525.31	4
24	12	12	3107.74	235.67	-2.40	3341.01	4
24	12	8	3107.74	299.33	1.15	3408.21	8
24	12	4	3107.74	353.52	1.80	3463.05	8
24	12	00	3107.74	374.25	1.47	3483.45	4
24	8	8	3107.74	293.42	5.34	3406.50	4
24	8	4	3107.74	288.41	5.56	3401.70	8
24	8	00	3107.74	286.50	4.71	3398.95	4
24	4	4	3107.74	233.03	8.66	3349.43	4
24	4	00	3107.74	211.85	9.87	3329.45	4
24	00	00	3107.74	183.30	12.56	3303.60	1
25	24	24	3311.74	116.73	-371.58	3056.88	4
25	24	20	3311.74	410.01	-111.06	3610.69	8
25	24	16	3311.74	464.41	-21.90	3754.25	8
25	24	12	3311.74	389.83	-70.92	3630.65	8
25	24	8	3311.74	273.85	-86.76	3498.83	8
25	24	4	3311.74	179.18	-43.64	3447.28	8
25	24	00	3311.74	143.44	-14.58	3440.60	4
25	20	20	3311.74	236.83	-53.43	3495.14	4
25	20	16	3311.74	203.83	-24.42	3491.14	8
25	20	12	3311.74	242.52	-12.81	3541.45	8

25	20	8	3311.74	304.48	-9.90	3606.32	8
25	20	4	3311.74	355.36	-10.14	3656.95	8
25	20	00	3311.74	374.60	-10.53	3675.80	4
25	16	16	3311.74	154.03	-12.88	3452.88	4
25	16	12	3311.74	214.23	-5.34	3520.62	8
25	16	8	3311.74	310.10	-2.39	3619.45	8
25	16	4	3311.74	388.75	-1.50	3698.98	8
25	16	00	3311.74	418.49	-1.31	3728.91	4
25	12	12	3311.74	248.52	-1.21	3559.05	4
25	12	8	3311.74	303.11	1.77	3616.62	8
25	12	4	3311.74	347.90	2.04	3661.68	8
25	12	00	3311.74	364.84	1.61	3678.18	4
25	8	8	3311.74	292.07	5.23	3609.04	4
25	8	4	3311.74	283.04	5.35	3600.12	8
25	8	00	3311.74	279.62	4.69	3596.04	4
25	4	4	3311.74	229.85	8.16	3549.75	4
25	4	00	3311.74	209.75	9.27	3530.76	4
25	00	00	3311.74	183.33	11.59	3506.66	1
26	24	24	3523.90	253.93	-244.58	3533.25	4
26	24	20	3523.90	364.67	-64.32	3824.25	8
26	24	16	3523.90	376.45	-24.57	3875.78	8
26	24	12	3523.90	335.75	-45.31	3814.34	8
26	24	8	3523.90	279.91	-48.88	3754.92	8
26	24	4	3523.90	235.68	-28.45	3731.13	8
26	24	00	3523.90	219.15	-15.61	3727.44	4
26	20	20	3523.90	204.43	-37.79	3690.53	4
26	20	16	3523.90	185.04	-18.32	3690.61	8
26	20	12	3523.90	238.21	-8.76	3753.35	8
26	20	8	3523.90	312.66	-6.35	3830.21	8
26	20	4	3523.90	371.90	-7.01	3888.78	8
26	20	00	3523.90	394.07	-7.62	3910.35	4
26	16	16	3523.90	162.11	-9.33	3676.68	4
26	16	12	3523.90	226.50	-3.96	3746.44	8
26	16	8	3523.90	316.46	-1.63	3838.73	8
26	16	4	3523.90	388.01	-.78	3911.13	8
26	16	00	3523.90	414.79	-.57	3938.12	4
26	12	12	3523.90	259.43	-.26	3783.06	4
26	12	8	3523.90	305.44	2.22	3831.55	8
26	12	4	3523.90	342.04	2.20	3868.14	8
26	12	00	3523.90	355.74	1.71	3881.35	4
26	8	8	3523.90	290.10	5.06	3819.06	4
26	8	4	3523.90	277.92	5.15	3806.97	8
26	8	00	3523.90	273.36	4.64	3801.90	4
26	4	4	3523.90	226.95	7.70	3758.55	4
26	4	00	3523.90	207.87	8.73	3740.49	4
26	00	00	3523.90	183.36	10.72	3717.98	1
27	24	24	3744.22	296.01	-144.11	3896.12	4
27	24	20	3744.22	314.73	-42.92	4016.03	8
27	24	16	3744.22	314.03	-22.42	4035.82	8
27	24	12	3744.22	303.03	-28.68	4018.57	8
27	24	8	3744.22	289.53	-28.37	4005.38	8
27	24	4	3744.22	279.17	-19.44	4003.95	8
27	24	00	3744.22	275.33	-14.17	4005.37	4

27	20	20	3744.22	179.43	-27.93	3895.71	4
27	20	16	3744.22	176.17	-13.61	3906.78	8
27	20	12	3744.22	239.90	-6.23	3977.89	8
27	20	8	3744.22	320.85	-4.39	4060.68	8
27	20	4	3744.22	383.59	-4.92	4122.88	8
27	20	00	3744.22	406.86	-5.39	4145.69	4
27	16	16	3744.22	173.06	-6.87	3910.41	4
27	16	12	3744.22	238.47	-2.89	3979.80	8
27	16	8	3744.22	321.47	-.98	4064.71	8
27	16	4	3744.22	385.78	-.25	4129.75	8
27	16	00	3744.22	409.64	-.08	4153.77	4
27	12	12	3744.22	268.47	.48	4013.17	4
27	12	8	3744.22	306.56	2.52	4053.30	8
27	12	4	3744.22	336.08	2.31	4082.60	8
27	12	00	3744.22	347.03	1.80	4093.04	4
27	8	8	3744.22	287.69	4.87	4036.78	4
27	8	4	3744.22	273.08	4.96	4022.26	8
27	8	00	3744.22	267.66	4.57	4016.45	4
27	4	4	3744.22	224.29	7.28	3975.79	4
27	4	00	3744.22	206.19	8.22	3958.63	4
27	00	00	3744.22	183.39	9.95	3937.56	1
28	28	28	3972.70	-240.08	-216.83	3515.79	4
28	28	24	3972.70	404.65	-198.59	4178.76	8
28	28	20	3972.70	622.43	-15.23	4579.90	8
28	28	16	3972.70	577.13	-47.34	4502.49	8
28	28	12	3972.70	402.85	-126.98	4248.57	8
28	28	8	3972.70	203.88	-118.81	4057.76	8
28	28	4	3972.70	54.69	-45.96	3981.43	8
28	28	00	3972.70	-0.	-5.16	3967.54	4
28	24	24	3972.70	291.85	-86.03	4178.52	4
28	24	20	3972.70	269.32	-31.92	4210.10	8
28	24	16	3972.70	271.00	-18.47	4225.22	8
28	24	12	3972.70	284.54	-18.14	4239.10	8
28	24	8	3972.70	300.73	-17.05	4256.37	8
28	24	4	3972.70	313.04	-13.73	4272.00	8
28	24	00	3972.70	317.57	-11.91	4278.36	4
28	20	20	3972.70	162.70	-20.97	4114.43	4
28	20	16	3972.70	174.57	-10.13	4137.14	8
28	20	12	3972.70	245.15	-4.64	4213.21	8
28	20	8	3972.70	328.39	-3.22	4297.87	8
28	20	4	3972.70	391.46	-3.47	4360.69	8
28	20	00	3972.70	414.67	-3.73	4383.63	4
28	16	16	3972.70	185.46	-5.13	4153.02	4
28	16	12	3972.70	249.59	-2.02	4220.26	8
28	16	8	3972.70	325.18	-.43	4297.45	8
28	16	4	3972.70	382.45	.14	4355.29	8
28	16	00	3972.70	403.52	.25	4376.47	4
28	12	12	3972.70	275.80	1.06	4249.56	4
28	12	8	3972.70	306.71	2.71	4282.12	8
28	12	4	3972.70	330.13	2.37	4305.20	8
28	12	00	3972.70	338.75	1.87	4313.32	4
28	8	8	3972.70	284.97	4.67	4262.34	4
28	8	4	3972.70	268.51	4.78	4245.99	8

28	8	00	3972.70	262.46	4.49	4239.64	4
28	4	4	3972.70	221.85	6.90	4201.44	4
28	4	00	3972.70	204.68	7.75	4185.12	4
28	00	00	3972.70	183.42	9.26	4165.37	1
29	28	28	4209.34	65.28	-287.87	3986.75	4
29	28	24	4209.34	384.84	-121.32	4472.86	8
29	28	20	4209.34	485.09	-17.79	4676.63	8
29	28	16	4209.34	449.82	-35.25	4623.91	8
29	28	12	4209.34	349.34	-71.00	4487.67	8
29	28	8	4209.34	238.42	-64.38	4383.38	8
29	28	4	4209.34	156.21	-29.22	4336.32	8
29	28	00	4209.34	126.19	-10.09	4325.44	4
29	24	24	4209.34	268.12	-55.11	4422.35	4
29	24	20	4209.34	232.33	-24.95	4416.71	8
29	24	16	4209.34	242.84	-14.41	4437.77	8
29	24	12	4209.34	275.60	-11.64	4473.30	8
29	24	8	4209.34	312.15	-10.71	4510.78	8
29	24	4	4209.34	339.33	-9.94	4538.72	8
29	24	00	4209.34	349.26	-9.58	4549.02	4
29	20	20	4209.34	153.50	-15.81	4347.02	4
29	20	16	4209.34	178.02	-7.61	4379.75	8
29	20	12	4209.34	252.31	-3.58	4458.07	8
29	20	8	4209.34	334.92	-2.43	4541.83	8
29	20	4	4209.34	396.31	-2.42	4603.22	8
29	20	00	4209.34	418.74	-2.52	4625.55	4
29	16	16	4209.34	198.30	-3.85	4403.78	4
29	16	12	4209.34	259.58	-1.30	4467.62	8
29	16	8	4209.34	327.71	.04	4537.08	8
29	16	4	4209.34	378.32	.43	4588.09	8
29	16	00	4209.34	396.82	.47	4606.62	4
29	12	12	4209.34	281.59	1.50	4492.43	4
29	12	8	4209.34	306.08	2.82	4518.23	8
29	12	4	4209.34	324.27	2.40	4536.01	8
29	12	00	4209.34	330.92	1.93	4542.19	4
29	8	8	4209.34	282.06	4.47	4495.86	4
29	8	4	4209.34	264.22	4.60	4478.15	8
29	8	00	4209.34	257.70	4.40	4471.43	4
29	4	4	4209.34	219.61	6.54	4435.48	4
29	4	00	4209.34	203.31	7.32	4419.97	4
29	00	00	4209.34	183.44	8.64	4401.42	1
30	28	28	4454.14	217.59	-213.84	4457.89	4
30	28	24	4454.14	367.17	-72.54	4748.77	8
30	28	20	4454.14	406.73	-18.37	4842.50	8
30	28	16	4454.14	379.03	-28.77	4804.39	8
30	28	12	4454.14	320.03	-44.87	4729.30	8
30	28	8	4454.14	257.82	-39.42	4672.54	8
30	28	4	4454.14	212.46	-21.09	4645.52	8
30	28	00	4454.14	196.01	-11.48	4638.66	4
30	24	24	4454.14	238.93	-38.36	4654.70	4
30	24	20	4454.14	204.60	-19.74	4639.00	8
30	24	16	4454.14	225.86	-10.95	4669.04	8
30	24	12	4454.14	272.97	-7.69	4719.42	8
30	24	8	4454.14	322.99	-7.07	4770.06	8

30	24	4	4454.14	359.54	-7.31	4806.36	8
30	24	00	4454.14	372.82	-7.49	4819.46	4
30	20	20	4454.14	150.49	-11.97	4592.66	4
30	20	16	4454.14	184.80	-5.81	4633.13	8
30	20	12	4454.14	260.28	-2.82	4711.59	8
30	20	8	4454.14	340.31	-1.84	4792.61	8
30	20	4	4454.14	398.78	-1.66	4851.26	8
30	20	00	4454.14	420.01	-1.65	4872.50	4
30	16	16	4454.14	210.92	-2.87	4662.18	4
30	16	12	4454.14	268.32	-.69	4721.77	8
30	16	8	4454.14	329.18	.42	4783.74	8
30	16	4	4454.14	373.64	.65	4828.43	8
30	16	00	4454.14	389.79	.62	4844.54	4
30	12	12	4454.14	286.04	1.82	4741.99	4
30	12	8	4454.14	304.83	2.87	4761.83	8
30	12	4	4454.14	318.56	2.41	4775.11	8
30	12	00	4454.14	323.54	1.98	4779.65	4
30	8	8	4454.14	279.02	4.27	4737.43	4
30	8	4	4454.14	260.18	4.43	4718.75	8
30	8	00	4454.14	253.34	4.30	4711.78	4
30	4	4	4454.14	217.55	6.20	4677.89	4
30	4	00	4454.14	202.07	6.92	4663.13	4
30	00	00	4454.14	183.46	8.08	4645.68	1
31	28	28	4707.10	281.75	-138.66	4850.18	4
31	28	24	4707.10	334.17	-46.71	4994.56	8
31	28	20	4707.10	344.57	-17.90	5033.77	8
31	28	16	4707.10	329.48	-22.21	5014.37	8
31	28	12	4707.10	302.99	-28.53	4981.56	8
31	28	8	4707.10	276.16	-24.82	4958.44	8
31	28	4	4707.10	256.90	-15.68	4948.32	8
31	28	00	4707.10	249.95	-11.06	4945.99	4
31	24	24	4707.10	211.30	-28.48	4889.92	4
31	24	20	4707.10	185.51	-15.57	4877.04	8
31	24	16	4707.10	217.10	-8.26	4915.93	8
31	24	12	4707.10	274.38	-5.30	4976.17	8
31	24	8	4707.10	332.80	-4.91	5034.98	8
31	24	4	4707.10	374.85	-5.43	5076.51	8
31	24	00	4707.10	390.03	-5.74	5091.39	4
31	20	20	4707.10	152.24	-9.11	4850.23	4
31	20	16	4707.10	193.59	-4.50	4896.19	8
31	20	12	4707.10	268.35	-2.23	4973.21	8
31	20	8	4707.10	344.55	-1.37	5050.28	8
31	20	4	4707.10	399.40	-1.09	5105.41	8
31	20	00	4707.10	419.20	-1.02	5125.27	4
31	16	16	4707.10	222.87	-2.09	4927.88	4
31	16	12	4707.10	275.81	-.19	4982.72	8
31	16	8	4707.10	329.76	.72	5037.58	8
31	16	4	4707.10	368.59	.81	5076.50	8
31	16	00	4707.10	382.61	.73	5090.44	4
31	12	12	4707.10	289.32	2.05	4998.47	4
31	12	8	4707.10	303.10	2.88	5013.07	8
31	12	4	4707.10	313.02	2.41	5022.53	8
31	12	00	4707.10	316.60	2.01	5025.71	4

31	8	8	4707.10	275.94	4.08	4987.12	4
31	8	4	4707.10	256.40	4.27	4967.77	8
31	8	00	4707.10	249.35	4.19	4960.63	4
31	4	4	4707.10	215.66	5.90	4928.65	4
31	4	00	4707.10	200.95	6.55	4914.59	4
31	00	00	4707.10	183.48	7.57	4898.15	1
32	32	32	4968.22	-268.25	-153.75	4546.21	4
32	32	28	4968.22	338.85	-183.11	5123.95	8
32	32	24	4968.22	595.48	-31.93	5531.76	8
32	32	20	4968.22	617.15	-12.65	5572.71	8
32	32	16	4968.22	501.60	-71.18	5398.63	8
32	32	12	4968.22	328.80	-105.22	5191.79	8
32	32	8	4968.22	160.94	-80.05	5049.11	8
32	32	4	4968.22	42.46	-28.64	4982.04	8
32	32	00	4968.22	-0.	-3.52	4964.69	4
32	28	28	4968.22	297.01	-87.68	5177.55	4
32	28	24	4968.22	296.92	-33.01	5232.13	8
32	28	20	4968.22	296.42	-16.31	5248.32	8
32	28	16	4968.22	295.44	-16.56	5247.09	8
32	28	12	4968.22	294.28	-18.29	5244.20	8
32	28	8	4968.22	293.23	-16.09	5245.36	8
32	28	4	4968.22	292.51	-11.89	5248.84	8
32	28	00	4968.22	292.25	-9.84	5250.63	4
32	24	24	4968.22	188.36	-21.94	5134.64	4
32	24	20	4968.22	173.80	-12.21	5129.81	8
32	24	16	4968.22	214.25	-6.28	5176.18	8
32	24	12	4968.22	278.24	-3.85	5242.60	8
32	24	8	4968.22	341.36	-3.57	5306.00	8
32	24	4	4968.22	386.20	-4.05	5350.36	8
32	24	00	4968.22	402.30	-4.33	5366.19	4
32	20	20	4968.22	157.47	-7.00	5118.68	4
32	20	16	4968.22	203.44	-3.52	5168.13	8
32	20	12	4968.22	276.07	-1.75	5242.54	8
32	20	8	4968.22	347.70	-.97	5314.94	8
32	20	4	4968.22	398.57	-.66	5366.13	8
32	20	00	4968.22	416.84	-.58	5384.48	4
32	16	16	4968.22	233.92	-1.45	5200.69	4
32	16	12	4968.22	282.08	.23	5250.53	8
32	16	8	4968.22	329.58	.96	5298.76	8
32	16	4	4968.22	363.31	.93	5332.46	8
32	16	00	4968.22	375.43	.81	5344.46	4
32	12	12	4968.22	291.61	2.21	5262.03	4
32	12	8	4968.22	301.01	2.85	5272.07	8
32	12	4	4968.22	307.69	2.40	5278.30	8
32	12	00	4968.22	310.09	2.04	5280.35	4
32	8	8	4968.22	272.85	3.90	5244.97	4
32	8	4	4968.22	252.85	4.12	5225.19	8
32	8	00	4968.22	245.67	4.08	5217.97	4
32	4	4	4968.22	213.91	5.61	5187.74	4
32	4	00	4968.22	199.93	6.20	5174.35	4
32	00	00	4968.22	183.50	7.11	5158.82	1

APPENDIX III

COMPUTER PROGRAMS

	Page
Computation of Heat Capacity between 60°K and 300°K	220
Computation of Heat Capacity below 60°K	233
Evaluation of energy levels for Hindered Rotor	240

Computation of Heat Capacity between 60°K and 320°K

A copy of pages 62 and 63 of Computation Book III "White Phosphorous" is reproduced on the next page. The method of calculating the heat capacity from the experimental measurements given on page 62 is given in the Appendix of the thesis of Maple. He also used the next page as his example. Page 63 shows the calculated quantities which lead to the value of the heat capacity.

Ten data cards are required to give all the information the computer program needs to calculate the heat capacity. The information from Page 62 that need be punched on data cards are given below:

Card 1.

C11 = 49200 C12 = 49180

CL11 = 20.1 CL12 = 22.8

CL13 = 0.0 CL15 = 20.7

C14 = 19.7

Card 2.

E11 = 18931 E12 = 18929

EL11 = 12.7 EL12 = 20.3

EL13 = 0.0 EL15 = 19.4

E14 = 19.2

C_p 5 cells

Oct. 16 '48

BB

I_R

1:39	41453	— 25.2	
½		25.2	(4.4)
40	41454	— 20.8	
	(23.5)		
41	Ch'k 0	— 23.8	

E_R

42	79165	— $23.7_{0.0}$	
44		$23.7_{0.1}$	
46		$23.5_{0.05}$	(2.6)
48		23.4	
49	79166	— 20.7	
	(22.5)		

I_R

50	41453	— 24.0	
	(22.2)		

E_R

51	79165	— $22.9_{0.15}$	
53		22.6	
55		$22.4_{0.1}$	
57		$22.2_{0.0}$	(2.6)
59		22.2	
2:00	79166	— 19.6	
	(20.6)		
01	Ch'k 0	— 20.7	

I_R

02	41453	— 23.0	
	(20.4)		
03	Start		
17	Stop		

I_R

27	41452	— 17.7	
½		17.7	(4.3)
28	41453	— 13.4	
	(14.8)		
29	Ch'k 0	— 17.0	

E_R

30	79447	— $17.8_{0.05}$	
32		$17.5_{0.2}$	
34		$17.3_{0.05}$	
36		17.2	

0	Start		

I

2:26	49200	— 20.1	
2:56	49180	— 22.8	(.24)
3:26		20.7	
	(19.7)		

E

6:30	18931	— 17.7	
7:00	18929	— 20.3	(1.8)
7:30		19.4	
	(19.2)		

I

10:34	49100	— 13.5	
11:04	49070	— 19.1	(.25)
11:34		17.1	
	(18.5)		1485.34
			645.35
14:00	Stop		839.99

38		17.2^{00}	(2.7)
39	79448	— 14.5	
	(15.5)		

I_R

40	41452	— 17.5	
	(15.4)		

E_R

41	79447	— $17.3_{0.05}$	
43		$17.2_{0.05}$	
45		$17.1_{0.05}$	(2.5)
47		17.0	
48	79448	— 14.5	
	(14.6)		
49	Ch'k 0	— 14.8	

I_R

50	41452	— 17.1	
	(14.5)		

$E = 18929.56$

$I = \frac{1}{2}(49192.5 + 49072.0) = 49132.3$

$E_T = 100455.6 \times 18929.56 \times 49132.6 = 98.4290$

	E_R	I_R	R
1:41	79165.00	41453.39	190.9735
:50	79165.27	41453.41	190.9741
2:02	79165.58	41453.58	190.9740
2:29	79447.33	41452.23	191.6600
:40	79447.72	41452.49	191.6597
:49	79447.88	41452.59	191.6596

$R_{49} - R_{02} = 0.6856$

$\Delta E/\Delta R = 136.273 - .082 = 136.191$

MT 37.743

98.448

$\Delta E/\Delta T = 37.367$

He $.013$

37.380

$C_p = 4.9278$

R_1	192.7465
F_2	.247
R_{49}	192.994
R_{AV}	191.317
δR	1.677

$A/E_T = .2513$

E_{RR}	−.0013
SS	+.0001
W	+.0003
TIME	.0000
$R_0/\Delta R$	+.0003
	−.0006

$\frac{dR}{dT} = .37956$

$T_{AV} = 189.336$

Card 3.

C21 = 49100 C22 = 49070

CL12 = 13.5 CL22 = 19.1

CL23 = 0.0 CL25 = 17.1

C14 = 18.5

Card 4.

C51 = 41453 C52 = 41454

CL51 = 24.0 CL52 = 19.6

CL53 = 24.0 CL55 = 0.0

C54 = 22.2

Card 5.

E51 = 79165 E54 = 22.2

EL51 = 22.9 E61 = 79166

EL53 = 22.0 EL61 = 19.6

E64 = 20.6

Card 6.

C61 = 41453 C62 = 41454

CL61 = 23.0 CL62 = 18.6

CL63 = 23.0 CL65 = 0.0

C64 = 20.4

Card 7.

C71 = 41452 C72 = 41453

CL71 = 17.5 CL72 = 13.2

CL73 = 17.5 CL75 = 0.0

C74 = 15.5

Card 8.

E71 = 79447 E74 = 15.4

EL71 = 17.3 E81 = 79448

E173 = 17.0 EL81 = 14.5

E84 = 14.6

Card 9.

C81 = 41452 C82 = 41453

CL81 = 17.1 CL82 = 12.8

CL83 = 17.1 CL85 = 0.0

C84 = 14.5

Card 10.

ITIME= 14 TIM = 28

SUM = 5.24 SUMO = 0

WATCH= 0.0

The potentiometer reading corresponding to EL53 and EL73 must be extrapolated to the time of the reading of EL81. ITIME is the length of the heating period. TIM is the total time of the run; it is used to make the adiabatic correction. SUM is the sum of the galvanometer readings used for the adiabatic correction. SUMO is equal to ϵ_o (long equilibrium period). WATCH is the "time" correction.

The program will not calculate correct adaibatic corrections $(R_N/\Delta R)$, if the correction is greater than 0.3%.

The program output looks like:

CASE 1

E1 = 18929.56	CT = 49132.30	ET = 93.42900	RA = 192.7465
E5 = 79165.27	C5 = 41453.41	RT5 = 190.9711	FA = .2470
E6 = 79165.58	C6 = 41453.58	RT6 = 190.9740	RW = 192.9949
E7 = 79447.72	C7 = 41452.49	RT7 = 191.6597	RE = 1.6770
E8 = 79447.88	C8 = 41452.59	RT8 = 191.6596	Z = .2513

EPR = -.0013	RDIFF = .68560	RAVE = 191.3168
W = .0003	DA = 136.27300	DRAV = .37946
SS = .0001	DCORR = - .08200	DRDT = .37956
SW = .0000	DSUM = 136.19100	T = 189.33600
ADIA = .0003	MT = 37.74300	
WAT = .0000	CSUM = 98.44800	
CORR = -.0006	CTOT = 37.36700	

CTOT corresponds to $\Delta E/\Delta T$ without the helium correction. RT8 and RT6 are the resistances used to calculate ΔR(RDIFF).

The stop watch correction used in this program is 0.0008.

The ten data cards given after the program on the following pages are for page 62. After these ten data cards are cards that give the temperature in terms of resistance and give the heat capacity of the empty calorimeter.

```
C      THIS PROGRAM DETERMINES THE HEAT CAPACITY OF A SUBSTANCE FROM THE
C      EXPERIMENTAL DATA IN THE LIQUID NITROGEN TEMPERATURE REGION
       READ 119, J
  119 FORMAT (I2)
     0DIMENSION C11(50),CL11(50),CL13(50),C12(50),CL12(50),CL15(50),
     1    C14(50)
     0READ 100,(C11(K),CL11(K),CL13(K),C12(K),CL12(K),CL15(K),C14(K),
     1   K  = 1,J)
  100 FORMAT (F6.0, 2F5.1, F6.0, 3F5.1)
     0DIMENSION E11(50),EL11(50),EL13(50),E12(50),EL12(50),EL15(50),
     1    E14(50)
     0READ 100,(E11(K),EL11(K),EL13(K),E12(K),EL12(K),EL15(K),E14(K),
     1   K  = 1,J)
     0DIMENSION C21(50),CL21(50),CL23(50),C22(50),CL22(50),CL25(50),
     1    C24(50)
     0READ 100,(C21(K),CL21(K),CL23(K),C22(K),CL22(K),CL25(K),C24(K),
     1   K  = 1,J)
     0DIMENSION C51(50),CL51(50),CL53(50),C52(50),CL52(50),CL55(50),
     1    C54(50)
     0READ 100,(C51(K),CL51(K),CL53(K),C52(K),CL52(K),CL55(K),C54(K) ,
     1   K  = 1,J)
     0DIMENSION  E51(50),EL51(50),EL53(50),E54(50),E61(50),EL61(50),
     1    E64(50)
     0READ 104,(E51(K),EL51(K),EL53(K),E54(K),E61(K),EL61(K),E64(K),
     1   K  = 1,J)
  104 FORMAT (F6.0, F5.1, F6.2, F5.1, F6.0, 2F5.1)
     0DIMENSION C61(50),CL61(50),CL63(50),C62(50),CL62(50),CL65(50),
     1    C64(50)
     0READ 100,(C61(K),CL61(K),CL63(K),C62(K),CL62(K),CL65(K),C64(K),
     1   K  = 1,J)
     0DIMENSION C71(50),CL71(50),CL73(50),C72(50),CL72(50),CL75(50),
     1    C74(50)
     0READ 100,(C71(K),CL71(K),CL73(K),C72(K),CL72(K),CL75(K),C74(K),
     1   K  = 1,J)
     0DIMENSION  E71(50),EL71(50),EL73(50),E74(50),E81(50),EL81(50),
     1    E84(50)
     0READ 104,(E71(K),EL71(K),EL73(K),E74(K),E81(K),EL81(K),E84(K),
     1   K  = 1,J)
     0DIMENSION C81(50),CL81(50),CL83(50),C82(50),CL82(50),CL85(50),
     1    C84(50)
     0READ 100,(C81(K),CL81(K),CL83(K),C82(K),CL82(K),CL85(K),C84(K),
     1   K  = 1,J)
      DIMENSION  ITIME(50), TIM(50), SUM(50), SUMO(50), WATCH(50)
     0READ 109,(ITIME(K),TIM(K),SUM(K),SUMO(K),WATCH(K),
     1   K  = 1,J)
  109 FORMAT (I3,F3.0,F6.2,F7.0,F6.4)
      DIMENSION  T(105), R(105), DR(105)
      READ 110,L,(N,T(N),R(N),DR(N),  N=1,L)
  110 FORMAT (I3/(I3, F4.0, F9.4, F6.5))
      DIMENSION  V(160), DHDR(160)
      READ 111, I,(M,V(M),DHDR(M),   M=1,I)
  111 FORMAT (I3/(I3, F6.0, F7.0))
      K = 1
```

```
702 C1 = X(CL11(K),CL12(K),CL13(K),C14(K),CL15(K),C11(K),C12(K))
    C2 = X(CL21(K),CL22(K),CL23(K),C24(K),CL25(K),C21(K),C22(K))
    E1 = X(EL11(K),EL12(K),EL13(K),E14(K),EL15(K),E11(K),E12(K))
    C5 = X(CL51(K),CL52(K),CL53(K),C54(K),CL55(K),C51(K),C52(K))
    C6 = X(CL61(K),CL62(K),CL63(K),C64(K),CL65(K),C61(K),C62(K))
    C7 = X(CL71(K),CL72(K),CL73(K),C74(K),CL75(K),C71(K),C72(K))
    C8 = X(CL81(K),CL82(K),CL83(K),C84(K),CL85(K),C81(K),C82(K))
    CT = (C1 + C2)/2.0
   0E5= E51(K)+(EL51(K)-E54(K)) *ABSF(E61(K)-E51(K))/ABSF(EL53(K)-
   1     EL61(K))
   0E6= E61(K)+(EL61(K)-E64(K)) *ABSF(E61(K)-E51(K))/ABSF(EL53(K)-
   1     EL61(K))
   0E7= E71(K)+(EL71(K)-E74(K)) *ABSF(E81(K)-E71(K))/ABSF(EL73(K)-
   1     EL81(K))
   0E8= E81(K)+(EL81(K)-E84(K)) *ABSF(E81(K)-E71(K))/ABSF(EL73(K)-
   1     EL81(K))
    TIME = ITIME(K)
    ITIM = ITIME(K)
   0GO TO (20,21,22,23,24,25,26,27,28,29,30,31,32,33,34,35,36,37,38,
   1      39),ITIM
 20 FT  =7175.4
    GO TO 40
 21 FT  =14350.8
    GO TO 40
 22 FT  =21526.2
    GO TO 40
 23 FT  =28701.6
    GO TO 40
 24 FT  =35876.9
    GO TO 40
 25 FT  =43052.3
    GO TO 40
 26 FT  =50227.7
    GO TO 40
 27 FT  =57403.1
    GO TO 40
 28 FT  =64578.5
    GO TO 40
 29 FT  =71753.9
    GO TO 40
 30 FT  =78929.3
    GO TO 40
 31 FT  =86104.7
    GO TO 40
 32 FT  =93280.0
    GO TO 40
 33 FT  =100455.4
    GO TO 40
 34 FT  =107630.8
    GO TO 40
 35 FT  =114806.2
    GO TO 40
 36 FT  =121981.6
```

```
      GO TO 40
   37 FT  =129157.0
      GO TO 40
   38 FT  =136332.4
      GO TO 40
   39 FT  =143507.8
   40 ET = FT*E1*CT*1.0E-12
      RT5 = 100.0*E5/C5
      RT6 = 100.0*E6/C6
      RT7 = 100.0*E7/C7
      RT8 = 100.0*E8/C8
      RAVE = (RT8 + RT6)/2.0
      RDIFF = RT8 - RT6
C      DA IS DELTA E/ DELTA R
      DA = ET/RDIFF
      WAT = WATCH(K)
      RA = 500.28*E1/CT
      FA = (6.60E-6)*RA**2
      RW = RA + FA
      RE = RW - RAVE
C      Z IS A/ET
      Z = RE*TIME/ET
      SS = RE/(10.0*RAVE*TIME)
      IF (RW - 128.)48,48,41
   41 IF (RW - 143.)49,49,42
   42 IF (RW - 158.)50,50,43
   43 IF (RW - 173.)51,51,44
   44 IF (RW - 188.)52,52,45
   45 IF (RW - 203.)53,53,46
   46 IF (RW - 218.)54,54,47
   47 IF (RW - 233.)55,55,56
   48 EPR  =-0.0008
      GO TO 57
   49 EPR  =-0.0009
      GO TO 57
   50 EPR  =-0.0010
      GO TO 57
   51 EPR  =-0.0011
      GO TO 57
   52 EPR  =-0.0012
      GO TO 57
   53 EPR  =-0.0013
      GO TO 57
   54 EPR  =-0.0014
      GO TO 57
   55 EPR  =-0.0015
      GO TO 57
   56 EPR  =-0.0016
   57 IF (RAVE - 139.)64, 64, 60
   60 IF (RAVE - 161.)65,65,61
   61 IF (RAVE - 187.)66,66,62
   62 IF (RAVE - 219.)67,67,68
   64 W=0.0000
```

```
      GO TO 69
   65 W=0.0001
      GO TO 69
   66 W=0.0002
      GO TO 69
   67 W=0.0003
      GO TO 69
   68 W=0.0004
   69 SW=0.0008
      IF (RAVE - 184.)600,600,601
  600 IF (RAVE - 167.5) 602,602,603
  602 IF (RAVE - 131.6) 604,604,605
  604 IF (RAVE - 130.)606,606,607
  606 DC  =0
      GO TO 621
  607 DC  =6.E-3
      GO TO 621
  605 IF (RAVE - 139.5) 608,608,609
  608 IF (RAVE - 134.5) 610,610,611
  610 DC  =5.E-3
      GO TO 621
  611 DC  =4.E-3
      GO TO 621
  609 DC  =3.E-3
      GO TO 621
  603 IF (RAVE - 176.)611,611,610
  601 IF (RAVE - 197.5) 612,612,613
  612 IF (RAVE - 189.5) 607,607,614
  614 IF (RAVE - 194.5) 615,615,616
  615 DC  =7.E-3
      GO TO 621
  616 DC  =8.E-3
      GO TO 621
  613 IF (RAVE - 202.5) 617,617,618
  617 DC  =9.E-3
      GO TO 621
  618 IF (RAVE - 206.0) 619,619,620
  619 DC  =1.E-2
      GO TO 621
  620 DC = (0.45*RAVE - 82.5)*1.0E-3
  621 ADIA = DC*(SUM(K)-SUMO(K)*TIM(K))/ET
      CORR = EPR + SS + W + SW + ADIA + WATCH(K)
      DCORR = DA*CORR
      DSUM = DA + DCORR
      IF (RAVE - 152.)500, 500, 501
  500 IF (RAVE - 134.)502, 502, 503
  501 IF (RAVE - 190.)504, 504, 505
  502 IF (RAVE - 130.)506, 506, 507
  503 IF (RAVE - 140.)508, 508, 509
  508 IF (RAVE - 136.)510, 510, 511
  509 IF (RAVE - 145.)512, 512, 513
  512 IF (RAVE - 142.)514, 514, 515
  513 IF (RAVE - 148.)516, 516, 517
```

```
504 IF (RAVE - 171.)518, 518, 519
518 IF (RAVE - 162.)520, 520, 521
520 IF (RAVE - 157.)522, 522, 523
521 IF (RAVE - 166.)524, 524, 525
519 IF (RAVE - 181.)526, 526, 527
526 IF (RAVE - 176.)528, 528, 529
527 IF (RAVE - 186.)530, 530, 531
505 IF (RAVE - 210.)532, 532, 533
532 IF (RAVE - 200.)534, 534, 535
534 IF (RAVE - 195.)536, 536, 537
535 IF (RAVE - 205.)538, 538, 539
533 IF (RAVE - 220.)540, 540, 541
540 IF (RAVE - 215.)542, 542, 543
541 IF (RAVE - 225.)544, 544, 545
507 IF (RAVE - 132.)546, 546, 547
546 N = 23
    M = 9
    GO TO 550
510 N = 37
    M = 29
    GO TO 550
511 N = 42
    M = 39
    GO TO 550
514 N = 48
    M = 47
    GO TO 550
515 N = 51
    M = 51
    GO TO 550
516 N = 55
    M = 57
    GO TO 550
517 N = 58
    M = 63
    GO TO 550
522 N = 60
    M = 68
    GO TO 550
523 N = 62
    M = 73
    GO TO 550
524 N = 64
    M = 78
    GO TO 550
525 N = 66
    M = 82
    GO TO 550
528 N = 69
    M = 87
    GO TO 550
529 N = 71
    M = 92
```

```
      GO TO 550
  530 N = 74
      M = 97
      GO TO 550
  531 N = 77
      M = 102
      GO TO 550
  536 N = 79
      M = 106
      GO TO 550
  537 N = 81
      M = 111
      GO TO 550
  538 N = 84
      M = 116
      GO TO 550
  539 N = 87
      M = 121
      GO TO 550
  542 N = 89
      M = 126
      GO TO 550
  543 N = 92
      M = 131
      GO TO 550
  544 N = 95
      M = 136
      GO TO 550
  545 N = 98
      M = 141
      GO TO 550
  547 N = 31
      M = 19
      GO TO 550
  550 IF (RAVE - R(N)) 551, 551, 552
  552 N = N + 1
      GO TO 550
  551 IF (RAVE - V(M)) 553, 553, 554
  554 M = M + 1
      GO TO 551
  553 DRDT = DR(N) - (R(N) - RAVE)*(DR(N) - DR(N-1))/(R(N)-R(N-1))
      DRAV = (DRDT + DR(N))/2.0
      TEMP = T(N) - (R(N) - RAVE)/DRAV
      CMT = DHDR(M-1) + (RAVE-V(M-1))*(DHDR(M)-DHDR(M-1))/(V(M)-V(M-1))
      CSUM = DSUM - CMT
      CTOT = CSUM*DRDT
      PRINT 131, K
  131 FORMAT (5H CASE I2///)
      PRINT  120,  E1, CT, ET, RA, EPR
 1200FORMAT (4H E1= F11.2, 5H  CT= F10.2, 5H  ET= F11.5, 5H  RA= F10.4,
     1    6H  EPR= F10.4)
      PRINT 121, E5, C5, RT5, FA, W
  121 FORMAT (5H E5= F10.2, 5H  C5= F10.2, 6H  RT5= F10.4,
```

```
     1   5H  FA= F10.4, 5H  W= F11.4)
         PRINT 122, E6, C6, RT6, RW, SS
 1220FORMAT  (4H E6= F11.2, 5H  C6= F10.2, 6H  RT6= F10.4,
     1   5H  RW= F10.4, 5H  SS= F11.4)
         PRINT 123, E7, C7, RT7, RE, SW
 1230FORMAT  (4H E7= F11.2, 5H  C7= F10.2, 6H  RT7= F10.4,
     1    5H  RE= F10.4, 5H  SW= F11.4)
         PRINT 124, E8, C8, RT8, Z, ADIA
 1240FORMAT  (4H E8= F11.2, 5H  C8= F10.2, 6H  RT8= F10.4,
     1   4H  Z= F11.4, 7H  ADIA= F 9.4)
         PRINT 125, RDIFF, RAVE, WAT
  125 FORMAT (8H RDIFF= F10.5, 7H  RAVE= F10.4, 27X, 5H WAT= F10.4)
         PRINT 126, DA, DRAV, CORR
  126 FORMAT (4H DA= F14.5, 7H  DRAV= F10.5, 27X, 6H CORR= F10.4)
         PRINT 127, DCORR, DRDT
  127 FORMAT  (8H DCORR= F10.5, 7H  DRDT= F10.5)
         PRINT 128, DSUM, TEMP
  128 FORMAT (6H DSUM= F12.5, 4H  T= F13.5)
         PRINT 140, CMT
  140 FORMAT (4H MT= F14.5)
         PRINT 129, CSUM
  129 FORMAT  (6H CSUM= F12.5)
         PRINT 130, CTOT
  130 FORMAT  (6H CTOT= F12.5////)
         IF (J - K) 700, 700, 701
  701 K = K + 1
         GO TO 702
  506 CONTINUE
  700 CALL EXIT
         END
         FUNCTION X(A, B, C, D, E, F, G)
         IF (E) 10, 11, 10
   10 S = ABSF((2.0*B - A - E)/(F - G))
         X = G + (B - D)/S
         RETURN
   11 S = ABSF((2.0*C - B - A)/(F - G))
         X = F + (C - D)/S
         RETURN
         END
*        DATA
 1
 49200 20.1 0000 49180 22.8 20.7 19.7
 18931 17.7 0000 18929 20.3 19.4 19.2
 49100 13.5 0000 49070 19.1 17.1 18.5
 41453 24.0 24.0 41454 19.6 0000 22.2
 79165 22.9 22.20 22.2 79166 19.6 20.6
 41453 23.0 23.0 41454 18.6 0000 20.4
 41452 17.5 17.5 41453 13.2 0000 15.4
 79447 17.3 16.95 15.3 79448 14.5 14.6
 41452 17.1 17.1 41453 12.8 0000 14.5
 14 29  5.24 000000  0000
104
  1  10 127.4891 01100
```

2	11	127.5024	01540
3	12	127.5202	02030
4	13	127.5432	02580
5	14	127.5720	03200
6	15	127.6074	03900
7	16	127.6502	04690
8	17	127.7014	05570
9	18	127.7620	06550
10	19	127.8328	07610
11	20	127.9146	08740
12	21	128.0078	09910
13	22	128.1128	11090
14	23	128.2297	12290
15	24	128.3587	13500
16	25	128.4998	14720
17	26	128.6532	15960
18	27	128.8190	17200
19	28	128.9972	18430
20	29	129.1876	19640
21	30	129.3900	20830
22	31	129.6042	21990
23	32	129.8298	23120
24	33	130.0664	24200
25	34	130.3136	25230
26	35	130.5709	26210
27	36	130.8378	27150
28	37	131.1138	28050
29	38	131.3986	28900
30	39	131.6917	29720
31	40	131.9929	30510
32	41	132.3018	31270
33	42	132.6182	32000
34	43	132.9417	32700
35	44	133.2720	33360
36	45	133.6087	33990
37	46	133.9516	34580
38	47	134.3003	35150
39	48	134.6546	35700
40	49	135.0142	36220
41	50	135.3789	36710
42	51	135.7483	37150
43	52	136.1219	37540
44	53	136.4992	37900
45	54	136.8798	38240
46	56	137.6508	38860
47	58	138.4338	39430
48	60	139.2276	39940
49	62	140.0310	40390
50	64	140.8428	40780
51	66	141.6617	41110
52	68	142.4867	41380
53	70	143.3166	41600
54	72	144.1504	41770

55	74	144.9869	41880
56	76	145.8252	41950
57	78	146.6645	41990
58	80	147.5041	42019
59	85	149.6059	42040
60	90	151.7069	41987
61	95	153.8035	41863
62	100	155.8924	41683
63	105	157.9712	41469
64	110	160.0388	41239
65	115	162.0947	40998
66	120	164.1383	40744
67	125	166.1689	40478
68	130	168.1860	40206
69	135	170.1896	39941
70	140	172.1805	39700
71	145	174.1601	39490
72	150	176.1298	39300
73	155	178.0903	39119
74	160	180.0418	38941
75	165	181.9844	38764
76	170	183.9182	38589
77	175	185.8433	38415
78	180	187.7598	38247
79	185	189.6681	38088
80	190	191.5687	37936
81	195	193.4618	37788
82	200	195.3476	37644
83	205	197.2263	37505
84	210	199.0982	37371
85	215	200.9635	37243
86	220	202.8226	37123
87	225	204.6758	37009
88	230	206.5235	36899
89	235	208.3658	36790
90	240	210.2026	36683
91	245	212.0341	36579
92	250	213.8606	36482
93	255	215.6824	36393
94	260	217.5000	36313
95	265	219.3138	36239
96	270	221.1240	36168
97	275	222.9307	36100
98	280	224.7340	36033
99	285	226.5340	35968
100	290	228.3308	35905
101	295	230.1245	35844
102	300	231.9152	35785
103	305	233.7030	35728
104	310	235.4880	35673

156

1	128.4	4.622
2	128.6	4.832

3	128.8	5.043
4	129.0	5.254
5	129.2	5.462
6	129.4	5.669
7	129.6	5.876
8	129.8	6.083
9	130.0	6.288
10	130.2	6.492
11	130.4	6.696
12	130.6	6.897
13	130.8	7.096
14	131.0	7.292
15	131.2	7.479
16	131.4	7.663
17	131.6	7.847
18	131.8	8.030
19	132.0	8.212
20	132.2	8.395
21	132.4	8.578
22	132.6	8.763
23	132.8	8.946
24	133.0	9.127
25	133.2	9.307
26	133.4	9.486
27	133.6	9.660
28	133.8	9.832
29	134.0	10.001
30	134.2	10.168
31	134.4	10.333
32	134.6	10.496
33	134.8	10.658
34	135.0	10.820
35	135.2	10.981
36	135.4	11.141
37	135.6	11.300
38	135.8	11.457
39	136.0	11.614
40	136.5	12.002
41	137.0	12.388
42	137.5	12.772
43	138.0	13.153
44	138.5	13.533
45	139.0	13.911
46	139.5	14.284
47	140.0	14.654
48	140.5	15.022
49	141.0	15.388
50	141.5	15.752
51	142.0	16.111
52	142.5	16.463
53	143.0	16.814
54	143.5	17.163
55	144.0	17.511

56	144.5	17.851
57	145.0	18.186
58	145.5	18.523
59	146.0	18.854
60	146.5	19.182
61	147.0	19.511
62	147.5	19.833
63	148.0	20.152
64	148.5	20.471
65	149	20.784
66	150	21.402
67	151	22.006
68	152	22.611
69	153	23.202
70	154	23.772
71	155	24.324
72	156	24.865
73	157	25.397
74	158	25.915
75	159	26.425
76	160	26.923
77	161	27.416
78	162	27.889
79	163	28.350
80	164	28.805
81	165	29.248
82	166	29.676
83	167	30.090
84	168	30.500
85	169	30.910
86	170	31.300
87	171	31.690
88	172	32.070
89	173	32.440
90	174	32.800
91	175	33.140
92	176	33.470
93	177	33.790
94	178	34.100
95	179	34.400
96	180	34.700
97	181	35.000
98	182	35.290
99	183	35.580
100	184	35.870
101	185	36.140
102	186	36.410
103	187	36.690
104	188	36.950
105	189	37.190
106	190	37.430
107	191	37.670
108	192	37.900

109	193	38.120
110	194	38.340
111	195	38.550
112	196	38.760
113	197	38.960
114	198	39.160
115	199	39.360
116	200	39.550
117	201	39.730
118	202	39.910
119	203	40.090
120	204	40.270
121	205	40.440
122	206	40.610
123	207	40.780
124	208	40.940
125	209	41.100
126	210	41.260
127	211	41.410
128	212	41.560
129	213	41.720
130	214	41.870
131	215	42.010
132	216	42.150
133	217	42.290
134	218	42.430
135	219	42.560
136	220	42.690
137	221	42.820
138	222	42.950
139	223	43.080
140	224	43.210
141	225	43.330
142	226	43.450
143	227	43.580
144	228	43.700
145	229	43.830
146	230	43.950
147	231	44.070
148	232	44.180
149	233	44.300
150	234	44.410
151	235	44.530
152	236	44.640
153	237	44.760
154	238	44.870
155	239	44.980
156	240	45.080

Computation of Heat Capacity below 60°K

The input data for this program is the same as for the previous program. Again, CTOT is $\Delta E/\Delta T$ without the helium correction.

No stop watch correction has been used in this program.

```
C      THIS PROGRAM DETERMINES THE HEAT CAPACITY OF A SUBSTANCE IN THE
C      LIQUID HYDROGEN TEMPERATURE REGION
       READ 119, J
  119 FORMAT (I2)
      0DIMENSION C11(50),CL11(50),CL13(50),C12(50),CL12(50),CL15(50),
      1    C14(50)
      0READ 100,(C11(K),CL11(K),CL13(K),C12(K),CL12(K),CL15(K),C14(K),
      1   K  = 1,J)
  100 FORMAT (F6.0, 2F5.1, F6.0, 3F5.1)
      0DIMENSION E11(50),EL11(50),EL13(50),E12(50),EL12(50),EL15(50),
      1    E14(50)
      0READ 100,(E11(K),EL11(K),EL13(K),E12(K),EL12(K),EL15(K),E14(K),
      1   K  = 1,J)
      0DIMENSION C21(50),CL21(50),CL23(50),C22(50),CL22(50),CL25(50),
      1    C24(50)
      0READ 100,(C21(K),CL21(K),CL23(K),C22(K),CL22(K),CL25(K),C24(K),
      1   K  = 1,J)
      0DIMENSION C51(50),CL51(50),CL53(50),C52(50),CL52(50),CL55(50),
      1    C54(50)
      0READ 100,(C51(K),CL51(K),CL53(K),C52(K),CL52(K),CL55(K),C54(K) ,
      1   K  = 1,J)
      0DIMENSION  E51(50),EL51(50),EL53(50),E54(50),E61(50),EL61(50),
      1    E64(50)
      0READ 104,(E51(K),EL51(K),EL53(K),E54(K),E61(K),EL61(K),E64(K),
      1   K  = 1,J)
  104 FORMAT (F6.0, F5.1, F6.2, F5.1, F6.0, 2F5.1)
      0DIMENSION C61(50),CL61(50),CL63(50),C62(50),CL62(50),CL65(50),
      1    C64(50)
      0READ 100,(C61(K),CL61(K),CL63(K),C62(K),CL62(K),CL65(K),C64(K),
      1   K  = 1,J)
      0DIMENSION C71(50),CL71(50),CL73(50),C72(50),CL72(50),CL75(50),
      1    C74(50)
      0READ 100,(C71(K),CL71(K),CL73(K),C72(K),CL72(K),CL75(K),C74(K),
      1   K  = 1,J)
      0DIMENSION  E71(50),EL71(50),EL73(50),E74(50),E81(50),EL81(50),
      1    E84(50)
      0READ 104,(E71(K),EL71(K),EL73(K),E74(K),E81(K),EL81(K),E84(K),
      1   K  = 1,J)
      0DIMENSION C81(50),CL81(50),CL83(50),C82(50),CL82(50),CL85(50),
      1    C84(50)
      0READ 100,(C81(K),CL81(K),CL83(K),C82(K),CL82(K),CL85(K),C84(K),
      1   K  = 1,J)
       DIMENSION  ITIME(50), TIM(50), SUM(50), SUMO(50), WATCH(50)
      0READ 109,(ITIME(K),TIM(K),SUM(K),SUMO(K),WATCH(K),
      1   K  = 1,J)
  109 FORMAT (I3,F3.0,F6.2,F7.0,F6.4)
       DIMENSION  T(105), R(105), DR(105)
       READ 110,L,(N,T(N),R(N),DR(N),  N=1,L)
  110 FORMAT (I3/(I3, F4.0, F9.4, F6.5))
       DIMENSION  V(160), DHDR(160)
       READ 111, I,(M,V(M),DHDR(M),    M=1,I)
  111 FORMAT (I3/(I3, F6.0, F7.0))
       K = 1
```

```
702 C1 = X(CL11(K),CL12(K),CL13(K),C14(K),CL15(K),C11(K),C12(K))
    C2 = X(CL21(K),CL22(K),CL23(K),C24(K),CL25(K),C21(K),C22(K))
    E1 = X(EL11(K),EL12(K),EL13(K),E14(K),EL15(K),E11(K),E12(K))
    C5 = X(CL51(K),CL52(K),CL53(K),C54(K),CL55(K),C51(K),C52(K))
    C6 = X(CL61(K),CL62(K),CL63(K),C64(K),CL65(K),C61(K),C62(K))
    C7 = X(CL71(K),CL72(K),CL73(K),C74(K),CL75(K),C71(K),C72(K))
    C8 = X(CL81(K),CL82(K),CL83(K),C84(K),CL85(K),C81(K),C82(K))
    CT = (C1 + C2)/2.0
   0E5= E51(K)+(EL51(K)-E54(K)) *ABSF(E61(K)-E51(K))/ABSF(EL53(K)-
   1     EL61(K))
   0E6= E61(K)+(EL61(K)-E64(K)) *ABSF(E61(K)-E51(K))/ABSF(EL53(K)-
   1     EL61(K))
   0E7= E71(K)+(EL71(K)-E74(K)) *ABSF(E81(K)-E71(K))/ABSF(EL73(K)-
   1     EL81(K))
   0E8= E81(K)+(EL81(K)-E84(K)) *ABSF(E81(K)-E71(K))/ABSF(EL73(K)-
   1     EL81(K))
    TIME = ITIME(K)
    ITIM = ITIME(K)
   0GO TO (20,21,22,23,24,25,26,27,28,29,30,31,32,33,34,35,36,37,38,
   1      39),ITIM
 20 FT  =7175.4
    GO TO 40
 21 FT  =14350.8
    GO TO 40
 22 FT  =21526.2
    GO TO 40
 23 FT  =28701.6
    GO TO 40
 24 FT  =35876.9
    GO TO 40
 25 FT  =43052.3
    GO TO 40
 26 FT  =50227.7
    GO TO 40
 27 FT  =57403.1
    GO TO 40
 28 FT  =64578.5
    GO TO 40
 29 FT  =71753.9
    GO TO 40
 30 FT  =78929.3
    GO TO 40
 31 FT  =86104.7
    GO TO 40
 32 FT  =93280.0
    GO TO 40
 33 FT  =100455.4
    GO TO 40
 34 FT  =107630.8
    GO TO 40
 35 FT  =114806.2
    GO TO 40
 36 FT  =121981.6
```

```
      GO TO 40
   37 FT  =129157.0
      GO TO 40
   38 FT  =136332.4
      GO TO 40
   39 FT  =143507.8
   40 ET = FT*E1*CT*1.0E-12
      RT5 = 100.0*E5/C5
      RT6 = 100.0*E6/C6
      RT7 = 100.0*E7/C7
      RT8 = 100.0*E8/C8
      TEMP1 = 0.0
      RAV = 0.0
  804 IF (RAV) 801, 800, 801
  801 RAV = RT8
      GO TO 805
  800 RAV = RT6
  805 IF (RAV  - 152.)900, 900, 901
  900 IF (RAV  - 134.)902, 902, 903
  902 IF (RAV  - 130.)906, 906, 907
  903 IF (RAV  - 140.)908, 908, 909
  908 IF (RAV  - 136.)910, 910, 911
  909 IF (RAV  - 145.)912, 912, 913
  912 IF (RAV  - 142.)914, 914, 915
  913 IF (RAV  - 148.)916, 916, 917
  907 IF (RAV - 132.0) 946, 946, 947
  906 N = 1
      GO TO 950
  946 N = 23
      GO TO 950
  910 N = 37
      GO TO 950
  911 N = 42
      GO TO 950
  914 N = 48
      GO TO 950
  915 N = 51
      GO TO 950
  916 N = 55
      GO TO 950
  917 N = 58
      GO TO 950
  947 N = 31
  950 IF (RAV  - R(N)) 951, 951, 952
  952 N = N + 1
      GO TO 950
  951 DRDT = DR(N) - (R(N) - RAV )*(DR(N) - DR(N-1))/(R(N)-R(N-1))
      DRAV = (DRDT + DR(N))/2.0
      IF (TEMP1) 802, 803, 802
  803 TEMP1= T(N) - (R(N) - RAV )/DRAV
      GO TO 804
  802 TEMP2= T(N) - (R(N) - RAV )/DRAV
      TDELTA = TEMP2 - TEMP1
```

```
      TEMP = (TEMP1 + TEMP2)/2.0
      RDIFF = RT8 - RT6
C       DA IS DELTA E/ DELTA R
      DA = ET/TDELTA
      IF (TEMP - 40.0) 630, 630, 631
  630 IF (TEMP - 25.0) 632, 632, 633
  632 IF (TEMP - 17.0) 634, 634, 635
  633 IF (TEMP - 32.0) 636, 636, 637
  631 IF (TEMP - 56.0) 638, 638, 639
  638 IF (TEMP - 47.0) 640, 640, 641
  634 N = 1
      GO TO 642
  635 N = 8
      GO TO 642
  636 N = 16
      GO TO 642
  637 N = 23
      GO TO 642
  640 N = 31
      GO TO 642
  641 N = 38
      GO TO 642
  639 N = 46
  642 IF (TEMP - T(N)) 643, 643, 644
  644 N = N + 1
      GO TO 642
 6430DTDR = 1.0/DR(N) - (T(N)-TEMP)*(1.0/DR(N)-1.0/DR(N-1))/(T(N)-T(N-1
     1))
      DTAV = (DTDR + 1.0/DR(N))/2.0
      RAVE = R(N) - (T(N) - TEMP)/DTAV
      WAT = WATCH(K)
      RA = 500.28*E1/CT
      FA = (6.60E-6)*RA**2
      RW = RA + FA
      RE = RW - RAVE
C       Z IS A/ET
      Z = RE*TIME/ET
      SS = RE/(10.0*RAVE*TIME)
      IF (RW - 128.)48,48,41
   41 IF (RW - 143.)49,49,42
   48 EPR  =-0.0008
      GO TO 57
   49 EPR  =-0.0009
      GO TO 57
   42 EPR = -0.0010
   57 IF (RAVE - 139.)64, 64, 60
   64 W=0.0000
      GO TO 69
   60 W = 0.0001
   69 SW = 0.0
  600 IF (RAVE - 167.5) 602,602,621
  602 IF (RAVE - 131.6) 604,604,605
  604 IF (RAVE - 130.05) 606, 607, 607
```

```
606 DC = 7.E-3
    GO TO 621
607 DC  =6.E-3
    GO TO 621
605 IF (RAVE - 139.5) 608,608,609
608 IF (RAVE - 134.5) 610,610,611
610 DC  =5.E-3
    GO TO 621
611 DC  =4.E-3
    GO TO 621
609 DC  =3.E-3
621 ADIA = DC*(SUM(K)-SUMO(K)*TIM(K))/ET
    CORR = EPR + SS + W + SW + ADIA + WATCH(K)
    DCORR = DA*CORR
    DSUM = DA + DCORR
    IF (RAVE - 152.)500, 500, 901
500 IF (RAVE - 134.)502, 502, 503
502 IF (RAVE - 130.5) 506, 506, 507
503 IF (RAVE - 140.)508, 508, 509
508 IF (RAVE - 136.)510, 510, 511
509 IF (RAVE - 145.)512, 512, 513
512 IF (RAVE - 142.)514, 514, 515
513 IF (RAVE - 148.)516, 516, 517
507 IF (RAVE - 132.)546, 546, 547
546 M = 11
    GO TO 550
510 M = 29
    GO TO 550
511 M = 39
    GO TO 550
514 M = 47
    GO TO 550
515 M = 51
    GO TO 550
516 M = 57
    GO TO 550
517 M = 63
    GO TO 550
547 M = 19
    GO TO 550
550 IF (RAVE - V(M)) 553, 553, 554
554 M = M + 1
    GO TO 550
553 CMT = DHDR(M-1) + (RAVE-V(M-1))*(DHDR(M)-DHDR(M-1))/(V(M)-V(M-1))
    DELRDT = RDIFF/TDELTA
    DELHDT = CMT*DELRDT
    GO TO 81
506 CMT = 0.0
    IF (TEMP - 15.0) 70, 70, 71
 70 TK = 4.774 - 0.101*(TEMP-10.0)/5.0
    GO TO 80
 71 IF (TEMP - 20.0) 72, 72, 73
 72 TK = 4.673 - 0.101*(TEMP-15.0)/5.0
```

```
      GO TO 80
   73 IF (TEMP - 25.0) 74, 74, 75
   74 TK = 4.572 - 0.101*(TEMP-20.0)/5.0
      GO TO 80
   75 IF (TEMP - 30.0) 76, 76, 77
   76 TK = 4.471 - 0.101*(TEMP-25.0)/5.0
      GO TO 80
   77 IF (TEMP - 35.0) 78, 78, 79
   78 TK = 4.369 - 0.101*(TEMP-30.0)/5.0
      GO TO 80
   79 TK = 4.268 - 0.101*(TEMP-35.0)/5.0
   80 DELHDT = TK*(TEMP**3)*1.0E-5
   81 CTOT = DSUM - DELHDT
      PRINT 131, K
  131 FORMAT (5H CASE I2///)
      PRINT  120,  E1, CT, ET, RA, EPR
 1200FORMAT (4H E1= F11.2, 5H  CT= F10.2, 5H  ET= F11.5, 5H  RA= F10.4,
     1    6H  EPR= F10.4)
      PRINT 121, E5, C5, RT5, FA, W
  121 FORMAT (5H E5= F10.2, 5H  C5= F10.2, 6H  RT5= F10.4,
     1   5H  FA= F10.4, 5H  W= F11.4)
      PRINT 122, E6, C6, RT6, RW, SS
 1220FORMAT  (4H E6= F11.2, 5H  C6= F10.2, 6H  RT6= F10.4,
     1   5H  RW= F10.4, 5H  SS= F11.4)
      PRINT 123, E7, C7, RT7, RE, SW
 1230FORMAT  (4H E7= F11.2, 5H  C7= F10.2, 6H  RT7= F10.4,
     1    5H  RE= F10.4, 5H  SW= F11.4)
      PRINT 124, E8, C8, RT8, Z, ADIA
 1240FORMAT  (4H E8= F11.2, 5H  C8= F10.2, 6H  RT8= F10.4,
     1   4H  Z= F11.4, 7H  ADIA= F 9.4)
      PRINT 125, RDIFF, RAVE, WAT
  125 FORMAT (8H RDIFF= F10.5, 7H  RAVE= F10.4, 27X, 5H WAT= F10.4)
      PRINT 126, DA,DELRDT,CORR
  126 FORMAT (4H DA= F14.5, 7H  DRDT= F10.5, 27X, 6H CORR= F10.4)
      PRINT 127, DCORR, CMT
  127 FORMAT  (8H DCORR= F10.5, 7H  CMT = F10.5)
      PRINT 128, DSUM, TEMP, TEMP1, TEMP2, TDELTA
 1280FORMAT (6H DSUM= F12.5, 4H  T= F13.5, 5H  T1= F13.5, 5H  T2= F13.5
     1, 7H  DIFF= F13.5)
      PRINT 140, DELHDT
  140 FORMAT (4H MT= F14.5)
      PRINT 130, CTOT
  130 FORMAT  (6H CTOT= F12.5////)
      IF (J - K) 700, 700, 701
  701 K = K + 1
      GO TO 702
  901 CONTINUE
  700 CALL EXIT
      END
      FUNCTION X(A, B, C, D, E, F, G)
      IF (E) 10, 11, 10
   10 S = ABSF((2.0*B - A - E)/(F - G))
      X = G + (B - D)/S
```

```
      RETURN
   11 S = ABSF((2.0*C - B - A)/(F - G))
      X = F + (C - D)/S
      RETURN
      END
```

```
C      THIS PROGRAM COMPUTES THE ENERGY LEVELS FOR  A SPHERICAL TOP
C      IN A CUBIC ENVIRONMENT. IT THEN COMPUTES THE HEAT CAPACITY FROM
C      THESE ENERGY LEVELS
C      IF IM1 = 0, DO NOT PUNCH OUT ANY CARDS
C      IF IM1 = 1, PUNCH ENERGY LEVELS FOR HEAT CAPACITY CALCULATION
C      IF IM1 = 2, PUNCH ENERGY LEVELS FOR THESIS
C      NIK = FIRST ROTATIONAL LEVELS TO BE COMPUTED, THOSE LEVELS BELOW
C      NIK ARE UNDER BARRIER TO ROTATION
C      DOU IS NUMBER OF LEVELS LEFT OUT BECAUSE THEY ARE UNDER J = NIK
C      K1 IS THE LOWEST TEMPERATURE THE HEAT CAPACITY IS TO BE CALCULATED
C      K2 IS THE HIGHEST TEMPERATURE THE HEAT CAPACITY IS TO BE CALCULATED
C      KN IS INTERVAL BETWEEN HEAT CAPACITY CALCULATIONS
C      TIN IS THE ROTATIONAL CONSTANT IN RECIPROCAL CM.
C      Y IS THE TORSIONAL FREQUENCY IN RECIPROCAL CM.
C      KAX IS THE HIGHEST ROTATIONAL LEVEL TO BE COMPUTED
C      TH IS THE AMOUNT OF CALORIES BELOW THE BARRIER A ROTATIONAL LEVEL
C      MAY APPEAR AT. USUALLY IS EQUAL TO 70 CALORIES.
       DIMENSION R(2000), E(2000)
  811  READ 103, K1, K2, KN, TIN, Y, KAX, TH, IM1, NIK, DOU, IM2
  103  FORMAT (3I4  , 2F7.0, I4, F7.0, 2I3, F5.0, 22X, I2)
       TELL = 2.8591*TIN
       OMEGA = 2.8591*Y + 5.0*TELL
       V = OMEGA**2/(16.0*TELL)
       VP = V/2.8591
       COUNT = 0.0
       DOUNT = DOU
       PRINT 160, V, VP
  160  FORMAT (20H1POTENTIAL BARRIER =F10.3, 6H CAL., F8.3, 15H RECIPROCA
      1L CM. ////)
       S = Y*1.439
       PRINT 150
  150  FORMAT (26H ANHARMONIC ENERGY LEVELS ////)
       KTOT = 0
       N = 1
  210  X = KTOT
       W = 0
       Z = 0
  900  TOT = X + W + Z
       IF (X - Z) 400, 401, 402
  402  IF (Z - W) 400, 404, 405
  401  IF (Z - W) 400, 403, 404
  403  R(N) = 1.0
       GO TO 406
  404  R(N) = 3.0
       GO TO 406
  405  R(N) = 6.0
  406  E(N) = TOT*OMEGA - (2.0*(X**2 + W**2 + Z**2) + 3.0*TOT + X*W + Z*W
      1+ Z*X)*TELL
       IF (V - E(N)) 506, 504, 504
  504  PIT = E(N)/2.8591
       PRINT 151, N, X, Z, W, R(N), PIT
  151  FORMAT (I4, 30X, 4F4.0, F14.4)
       COUNT = COUNT + R(N)
```

```
      IF (IM1 - 1) 801, 800, 801
  800 PUNCH 880, R(N), PIT
  880 FORMAT (2F10.4)
  881 FORMAT (20X, 3F6.0, F12.2, F7.0)
  801 IF (IM1 - 2) 802, 803, 802
  803 PUNCH 881, X, Z, W, PIT, R(N)
  802 N = N + 1
      W1 = 0.0
  204 IF (Z - W - 1.0) 200, 200, 203
  203 Z = Z - 1.0
      W = W + 1.0
      GO TO 900
  200 IF (W) 22, 23, 22
   22 W1 = W
      Z = Z + W
      W = 0.0
   23 IF (X - Z - 1.0) 202, 202, 201
  201 X = X - 1.0
      Z = Z + 1.0
      GO TO 900
  202 IF (W1) 842, 30, 842
   30 IF (X - W - 1.0) 205, 205, 206
  206 X = X - 1.0
      W = W + 1.0
      GO TO 900
  842 W = W1
      Z = Z - W1
      IF (X - Z - 1.0) 841, 841, 831
  831 X = X - 1.0
      Z = Z + 1.0
      GO TO 900
  841 IF (X - W - 1.0) 205, 205, 840
  840 X = X - 1.0
      W = W + 1.0
      IF (X - Z) 205, 900, 900
  205 KTOT = KTOT + 1
      PRINT 175
  175 FORMAT (1H0)
      GO TO 210
  506 PRINT 152
  152 FORMAT (26H0ROTATIONAL ENERGY LEVELS ///)
      DO 550 M = NIK,KAX
      T0 = M/4
      T = 4.0*T0
      T1 = M
      T2 = T
  553 T3 = T2
  552 CALL ENER(TELL, V    , OMEGA, T1, T2, T3, EN, E0, E1, E2, 4.0)
      E(N) = EN
      CALL DEGEN (TIN    , T1, T2, T3, D, DNS)
      R(N) = D
      BAT = E(N)/2.8591
      BAT0 = E0/2.8591
```

```
      BAT1 = E1/2.8591
      BAT2 = E2/2.8591
      IF (E(N) - V + TH) 21, 91, 91
   21 DOUNT = DOUNT + R(N)
      PRINT 153, N, T1, T2, T3, R(N), DNS, BAT, BAT0, BAT1, BAT2
  153 FORMAT (2X, I5, 20X, 3F4.0, 2F12.5, 4F14.4)
      GO TO 809
   91 PRINT 882, N, T1, T2, T3, R(N), DNS, BAT, BAT0, BAT1, BAT2
  882 FORMAT (I5, 20X, 3F4.0, 2F12.5, 4F14.4)
      IF (IM1 - 1) 805, 806, 805
  806 PUNCH 880, R(N), E(N)
  805 IF (IM1 -2) 807, 808, 807
  808 PUNCH 80, T1, T2, T3, BAT0, BAT1, BAT2, BAT, R(N)
   80 FORMAT (7X, 3F4.0, 4F11.2, F5.0)
  807 N = N + 1
  809 T3 = T3 - 4.0
      IF (T3) 551, 552, 552
  551 T2 = T2 - 4.0
      IF (T2) 550, 553, 553
  550 CONTINUE
      E(N) = V
      R(N) = DOUNT - COUNT
      PRINT 883, R(N), VP
  883 FORMAT (1H0, 51X, F5.0, F11.4)
      PRINT 884
  884 FORMAT (30H1 TEMPERATURE   HEAT CAPACITY )
      DO 810 I = K1, K2, KN
      TEMP = I
      CALL ROT(E, R, TEMP, N, S, CP)
  810 CONTINUE
      IF (IM2) 400, 811, 400
  400 CALL EXIT
      END
      SUBROUTINE DEGEN (TIN, T1, T2, T3, R, RNS)
C     DETERMINED DEGENERACY OF ROTATIONAL LEVELS
      D = 1.0
      IF (T2) 100, 101, 100
  101 R = 1.0
      RNS = R*D
      RETURN
  100 IF (T2 - T3) 102, 103, 102
  103 R = 4.0
      RNS = R*D
      RETURN
  102 IF (T3) 104, 105, 104
  105 R = 4.0
      RNS = R*D
      RETURN
  104 R = 8.0
      RNS = R*D
      RETURN
      END
      SUBROUTINE ENER(TELL, V, OMEGA, X, Y, Z, EN, E0, E1, E2, PIN)
```

```
C      CALCULATES ENERGIES OF ROTATIONAL LEVELS
       AA =            Y*Z/(X*(X + 1.0))
       AD=2.0*SQRTF((X - Y + 1.0)*(X + Y + 1.0)*(X - Z + 1.0)*(X + Z + 1.
      10)/((2.0*X + 1.0)*(2.0*X + 3.0)))/(2.0*X + 2.0)
       AG=2.0*SQRTF((X**2 - Y**2)*(X**2 - Z**2)/(4.0*X**2 - 1.0))/(2.0*X)
       E0 = X*(X + 1.0)*TELL - 1.5*OMEGA + 15.0*TELL*PIN**2/64.0 + 15.0*V
      1/16.0
       E1 = V/2.0*(-49.0/8.0*(AA**4 +12.0*AA**2*AD*AG + 6.0*AD**2*AG**2)
      1  + 21.0/4.0*(AA**2 + 2.0*AD*AG))
       A1 = - 49.0*(AD*AA**3 + 3.0*AA*AG*AD**2)/2.0 + 21.0*AA*AD/2.0
       A2 = - 49.0*(6.0*AA**2*AD**2 + 4.0*AG*AD**3)/8.0 + 21.0*AD**2/4.0
       A3 = - 49.0*AA*AD**3/2.0
       A4 =-49.0*AD**4/8.0
       A11 = - 49.0*(AG*AA**3 + 3.0*AA*AD*AG**2)/2.0 + 21.0*AA*AG/2.0
       A12 = - 49.0*(6.0*AA**2*AG**2 + 4.0*AD*AG**3)/8.0 + 21.0*AG**2/4.0
       A13 = - 49.0*AA*AG**3/2.0
       A14 = - 49.0*AG**4/8.0
       E2 =-V**2/(8.0*TELL)*(A1**2/(X + 1.0) + A2**2/(2.0*X + 3.0) + A3**
      12/(3.0*X + 6.0) + A4**2/(4.0*X + 10.0) - A11**2/X - A12**2/(2.0*X-
      21.0) - A13**2/(3.0*X - 3.0) - A14**2/(4.0*X - 6.0))
       EN = E0 + E1 + E2
       RETURN
       END
```

REFERENCES

1. D. W. Osborne and E. F. Westrum, J. Chem. Phys., 21, 1884, (1953)

2. J. W. Stout and E. Catalano, J. Chem. Phys., 23, 2013, (1955)

3. C. C. Stephenson, D. R. Bentz, and D. A. Stevenson, J. Am. Chem. Soc., 77, 2161, (1955)

4. C. C. Stephenson, C. A. Wulff, and O. R. Lundell, J. Chem. Phys., 40, 967, (1964)

5. A. G. Cole, "The Heat Capacities of NH_4Br and NH_4I, etc." thesis, MIT, (1952)

6. A. Einstein, Ann. d. Physik, 22, 180, (1907); 34, 170, (1911)

7. P. Debye, Ann. Physik, 39, 789, (1912)

8. A. J. Karo, J. Chem. Phys., 31, 1489, (1959)

9. E. W. Kellermann, Trans. Royal Soc. (London), 238, 513, (1940)

10. E. W. Kellermann, Proc. Royal Soc. (London), A178, 17, (1941)

11. A. J. Karo, J. Chem. Phys., 33, 7, (1960)

12. C. C. Stephenson, unpublished data

13. B. Yates and C. H. Panter, Proc. Phys. Soc., 80, 373, (1962)

14. W. T. Berg and J. A. Morrison, Proc. Royal Soc. (London), 242, 467, (1957)

15. M. P. Tosi and F. G. Fumi, Phys. Rev., 131, 1458, (1963)

16. G. Leibfried and W. Ludwig in Solid-State Physics, edited by F. Seitz and D. Turnbull, Academic Press, Inc., New York, Volume 12, 275, (1961)

17. C. C. Stephenson, R. W. Blue and J. W. Stout, J. Chem. Phys. 20, 1046, (1952)

18. L. Pauling, Phys. Rev., 36, 430, (1930)

19. L. Frenkel, Acta Physicochim. URSS, 3, 23, (1935)

20. C. C. Stephenson, L. A. Landers, and A. G. Cole, J. Chem. Phys., 20, 1044, (1952)

21. R. S. Orehotsky, "The Heat Capacity of Ammonium and Deutero-Ammonium Fluoborate between 25°K and 300°K," thesis, MIT, (1963)

22. G. S. Morfee, L. A. K. Staveley, S. T. Walters, and D. L. Wigley, J. Phys. Chem. Solids, 13, 132, (1960)

23. P. W. Anderson in Solid-State Physics, edited by F. Seitz and D. Turnbull, Academic Press Inc., New York, Vol. 14, 99, (1963)

24. J. A. Hoffmann, A. Paskin, K. J. Tauer, R. J. Weiss, J. Phys. Chem. Solids, 1, 45, (1956)

25. T. Oguchi, Prog. Theor. Phys., 13, 148, (1955)

26. O. Nagai, J. Phys. Soc. Japan, 18, 510, (1963)

27. W. Marshall, J. Phys. Chem. Solids, 7, 159, (1958)

28. H. E. Adams, "The Heat Capacity of Manganese Fluoride, etc.", thesis, MIT, (1942)

29. R. W. Blue and J. F. G. Hicks, J. Am. Chem. Soc., 52, 1962, (1937)

30. T. G. Maple, "Thermodynamic Properties of Elemental Phosphorous", thesis, MIT, (1949)

31. J. H. Van Vleck, J. Chem. Phys., 5, 320, (1937)

32. C. H. Shomate, J. Am. Chem. Soc., 68, 964, (1946)

33. R. J. Weiss and K. J. Tauer, Phys. Rev., 100, 1223, (1955)

34. H. Forstat, G. Taylor and R. D. Spence, Phys. Rev., 116, 897, (1959)

35. W. K. Robinson and S. A. Friedberg, Phys. Rev., 117, 402, (1960)

36. S. A. Friedberg, Physica, 18, 714, (1952)

37. S. A. Friedberg and J. D. Wasscher, Physica, 19, 1072, (1953)

38. A. R. Miedema, H. van Kempen and W. J. Huiskamp, Physica, 29, 1266, (1963)

39. D. G. Kapadnis and R. H. Hartmans, Physica, 22, 181, (1956)

40. H. Forstat and D. R. McNeeley, J. Chem. Phys., 35, 1594, (1961)

41. R. D. Spence, H. Forstat, G. A. Khan and G. Taylor, J. Chem. Phys., 31, 555, (1955)

42. T. Haseda and A. R. Miedema, Physica, 27, 1102, (1961)

43. F. J. du Chatenier, B. M. Boerstoel, and J. de Nobel, Physica, 30, 1625, (1964)

44. H. van Kempen, W. T. Duffy Jr., A. R. Miedema, and W. J. Huiskamp, Physica, 30, 1131, (1964)

45. H. Forstat, G. Taylor, and B. R. King, J. Chem. Phys., 31, 929, (1959)

46. W. B. Hadley and J. W. Stout, J. Chem. Phys., 39, 2205, (1963)

47. G. T. Furukawa, T. B. Douglas, R. E. McCoskey, and D. C. Ginnings, NBS J. Res., 57, 67, (1956)

48. C. H. Shomate, J. Am. Chem. Soc., 68, 310, (1946)

49. F. Gronvold and E. F. Westrum, J. Am. Chem. Soc., 81, 1780, (1959)

50. C. T. Anderson, J. Am. Chem. Soc., 59, 488, (1937)

51. C. T. Anderson, J. Am. Chem. Soc., 58, 564, (1936)

52. K. K. Kelley, F. S. Boeriche, G. E. Moore, E. H. Huffman, and W. M. Bangert, "Thermodynamic Properties of Carbides of Chromium", Bureau of Mines Tech. Raper 662, (1944)

53. G. S. Heller, J. J. Stickler, J. B. Thaxter, J. Appl. Phys., 32, 307S, (1961)

54. E. P. Warekois, J. Appl. Phys., 31, 346S, (1960)

55. A. J. MacMillan, "Electric and Magnetic Properties of V_2Q_3 and Related Sesquioxides", Laboratory of Insulation Research, MIT Tech. Report 172, (1962)

56. J. W. Stout and H. E. Adams, J. Am. Chem. Soc., 64, 1535, (1942)

57. E. Catalano and J. W. Stout, J. Chem. Phys., 23, 1803, (1955)

58. E. Catalano and J. W. Stout, J. Chem. Phys., 23, 2013, (1955)

59. S. S. Todd, J. Am. Chem. Soc., 71, 4115, (1949)

60. E. Catalano, J. Phys. Soc. Japan Suppl. BI, 517, (1962)

61. K. K. Kelley and G. E. Moore, J. Am. Chem. Soc., 65, 1264, (1943)

62. J. W. Stout and R. C. Chisholm, J. Chem. Phys., 36, 979, (1962)

63. R. C. Chisholm and J. W. Stout, J. Chem. Phys., 36, 972, (1962)

64. R. B. Murray, Phys. Rev., 100, 1071, (1955)

65. R. A. Butera and W. F. Giauque, J. Chem. Phys., 40, 2379, (1964)

66. W. F. Giauque, E. W. Hornung, R. A. Fisher, and G. E. Brodale, J. Chem. Phys., 42, 835, (1965)

67. J. J. McBride, "Low Temperature Heat Capacities of Layer and Chain Type Crystalline Structures", thesis, U. of Michigan, (1956)

68. R. H. Busey and W. F. Giauque, J. Amer. Chem. Soc., 74, 4443, (1952)

69. J. W. Stout and S. A. Reed, J. Am. Chem. Soc., 76, 5279, (1954)

70. R. C. Chisholm, "Thermal Effects Associated with Magnetic Ordering in Iron Group Chlorides, etc.", thesis, Univ. of Chicago, (1960)

71. J. Hu and H. L. Johnston, J. Am. Chem. Soc., 75, 2471, (1953)

72. R. E. Newnham and Y. M. deHaan, Zeit. fur Krist., 117, S235, (1962)

73. Y. Ishikawa and S. Akimoto, J. Phys. Soc. Japan, 13, 1110, (1958)

74. G. Shirane, D. E. Cox, W. J. Takei, and S. L. Ruby, J. Phys. Soc. Japan, 17, 1598, (1962)

75. R. W. G. Wyckoff, Crystal Structures, Second edition, Interscience Publishers, New York, 1963, 2 vol.

76. A. Ferrari, A. Braibanti, and G. Bigliardi, Acta Crysta, 16, 846, (1963)

77. J. W. Tracy, N. W. Gregory, E. C. Lingafelter, J. D. Dunitz, H. C. Mez, R. E. Rundle, C. Scheringer, H. L. Yakel Jr., and M. K. Wilkinson, Acta Crysta, 14, 927, (1961)

78. T. Shinoda, H. Chihara, and S. Seki, J. Phys. Soc. Japan, 19, 1647, (1964)

79. M. E. Lines, Phys. Rev., 131, 546, (1963)

80. H. Bizette, C. Terrier, and B. Tsai, C. R. Acad. Sci. Paris, 243, 1295, (1956)

81. Y. Y. Li, Phys. Rev., 102, 1015, (1956)

82. J. Wucher, C. R. Acad. Sci. Paris, 241, 288, (1955)

83. L. Rimai, H. Statz, M. J. Weber, and G. A. de Mars, Phys. Rev. Letters, 4, 125, (1960)

84. F. J. Milford, M. Kretman, and J. G. Daunt, Eighth International Conference on Low Temperature Physics, Butteworthes, London, 1962, p. 220

85. M. O'Keeffe and F. S. Stone, J. Phys. Chem. Solids, 23, 261, (1962)

86. R. Ingalls, Phys. Rev., 133, A787, (1964)

87. A. Okiji and J. Kanamori, J. Phys. Soc. Japan, 19, 908, (1964)

88. S. Kern and B. Feldman, Solid State Research Report, Lincoln Laboratory, M.I.T., (1962), #2, p. 35 (unpublished)

89. R. Newnham, private communication

90. E. B. Wilson, Chemical Reviews, 27, 17, (1940)

91. "Tables Relating to Mathieu Functions", prepared by the Computation Laboratory of the National Applied Mathematics Laboratories, National Bureau of Standards, Columbia University Press, New York, (1951)

92. G. N. Lewis, M. Randall, K. S. Pitzer, and L. Brewer, Thermodynamics, Second edition, Mc-Graw Hill Co., New York, (1961)

93. H. S. Gutowsky, G. E. Pake, and R. Bersohn, J. Chem. Phys., 22, 643, (1954)

94. H. Rademacher and F. Reiche, Zeit. f. Physik, 41, 453, (1927)

95. C. H. Townes and A. L. Schawlow, Microwave Spectroscopy, McGraw-Hill Co., New York, (1955), p. 96

96. E. B. Wilson, J. Chem. Phys., 3, 276, (1935)

97. J. G. Marshall, L. A..K. Staveley, and K. R. Hart, Trans. Faraday Soc., 52, 19, (1956)

98. C. W. Garland and J. S. Jones, J. Chem. Phys., 39, 2874, (1963)

99. E. L Wagner and D. F. Hornig, J. Chem. Phys., 18, 296, (1950)

100. V. T. Deshpandi and D. B. Sirdeshmukh, Acta Crysta, 14, 353, (1961)

101. F. Yarnell, private communication

102. A. M. Karo, "The Heat Capacity of Deutero-Ammonium Bromide from 17°K to 300°K", thesis, M.I.T., (1952)

103. L. A. Landers, "The Heat Capacity of Solid Solutions of Ammonium Iodide and Patassium Iodide from 15°K to 300°K etc.," thesis, M.I.T., (1952)

104. H. L. Johnston and N. C. Hallet, J. Am. Chem. Soc., 75, 1467 (1953)

105. C. J. H. Schutte, Spectrochim Acta, 16 , 1054, (1960)

106. A. Altschuller, J. Am. Chem. Soc., 77, 5455, (1955)

107. T. B. Douglas and A. W. Harman, J. Res. NBS, 60 117, (1958)

108. W. H. Stockmayer and C. C. Stephenson, J. Chem. Phys., 21, 1311, (1953)

109. G. T. Furukawa, M. L. Reilley, and J. H. Piccirelli, J. Res. NBS, 68A, 651, (1964)

110. T. C. Waddington, J. Chem. Soc., 4783, (1958)

111. D. Welsh, "An X-ray Investigation of the Lamba Point, etc.", thesis, M.I.T., (1962)

112. S. C. Abrahams and J. Kalmajs, J. Chem. Phys., 22, 434, (1954)

113. P. T. Ford and H. M. Powell, Acta Crysta, 7, 604, (1954)

114. C. A. Wulff, J. Chem. Phys., 39, 1227, (1963)

115. K. Clusius, J. Goldman, and A. Perilick, Z. Naturforsch, 4, 424, (1949)

116. G. Shirane, S. J. Pickart, and Y. Ishikawa, J. Phys. Soc. Japan, 14, 1352, (1959)

117. E. Benjamins and E. F. Westrum, J. Am. Chem. Soc., 79, 287, (1957)

118. R. C. Plumb and D. F. Hornig, J. Chem. Phys., 23, 947, (1955)

119. P. M. Harris and E. P. Meibohm, J. Am. Chem. Soc., 69, 1231, (1947)

120. N. C. Hallet and H. L. Johnston, J. Am. Chem. Soc., 75, 1496, (1953)

121. J. L. Hoard and V. Blair, J. Am. Chem. Soc., 57, 1985, (1936)

122. Gmelins Handbuch der Anorganishen Chemie, Eighth edition, Vol. 23, p. 93 et. seq., (1936)

123. J. C. Southard and R. A. Nelson, J. Am. Chem. Soc., 55, 4865, (1933)

124. W. V. Smith, O. L. I. Brown, K. S. Pitzer, J. Am. Chem. Soc., 59, 1213, (1937)

125. W. M. Latimer and J. E. Ahlberg, J. Am. Chem. Soc., 52, 549, (1930)

126. E. R. Lippincott and R. D. Nelson, J. Am. Chem. Soc., 77, 4990, (1955)

127. W. Vedder and D. F. Hornig, J. Chem. Phys., 35, 1560, (1961)

128. K. Mikki and A. K. Kroh in Inelastic Neutron Scattering in Solids and Liquids, International Atomic Energy Commission, Vienna, (1963), p. 237, Vol. 2

129. G. Venkataraman in Inelastic Neutron Scattering in Solids and Liquids, International Atomic Energy Commission, Vienna, (1963), p. 253, Vol. 2

130. E. L. Wagner and D. F. Hornig, J. Chem. Phys., 18, 305, (1950)

131. W. C. Plumb and D. F. Hornig, J. Chem. Phys., 21, 366, (1953)

132. T. Ernst, Z. physik Chem., B20, 65, (1933)

133. H. Dachs, Zeit. fur Krist., 112, 60, (1959)

134. J. D. Bernal, H. D. Megaw, Proc. Royal Soc. (London), A151, 384, (1935)

135. H. E. Petch and H. D. Megaw, J. Opt. Soc. Am., 44, 744, (1954)

136. W. R. Busing and H. A. Levy, J. Chem. Phys., 26, 563, (1957)

137. N. Ockman, Advances in Phys., 7, 199, (1958)

138. T. W. Bauer, H. J. Johnston, and E. C. Kerr, J. Am. Chem. Soc., 72, 5174, (1950)

139. L. E. Murch and W. F. Giauque, J. Phys. Chem., 66, 2052, (1962)

140. W. F. Gaiuque and R. C. Archibald, J. Am. Chem. Soc., 59, 561, (1937)

141. W. E. Hatton, D. L. Hildebrand, G. C. Sinke, and D. R. Stull, J. Am. Chem. Soc., 81, 5028, (1959)

142. S. S. Mitra in Solid-State Physics, edited by F. Seitz and D. Turnbull, Academic Press Inc., New York, Vol. 12, p. 1, (1961)

143. G. C. Pimental and A. L. McClellan, The Hydrogen Bond, W. H. Freeman and Co., San Francisco, (1960), p. 126

144. A. D. B. Woods, B. N. Brockhouse, M. Sakamoto, R. N. Sinclair, "Energy Distributions of Neutrons Scattered by Graphite, etc." AECL #1088, (1960)

145. E. A. Moelwyn-Hughes, Physical Chemistry, Pergamon Press, London, Second Revised Edition, (1961)

146. R. W. Blue, J. Chem. Phys., 22, 280, (1954)

147. S. C. Abrahams, R. L. Collin, and W. N. Lipscome, Acta Crysta, 4, 15, (1951)

148. P. A. Giguere, D. I. Liu, J. S. Dugdale, and J. A. Morrison, Can. J. Chem., 32, 117, (1954)

149. P. A. Giguere and K. B. Harvey, J. Mol. Spectroscopy, 3, 36, (1959)

150. R. C. Taylor, paper presented at the "Symposium on Molecular Structure and Spectroscopy", Columbus, Ohio, (1957)

151. R. P. Bell. Proc. Royal Soc. (London), A183, 328, (1945)

152. A. Danti, W. J. Lafferty, and R. C. Lord, J. Chem Phys., 33, 294, (1961)

153. S. I. Chan, J. Zinn, J. Fernandez, and W. D. Gwinn, J. Chem. Phys., 33, 295, 1643, (1960); 34, 1319, (1961)

154. G. W. Rathjens and W. D. Gwinn, J. Am. Chem. Soc., 75, 5629, (1953)

155. D. W. Scott, H. L. Finke, W. N. Hubbard, J. P. McCullough, C. Katz, M. E. Gross, J. F. Messerly, R. E. Pennington, G. Waddington, J. Am. Chem. Soc., 75, 2795, (1953)

156. S. I. Chan, D. Stelman and L. E. Thompson, J. Chem. Phys., 41, 2828, (1964)

157. R. C. Lord and I. Nakagawa, J. Chem. Phys., 39, 2951, (1963)

158. L. N. Mulay and A. Attalla, J. Am Chem. Soc., 85, 702, (1963)

159. J. R. Durig, "Far Infrared Studies of Centrifugal Distortion and Anharmonic Vibrations in Polyatomic Molecules", thesis, M.I.T., (1962)

160. J. D. Duntz and L. E. Orgel, Nature, 171, 121, (1953)

161. P. F. Eiland and R. Pepinsky, J. Am. Chem. Soc., 74, 4971, (1952)

162. W. K. Winter, B. Cornutte, and S. E. Whitcomb, Spectrochim Acta, 15, 1085, (1959)

163. J. W. Edwards, G. L. Kington, and R. Mason, Trans. Frarday Soc., 56, 660, (1960)

164. J. W. Edwards and G. L. Kington, Trans. Frarday Soc., 58, 1334, (1962)

165. W. F. Giauque and J. W. Stout, J. Am. Chem. Soc., 58, 1144, (1936)

166. E. A. Long and J. D. Kemp, J. Am. Chem. Soc., 58, 1829, (1936)

167. J. B. Goodenough, Magnetism and the Chemical Bond, New York, Interscience Publishers, (1963)

168. J. J. Stickler and G. S. Heller, J. Appl. Phys., 33, 1302S, (1962)

BIOGRAPHICAL SKETCH

The author was born on November 7, 1939 in Fall River, Massachusetts. He was educated in the public schools of Fall River, graduating from B. M. C. Durfee High School June 1957. He received his undergraduate education at Providence College from which he received a Bachelor of Science degree, magna cum laude, in June 1961. While at Providence he was elected to membership in Delta Epsilon Sigma. He entered the Massachusetts Institute of Technology September 1961 to begin his graduate study for the degree of Doctor of Philosophy in physical chemistry. Professor Clark C. Stephenson supervised the author's thesis work. The author was elected to Sigma Xi while at the Massachusetts Institute of Technology.